Particulate Monitoring Analysis for the Paso del Norte Airshed in the United States – Mexico Border Region

November 13, 2008-April 30, 2009

New Mexico Environment Department Air Quality Bureau

Particulate Monitoring Analysis for the Paso del Norte Airshed in the United States – Mexico Border Region

November 13, 2008-April 30, 2009

New Mexico Environment Department Air Quality Bureau

Acknowledgements

- The Ecologia y Protección Civil, Normativo Ambiental air monitoring staff collected the data in Mexico. Thanks to Daniel Terrazas, Pedro Mora, Ricardo Aragon and Lic. Hector A. Sandoval Quesney, Director Normativo Ambiental, Dr. Gral. De Ecologia y Protección Civil, Venida Francisco Villa No. 950 nte. Ciudad Juárez, Chihuahua 32000 Tel. 207-88-00 Ext. 2448 Email: hsandovalq@juarez.gob.mx . Thanks also to Ing. Bernardo Escudero O. Director, Ecologia y Protección Civil, Presidencia Municipal Ciudad Juárez, Chihuahua 32300.

- The New Mexico Environment Department air monitoring staff collected the data in New Mexico. Thanks to Abel Ramirez, Daniel Galindo, Michaela Lane-Sanchez and Terry Hertel, Manager, Ambient Air Monitoring Program, NMED Air Quality Bureau, 1301 Siler Road Building B, Santa Fe, NM 87505, phone 505 476-4316 Email: terry.hertel@state.nm.us .

- The data was analyzed and a report prepared (*Sunland Park Low-Wind $PM_{2.5}$ Exceedances Study*) by David DuBois, Ricky Tropp and Ilias Kavouras of the Desert Research Institute, 755 East Flamingo Road, Las Vegas, Nevada 89119, phone 702 862-5468.

This project was funded by the U.S. Environmental Protection Agency Region VI, Dallas, Texas ,U.S./Mexico Border Air Quality Grant Program FY 2006/2007 grant number XA-96648101 and the New Mexico Environment Department.

Cover photos: Webcam views of the project area in the Rio Grande Valley, looking west/northwest from Ranger Peak, El Paso, Texas. Top view, 03/03/08; bottom view, 04/10/08.

Executive Summary

A saturation monitoring network for $PM_{2.5}$ was operated at 13 sites in the binational border region of Sunland Park, New Mexico, El Paso, Texas and Ciudad Juárez, Mexico. The purpose of this network was to assess the spatial extent of high $PM_{2.5}$ during low wind, stagnation episodes and to investigate possible source areas. This study successfully investigated the spatial and temporal behavior of $PM_{2.5}$ during numerous episodes. During this 181 day study which occurred from October 31, 2008 to April 30, 2009, we quantified over 63 episodes where the hourly $PM_{2.5}$ concentration exceeded 30 $\mu g/m^3$ over one or more hours with winds less than 2 mph (0.89 m/s). During the study the NMED Air Quality Bureau sites did not exceed the EPA 24-hour National Ambient Air Quality Standard of 35 $\mu g/m^3$ for particles with aerodynamic diameter 2.5 µm or less ($PM_{2.5}$). The highest $PM_{2.5}$ measured at the Sunland Park City Yard site was 30.8 $\mu g/m^3$, 88 percent of the standard. However, four exceedances of the standard were observed at the saturation sites in New Mexico. Exceedances occurred at Ardovino's (Dec. 16, 2008), Dona Ana Community College (Dec. 25, 2008), Riverside Elementary (Feb. 25, 2009) and at the Sunland Park Race Track (April 28, 2009). The majority of the episodes occurred during the hours between 18:00 and 20:00 MST. Episodes occurred on average every 3 days and varied in duration between one and nine hours and often went past midnight. Historical $PM_{2.5}$ measurements from the NMED Air Quality Bureau sites indicate that the annual 15 $\mu g/m^3$ standard will not be exceeded. While a few $PM_{2.5}$ concentrations have exceeded the 24-hour standard during spring and winter, their number so far is not sufficient to cause non-attainment of the 24-hour standard in the near future.

Airmass backtrajectories have proven to be useful tools in exploring locations of sources and where those emissions are being transported. In this study we have compared a commonly used meteorological input with measurements in an area of complex terrain. For this small region, single station wind fields used in the trajectory model have shown better agreement with wind measurements observed during this study. We acknowledge that a spatially homogeneous wind field based on a single station is not the best choice, we demonstrate that useful information about air mass trajectories for short distances can be obtained. Using the backtrajectory model for six episodes, we isolated a source area south of Sunland Park within a distance of around 3 to 4 kilometers. Based on this effort, the locations of particulate emission sources leading to the low-wind exceedances can be localized in this area.

Table of Contents

List of Figures

List of Tables

Acronyms

BAM	Beta Attenuation Monitor
CD	Central Database
COD	Coefficient of Divergence
DRI	Desert Research Institute
EC	Elemental Carbon
EDAS	Eta Data Assimilation System
EMNRD	Energy, Minerals and Natural Resources Division
FAA	Federal Aviation Authority
GIS	Geographic Information System
GPS	Global Positioning System
HYSPLIT	HYbrid Single-Particle Lagrangian Integrated Trajectory model
IMPROVE	Interagency Monitoring of Protected Visual Environments
MM5	Mesoscale Meteorological model version 5
NAM	North American Model
NMED, AQB	New Mexico Environment Department, Air Quality Bureau
NOAA	National Oceanic and Atmospheric Administration
NOx	Nitrogen oxides
O_3	Ozone
OC	Organic Carbon
PAHs	Polycyclic Aromatic Hydrocarbons
PdN	Paso del Norte
PM_{10}	Particles with aerodynamic diameter 10 µm or less
$PM_{2.5}$	Particles with aerodynamic diameter 2.5 µm or less
PMF	Positive Matrix Factorization
QA	Quality Assurance
SOA	Secondary Organic Aerosol
SOP	Standard Operation Procedure
TBD	To be determined
TCEQ	Texas Commission on Environmental Quality
TEOM	Tapered Element Oscillating Microbalance
USEPA	United States Environmental Protection Agency
UTC	Coordinated Universal Time
UTEP	University of Texas at El Paso
VOC	Volatile Organic Compounds
WRF	Weather Research and Forecasting model

1 Introduction

1.1 Sunland Park and Air Quality

The Paso del Norte (PdN) region is situated at the intersection of three states (Texas, New Mexico, and Chihuahua), between the Franklin Mountains to the north and Sierras de Juárez to the south, with the Rio Grande River being the border between the U.S. and Mexico and elevations ranging from 3,773 feet at the Rio Grande bed to 6,070 feet at Range Peak. The cities of El Paso in Texas, Las Cruces in New Mexico, and Ciudad Juárez in Chihuahua, with a combined population of approximately 2.25 million people, are located within the boundaries of PdN. The region also encompasses smaller towns and communities. El Paso is located on the southwest tip of the State of Texas. The city's elevation is 3,800 feet above sea level and covers a total area of 250.5 square miles. The population of El Paso was about 736,310 in 2006, with a density of 2,939 people per square mile. Las Cruces is located in Doña Ana County, New Mexico, in the Mesilla Valley, east of the Rio Grande River. The city covers an area of 52.11 square miles. The estimated population for 2007 was 89,722, with a population density of 1,725 people per square mile (550.5/km^2). The estimated population of Ciudad Juárez is about 1.5 million people, and this urban area is expanding at a higher rate than the rest of Mexico.

There are two distinct regimes of degraded air quality in the region's conceptual model. The first occurs when great quantities of dust are lifted from the earth's surface during high winds events. These dust storms occur annually mainly during the spring and many are regional in extent. The second condition, and the focus of this study, occurs when winds are low and temperature inversions trap pollutants into air basins. The most noticeable low wind high pollutant events are observed near the highly urbanized areas along the border. These air stagnation events can occur anytime of the year but have the most impact during the colder months of December through February. During these low wind events, particulate emissions are found from unpaved roads, residential heating, brick kilns, open burning as well as gas phase organic compounds from combustion sources.

Based on past field studies (Li et al., 2001) and routine continuous PM_{10} and $PM_{2.5}$ compliance monitors in the area, most of the particulate is composed of geologic materials with the $PM_{10\text{-}2.5}$ size fraction dominating the total PM_{10} mass. Li et al. conducted a seven month measurement study of particulate in the Paso del Norte and found that approximately 25 percent of the PM_{10} is in the $PM_{2.5}$ size range. Complex terrain in the area defines the flow of pollutants during the evening. Cooler air flows down from higher to lower terrain and travels along ravines and natural drainage patterns toward the Rio Grande River channel. This event is most evident at the southernmost New Mexico monitoring site in the Paso del Norte airbasin. At the Sunland Park City Yard monitoring site, hourly PM_{10} and $PM_{2.5}$ regularly increase rapidly after sunset but decrease by midnight. At this site, unpaved roads and various combustion activities from south of the border are the suspected contributors. A study to characterize wind patterns during the summer of 1994 using a lidar, found plumes of particulate matter, flowing from higher to lower elevation, coming from Mexico in the morning (Barr et al., 1994). During that study, they observed morning mixing heights on the order of 200 meters and increasing throughout the day to between 3000 and 4000 meters by mid-afternoon.

1.2 Sources of $PM_{2.5}$

Road dust from unpaved and paved roads constitutes as one of the most important sources of PM_{10} and $PM_{2.5}$ in the Paso del Norte. A recent emission inventory for Cd. Juárez estimated 26 percent of the annual $PM_{2.5}$ emissions come from unpaved roads (PNEG, 2003). In Ciudad Juárez, unpaved road dust is a critical issue since many busy urban roads are unpaved (~ 50%) and paving has not kept up with the urban sprawl toward the city flanks. Approximately half a million vehicles (passenger cars and trucks) are registered in each city with nearly 50,000 vehicles crossing the U.S.-Mexican border into El Paso each day (US BTS, 2009).

Dust emissions from agricultural activities are expected to be the greatest between January and March when major land preparation activities occur in the Mesilla Valley and areas south of El Paso on both sides of the border. The figure below shows the locations of some of these sources based on digital landuse data, aerial photo interpretation and tabular data from annual reports (EMNRD, 2001; Orris, 2000; Pfeil, 2001; DuBois, 2003).

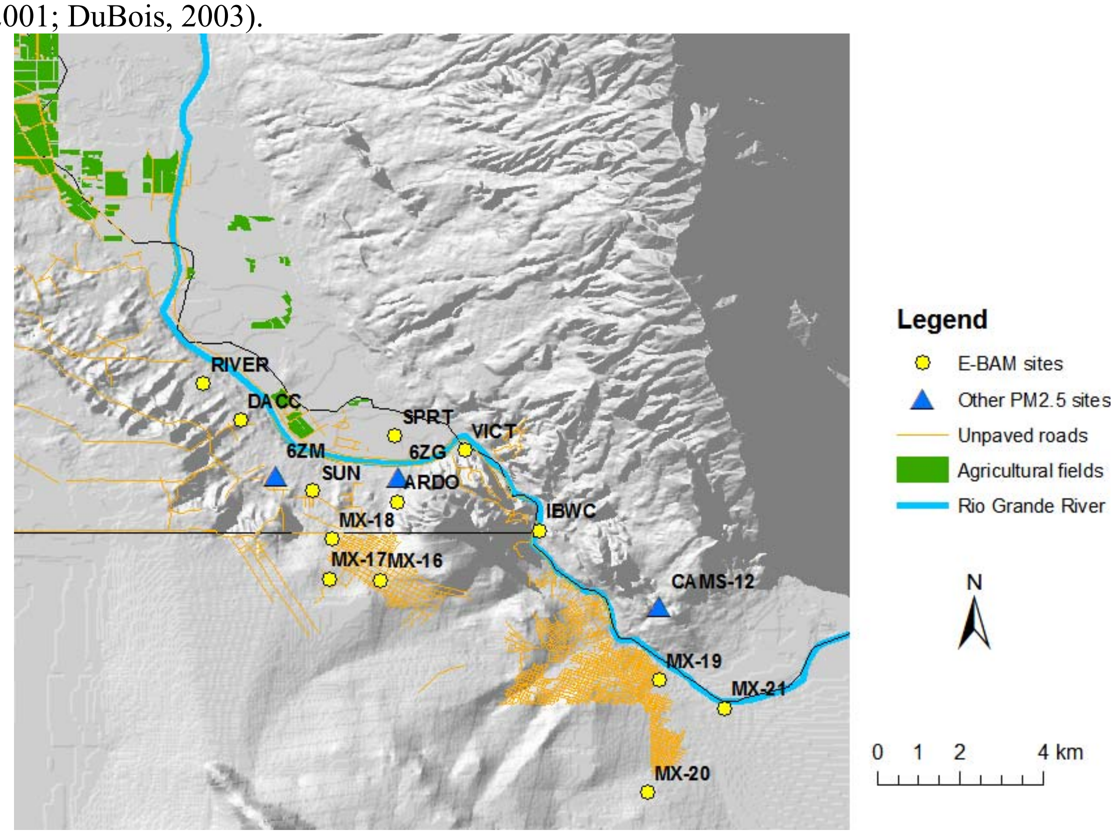

Figure 1-1. Sources of fugitive dust near the saturation sampling network.

Locations of unpaved roads and agricultural fields were estimated based on manual interpretation of aerial photos from 2001. The gap in coverage of unpaved roads in Figure 1-1 is based on the missing aerial photos for that area.

Unpaved road dust can be a significant contributor to the overall PM especially during agricultural harvests when vehicles travel down the numerous farm roads. Most urban roads are paved but many small settlements or colonias have unpaved roads with little or no dust control.

Particulates from combustion sources have been detected at urban and non-urban receptors throughout the year, but they are most abundant during the wintertime holiday season at urban sites. Particulates from residential heating account for as much as 44 percent of the annual $PM_{2.5}$ in Cd. Juárez. Small space heaters are widely used in Cd. Juárez in the cool months in homes without central heating. Some of these heaters are fueled by propane but still many are fueled with wood or other combustibles and can include refuse. As much as 60 percent of the lower income family houses use an unvented gas space heater or wood burning heater (Graham et al., 2004, 2005). As in many areas in the west, spatially dense monitoring studies have shown that the residential wood smoke contributions are more variable in space than motor vehicle exhaust emissions, with much higher contributions in residential neighborhoods than in commercial districts just a few kilometers away.

Atmospheric oxidation reactions of nitrogen oxides ($NO + NO_2 = NO_x$), sulfur dioxide (SO_2), and volatile organic compounds (VOCs) during winter contribute to the formation of condensable nitrate (NO_3^-), sulfate (SO_4^{2-}), and organic compounds that, under certain meteorological conditions, favor the formation of new particles with aerodynamic diameters less than 2.5 µm. Onroad and nonroad mobile sources are a significant source of NOx in the Paso del Norte air basin. Sulfur dioxide and oxides of nitrogen emissions are most intense along the major roadways, as well as in population centers where many vehicle miles are logged each day. Particulate matter emissions are largest in the population centers and are minor at the point source locations.

1.3 Project Objectives

The objectives of this effort were to examine temporal variations and spatial patterns in particulate mass around Sunland Park, New Mexico and to identify potential emission source locations contributing to the particulate matter spikes during low wind periods. The project made use of hourly $PM_{2.5}$ from MetOne E-BAM instruments and meteorological data surrounding the Sunland Park area obtained from a 13 site saturation monitoring network operated from November 2008 to April 2009.

2 Methods

This section presents information on data availability, data sources, quality checks and the components of the central database (CD).

2.1 Data

Table 2-1 shows the locations and names of the sampling sites investigated in this study. In total there were 13 saturation $PM_{2.5}$ sampling sites in operation. Seven of the sites were in New Mexico and the remainder in various locations in Ciudad Juárez. The network covered an area of about 104.7 km^2 (40.4 mi^2). The nearest saturation site to the Sunland Park City Yard (SPCY) was ARDO at 0.6 km south. Five of the saturation sites were within 2 km of the SPCY site. The furthest site from SPCY was the MX-20 site at 9.1 km in the easterly direction. Site elevations ranged from a low of 1125 m at MX-21 to a high of 1240 m at MX-17. The SPCY site sits at an elevation of 1142 m and the Desert View site is at 1170 m. To help define $PM_{2.5}$ gradients and wind patterns within the Paso del Norte, 6 additional existing sites were chosen. Five of those were located in the City of El Paso and one in Ciudad Juárez. Photos of each site and its surroundings are provided in Appendix A.

2.1.1 Data Completeness

Table 2-2 shows the dates that each site collected data. All sites were terminated on April 30, 2009 but not all sites were started at the same time. Three sites with the longest record are ARDO, RIVER and DACC at 182 days. The VICT site had the shortest record at 107 days since it started on January 13, 2009.

Table 2-1. Locations of PM_{10}, $PM_{2.5}$ and meteorological monitoring sites

Code	Description	AIRS Code	Country	State	County	City	Latitude	Longitude	Agency
	$PM_{2.5}$ Saturation Network Sites								
IBWC	International Boundary and Water Commission		USA	Texas	El Paso	El Paso	31.784361	106.52711	
SPRT	Sunland Park Race Track		USA	New Mexico	Dona Ana	Sunland Park	31.804722	106.55825	
ARDO	Ardovino's Restaurant		USA	New Mexico	Dona Ana	Sunland Park	31.790500	106.55772	
RIVER	Riverside Elementary School		USA	New Mexico	Dona Ana	Sunland Park	31.816056	106.59958	
DACC	Dona Ana Community College		USA	New Mexico	Dona Ana	Las Cruces	31.808111	106.59150	
SUN	Sunland Park Elementary School		USA	New Mexico	Dona Ana	Sunland Park	31.792861	106.57594	
VICT	Victoria Templo Anapra Church		USA	New Mexico	Dona Ana	Sunland Park	31.801611	106.54314	
MX-16	Central de Bomberos de Anapra		Mexico	Chihuahua		Anapra	31.773683	106.56134	
MX-17	Materiales La Mas Barata No. 4		Mexico	Chihuahua		Anapra	31.773908	106.57227	
MX-18	Iglesia Anglicana de San Jose de Anapra		Mexico	Chihuahua		Anapra	31.782611	106.57180	
MX-19	Maquiladora ACS		Mexico	Chihuahua		Juárez	31.752222	106.50111	
MX-20	Secundaria Federal No. 3		Mexico	Chihuahua		Juárez	31.728056	106.50361	
MX-21	Estacion de Bomberos		Mexico	Chihuahua		Juárez	31.746111	106.48722	
	Existing Network Sites								
6ZG	Sunland Park - City Yard	350130017	USA	New Mexico	Dona Ana	Sunland Park	31.79583	106.55750	NMED - AQB
6ZM	Sunland Park - Desert View Elementary School	350130021	USA	New Mexico	Dona Ana	Sunland Park	31.79611	106.58389	NMED - AQB
C12	El Paso UTEP	481410037	USA	Texas	El Paso	El Paso	31.76805	106.50111	TCEQ Reg 6
C41	Chamizal	481410044	USA	Texas	El Paso	El Paso	31.76555	106.45500	TCEQ Reg 6
C413	Tillman	481410002	USA	Texas	El Paso	El Paso	31.75750	106.48277	City of El Paso
C414	Ivanhoe	481410029	USA	Texas	El Paso	El Paso	31.78638	106.32416	City of El Paso
C415	Moon City	481410050	USA	Texas	El Paso	El Paso	31.67277	106.28416	City of El Paso
C662	Cd Juárez 20-30 Club	800060006	Mexico	Chihuahua		Juárez	31.73555	106.45972	Ciudad Juárez Health Dept

Table 2-2. Measured parameters and completeness of hourly data for each site

Code	Monitoring Period	PM_{10}	$PM_{2.5}$	Wind conditions	Other
	$PM_{2.5}$ Saturation Network Sites				
IBWC	Nov. 13, 2008 – Apr. 30, 2009		x	x	
SPRT	Nov. 13, 2008 – Apr. 30, 2009		x	x	
ARDO	Oct. 30, 2008 – Apr. 30, 2009		x	x	
RIVER	Oct. 30, 2008 – Apr. 30, 2009		x	x	
DACC	Oct. 30, 2008 – Apr. 30, 2009		x	x	
SUN	Nov. 13, 2008 – Apr. 30, 2009		x	x	
VICT	Jan. 13, 2009 – Apr. 30, 2009		x	x	
MX-16	Nov. 18, 2008 – Apr. 30, 2009		x	x	
MX-17	Nov. 18, 2008 – Apr. 30, 2009		x	x	
MX-18	Nov. 18, 2008 – Apr. 30, 2009		x	x	
MX-19	Nov. 18, 2008 – Apr. 23, 2009		x	x	
MX-20	Nov. 18, 2008 – Apr. 23, 2009		x	x	
MX-21	Dec. 01, 2008 – Apr. 30, 2009		x	x	
	Existing Network Sites				
6ZG	Oct. 29, 2008 – Apr. 30, 2009	x	x	x	x
6ZM	Oct. 29, 2008 – Apr. 30, 2009	x	x	x	x
C12	Oct. 01, 2008 – Apr. 30, 2009	x	x	x	x
C41	Oct. 01, 2008 – Apr. 30, 2009	x	x	x	x
C413	Oct. 01, 2008 – Apr. 30, 2009			x	x
C414	Oct. 01, 2008 – Apr. 30, 2009			x	x
C415	Oct. 01, 2008 – Apr. 30, 2009			x	x
C662	Oct. 01, 2008 – Apr. 30, 2009			x	x

2.1.2 Quality Control

Table 2-3 shows the percent of valid hourly $PM_{2.5}$ concentrations after removing the flagged data. Hourly data was flagged if concentrations during an individual hour were negative or if the sampler flow was more than 5% of the reference flow rate of 16.7 liters per minute. Saturation sites with the most valid hourly $PM_{2.5}$ include IBWC (95%), MX-17 (90%) and MX-20 (89%).

Table 2-3. Measured parameters and completeness of hourly data for each site. Concentrations are rounded to the nearest $\mu g/m^3$

Code	N_{valid} for $PM_{2.5}$	% valid $PM_{2.5}$
IBWC	3824	95
SPRT	3513	83
ARDO	3432	79
RIVER	3384	78
DACC	3103	71
SUN	3559	84
VICT	2124	83
MX-16	3265	83
MX-17	3529	90
MX-18	3388	87
MX-19	3069	82
MX-20	3334	89
MX-21	2943	82
6ZG	3976	91
6ZM	4121	94
C12	4963	98
C41	4993	98

Note that in the above table the VICT site started much later than the remaining sites resulting in a smaller sample size.

Deviations of the sampling flow rate of BAM monitors were recorded during the study that influence the performance of $PM_{2.5}$ sharp-cut cyclone and the measurement of $PM_{2.5}$ mass. For this reason, the performance of the $PM_{2.5}$ cyclone was evaluated based on the calibration curve provided by the manufacturer and the $PM_{2.5}/PM_{10}$ ratio. We did not assess the influence of flow rate on the performance of PM10 sampling inlet, because possible artifacts did not have an immediate effect on $PM_{2.5}$ measurements.

Figure 2-1 shows the estimated cut-point for the BGI $PM_{2.5}$ SCC using the equation provided from the manufacturer (D_{50}=64.73 $Q^{-1.1566}$). The cut-point of the cyclone for a decrease of the flow rate by 5 percent was 2.65 µm (a difference of 6 percent from the design value of 2.5), while a flow rate deviation of 10 percent will allow the penetration of particles with diameter up to 2.82 µm (a difference of 13 percent). In addition, lower flow rate also influences the sharpness of the curve (less steep curve) that result in the penetration of larger particles.

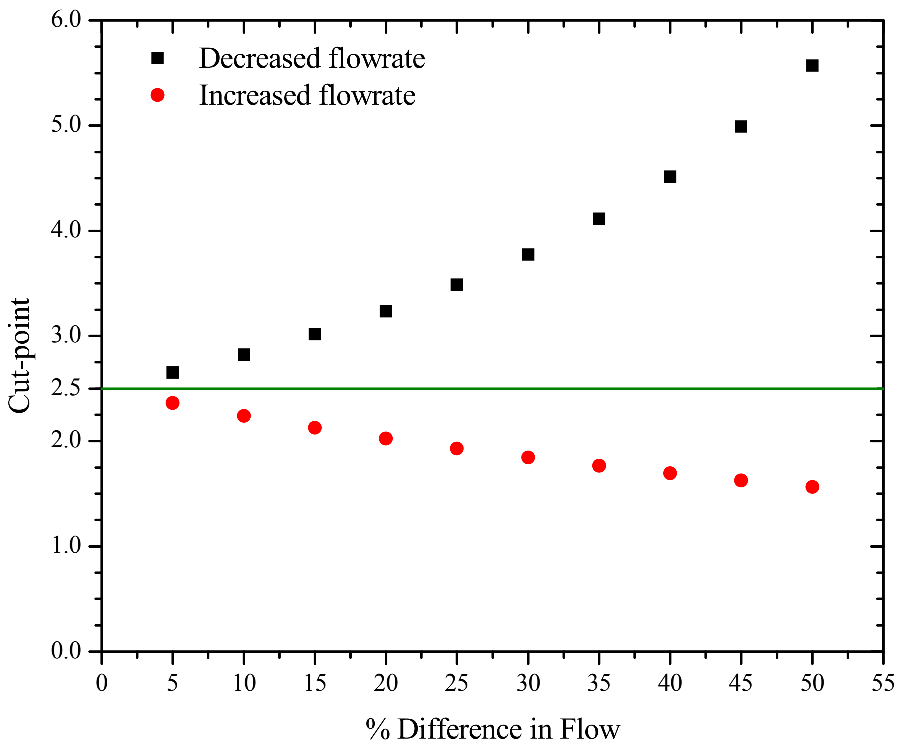

Figure 2-1. Estimated cyclone cutpoint for flowrate deviations from ±5 to ±50 percent

Table 2-4 shows the mean hourly $PM_{2.5}/PM_{10}$ ratios in 6ZG and 6ZM sites in New Mexico and C12 and C41 in El Paso, Texas using TEOM. For all locations, coarse particles ($PM_{10-2.5}$) represented from 75 percent to about 90 percent of PM_{10}. These values indicated that sampling artifacts (e.g low flowrates) that influence the cutpoint of the $PM_{2.5}$ cyclone (i.e. higher cutpoint) may result in inadequate classification of particles and significant impacts on measured $PM_{2.5}$ mass concentrations.

Table 2-4. Mean $PM_{2.5}/PM_{10}$ ratios in the study area

Monitoring site	Mean (± Standard error) 1-hr $PM_{2.5}/PM_{10}$
6ZG	0.12 ± 0.01
6ZM	0.11 ± 0.01
C12	0.22 ± 0.02
C41	0.23 ± 0.01

Overall, while the number of particles that may be misclassified because of changes of the cyclone cutpoint is strongly related to the size distribution of particulate matter (was not measured in this study), it is reasonable to assume that for low $PM_{2.5}/PM_{10}$ ratios, a large error may be introduced to $PM_{2.5}$ measurements when flowrate deviates more than 5 percent. To minimize this artifact, $PM_{2.5}$ mass measurements in which flowrate was higher than 17.5 liters/min or lower than 15.3 liters/min were excluded from the analysis. However, these data are flagged and included in the central database.

2.2 Database Development

The following table shows the data fields in the master database.

Table 2-5. Master database field description

Site ID	Site ID (see code names in Table 2-1)
Datetime	Date and time (mm/dd/yyyy hh:mm)
Date_mmddyyyy	Date (mm/dd/yyyy)
Time_hhmm	Time (hh)
PM10 (µg/m3)	PM_{10} mass concentration (µg/m^3)
PM25mass_ugm3	$PM_{2.5}$ mass concentration (µg/m^3)
PM25Monitor	Type of $PM_{2.5}$ monitor (TEOM or BAM)
Windspeed_ms	Wind speed (m/s)
Winddirection_degrees	Wind direction (degrees)
Temperature_C	Ambient Temperature (^{o}C) measured at BAM locations
Relativehumidity_%	Relative humidity (%)
Solar (w/m2)	Incoming solar radiation (W/m^2)
T2m (C°)	Ambient Temperature (^{o}C) measured at 2 meters
T10m (C°)	Ambient Temperature (^{o}C) measured at 10 meters
DeltaT (C°)	Difference of Temperature (^{o}C) measured at 2 and 10 meters
Sigma Deg	Wind direction deviation (degrees)
WSmax (m/s)	Maximum wind speed (m/s)
NOX ppm	NOx concentration (ppm)
NO ppm	NO concentration (ppm)
NO2 ppm	NO2 concentration (ppm)
O3 ppm	O3 concentration (ppm)
Flag_flow	Flow flag (CXX where XX denotes the percentage deviation)
flagflow	1=flow deviation more than 10%; 0=flow deviation less than 10%

Flagnegconc	1=Negative P2.5 mass concentration; 0=Non-Negative P2.5 mass concentration
Flagless18	1=Day with less than 18 valid hourly measurements; 0=Day with more than 18 valid hourly measurements
Flagmore8negs	1=Day with more than 8 negative PM2.5 mass measurements; 0=Day with less than 8 negative PM2.5 mass measurements

3 Results

This section presents the descriptive statistics and time series of $PM_{2.5}$ (and PM_{10}) mass concentrations and meteorological conditions collected in the Sunland Park, Ciudad Juárez and El Paso, Texas.

3.1 PM_{10} and $PM_{2.5}$ Mass Concentrations

While there are no National Ambient Air Quality Standards for hourly PM_{10} or $PM_{2.5}$, it is useful to examine them as a way to understand the nature of the sources and variations that contribute to the 24-hour averages. Table 3-1summarizes hourly $PM_{2.5}$ along with the mean and median concentrations for all sites during this study. This table clearly shows much higher hourly $PM_{2.5}$ in the Ciudad Juárez sites compared to site in New Mexico and in El Paso.

Table 3-1. Maximum, Mean and Median hourly $PM_{2.5}$ measured at each site. Concentrations are rounded to the nearest $\mu g/m^3$ to allow for easier comparison between sites

Code	Max $PM_{2.5}$	Mean $PM_{2.5}$	Median $PM_{2.5}$
IBWC	184	12	9
SPRT	194	14	10
ARDO	844	10	7
RIVER	145	9	7
DACC	1189	12	7
SUN	234	10	7
VICT	125	11	9
MX-16	2417	27	14
MX-17	734	23	15
MX-18	759	18	10
MX-19	342	21	11
MX-20	444	21	11
MX-21	469	20	13
6ZG	184	10	6
6ZM	76	7	5
C12	90	9	7
C41	99	9	7

Figure 3-2 and Figure 3-4 show the box plots of 24-hr $PM_{2.5}$ mass concentration measured at two monitoring sites in Sunland Park, New Mexico (6ZG and 6ZM) and two monitoring sites in El Paso, Texas (C12 and C41) using TEOM monitors, respectively. In addition, the levels of 24-hr PM mass concentrations measured at seven locations in New Mexico and six locations in Ciudad Juárez, Mexico using BAM monitors are presented in Figure 3-3. The boxes represent the 25%, 50% (median) and 75% percentiles, and whiskers show the 5% and 95% percentiles. The open squares show the mean value. The "x" show the 1st and 99th percentile while the "-" denote the maximum and minimum values.

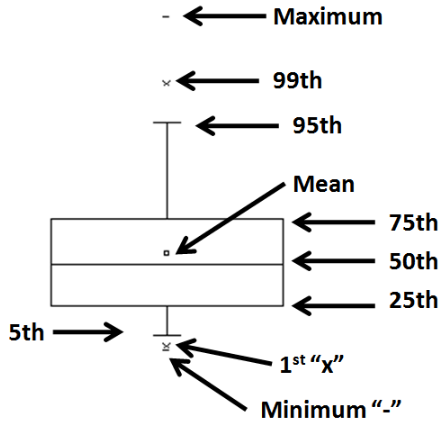

Figure 3-1. Box plot convention showing the various percentiles

Table 3-2 provides a summary of 24-hour averaged or daily $PM_{2.5}$ concentrations throughout the study. Minimum daily $PM_{2.5}$ levels ranged from a 1 to 2 $\mu g/m^3$ at 6ZG and 6ZM to 7.1 $\mu g/m^3$ at MX-21. The maximum daily $PM_{2.5}$ levels ranged from 20.2 $\mu g/m^3$ at 6ZM to 230.3 $\mu g/m^3$ at MX-16. The sites with the most variability were MX-16 and MX-19 with the spread between the 25th and 75th percentile of 15.8 $\mu g/m^3$. In comparison the 25th and 75th percentile differences for 6ZG and 6ZM were 7.3 and 5.2 $\mu g/m^3$.

With respect to the revised 24-hr $PM_{2.5}$ National Ambient Air Quality Standard of 35 $\mu g/m^3$, $PM_{2.5}$ levels were not exceeded the current standard at the 6ZG and 6ZM. The same was true for the two sites (C12 and C41) in El Paso, Texas. However, a total of four exceedances were observed at the supplemental sites in New Mexico using BAM monitors (on December 16, 2008 at ARDO site (54.0 $\mu g/m^3$), on December 25, 2008 at DACC site (36.3 $\mu g/m^3$), on February 25, 2009 at RIVER site (37.7 $\mu g/m^3$) and, on April 28, 2009 on SPRT site (43.2 $\mu g/m^3$)). For sites located in Ciudad Juárez, 24-hr $PM_{2.5}$ mass concentrations were more frequently higher than 35 $\mu g/m^3$ (19 days at MX-16, 13 days at MX-17, 11 days at MX-18, 17 days at MX-19, 19 days at MX-20 and 8 days at MX-21).

Table 3-2. Summary of daily $PM_{2.5}$ concentrations during the study

Statistic	**6ZG**	**6ZM**	**C12**	**C41**	**SUN**	**ARDO**	**DACC**	**IBWC**	**RIVER**	**SPRT**	**VICT**	**MX-16**	**MX-17**	**MX-18**	**MX-19**	**MX-20**	**MX-21**
Mean	10.4	7.1	8.6	9.2	10.3	10.0	11.1	11.8	9.7	14.5	10.7	26.4	22.6	18.0	20.5	20.6	20.8
Standard Dev	6.0	3.8	3.7	4.1	5.5	6.6	5.0	5.4	5.9	6.2	4.0	23.8	10.5	12.3	13.2	15.7	11.1
Minimum	1.7	0.9	2.3	2.5	3.4	4.0	3.8	4.5	3.1	5.7	5.1	6.1	6.1	4.0	5.6	2.4	7.1
5th percentile	3.3	2.0	3.8	4.2	4.4	4.5	5.0	6.1	4.2	7.4	6.0	8.3	10.7	6.3	7.0	7.2	8.9
25th percentile	5.8	4.4	6.0	6.6	6.7	6.3	7.0	7.9	6.1	10.1	7.7	14.6	15.5	10.6	10.5	10.2	12.5
Median	9.2	6.2	8.3	8.4	8.6	7.9	10.0	9.9	8.3	13.4	10.0	20.3	21.0	14.4	17.0	16.0	18.0
75th percentile	13.1	9.6	10.2	11.5	12.4	11.7	13.6	14.6	11.5	17.3	12.8	30.3	28.4	21.5	26.3	25.2	25.6
95th percentile	21.6	13.8	15.8	17.1	21.6	19.2	19.0	23.5	22.6	24.7	17.6	68.5	41.4	41.3	42.5	51.5	44.2
Maximum	38.9	20.2	22.6	23.7	32.4	62.0	28.2	28.7	37.7	50.8	22.2	230.3	72.6	79.9	88.9	90.9	56.9

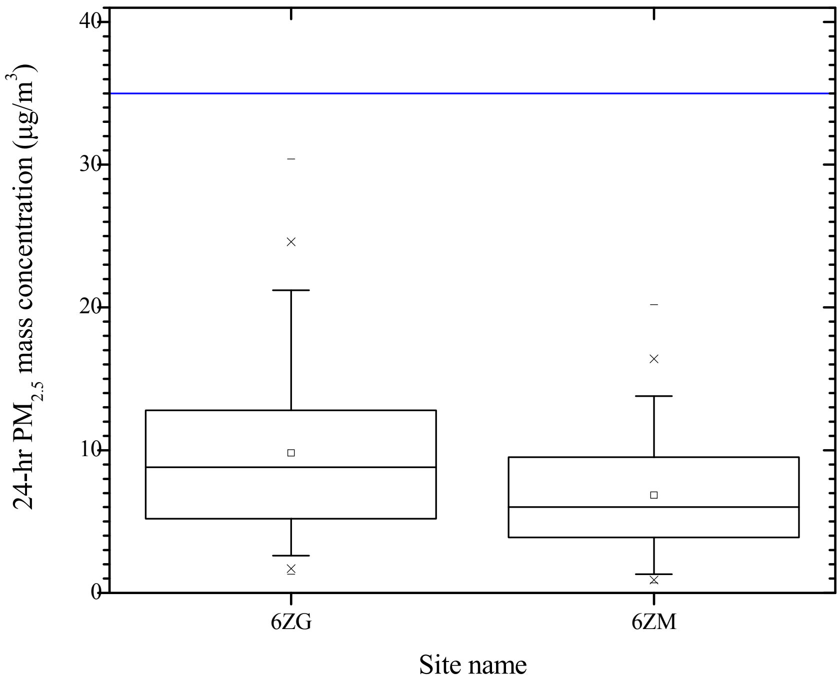

Figure 3-2. Box plots of 24-hr $PM_{2.5}$ mass concentrations at 6ZG and 6ZM sites in Sunland Park, New Mexico measured by TEOM. The blue line shows the 24-hr $PM_{2.5}$ NAAQS of 35 µg/m^3

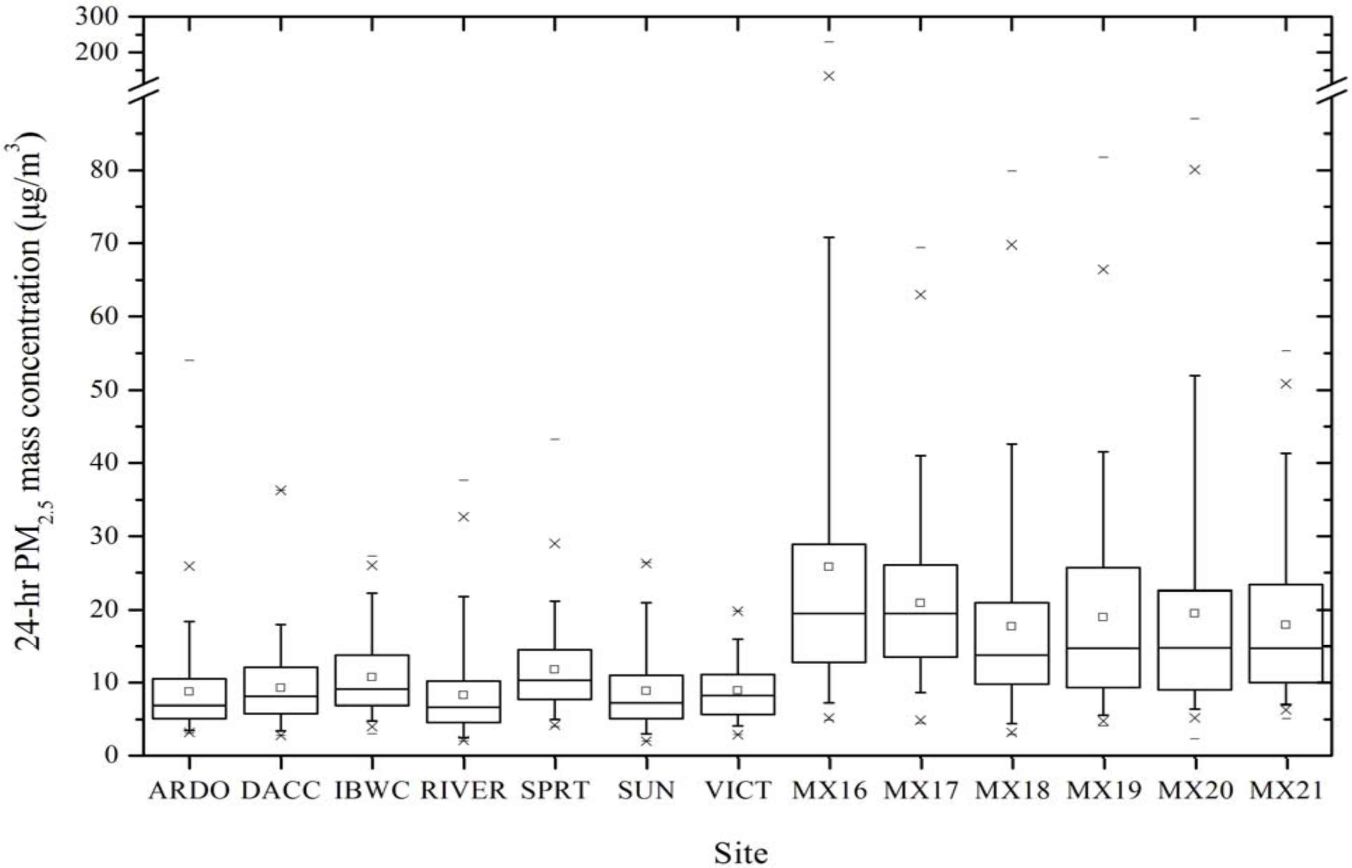

Figure 3-3. Box plot of 24-hr $PM_{2.5}$ mass concentrations at all E-BAM sites

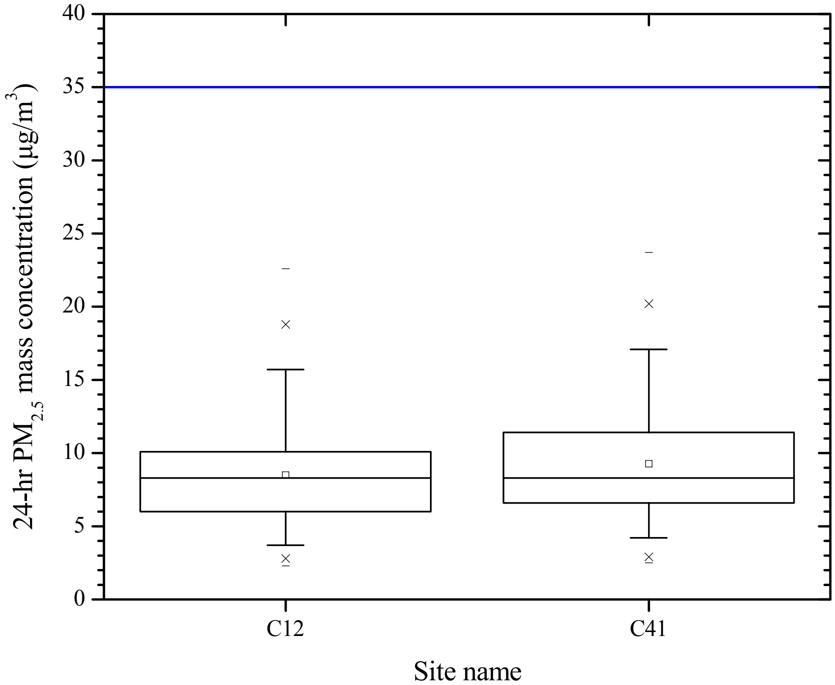

Figure 3-4. Box plots of 24-hr $PM_{2.5}$ mass concentrations at C12 and C41 sites in El Paso, Texas measured by TEOM. The blue line shows the 24-hr $PM_{2.5}$ NAAQS

Figure 3-5 shows the box plots of 24-hr PM_{10} mass concentration measured at two monitoring sites in Sunland Park, New Mexico (6ZG and 6ZM) and two monitoring sites in El Paso, Texas (C12 and C41) using TEOM monitors, respectively. Daily PM_{10} levels at all sites ranged from 8.0 $\mu g/m^3$ to 217.2 $\mu g/m^3$ at 6ZG, from 6.0 $\mu g/m^3$ to 161.1 $\mu g/m^3$ at 6ZM, from 9.0 $\mu g/m^3$ to 91.7 $\mu g/m^3$ at C12 and from 8.5 $\mu g/m^3$ to 94.0 $\mu g/m^3$ at C41, with average concentrations of 67.3 $\mu g/m^3$ at 6ZG, 49.1 $\mu g/m^3$ at 6ZM, 31.6 $\mu g/m^3$ at C12 and 35.3 $\mu g/m^3$ at C41. Comparison of daily PM_{10} and $PM_{2.5}$ mass concentrations (Figure 3-6 and Figure 3-7) showed that coarse particles accounted for the largest fraction of particulate matter in the region.

Figure 3-8 through Figure 3-11 show the time series of $PM_{2.5}$ at locations in Sunland Park, New Mexico, Ciudad Juárez, Mexico and El Paso, Texas. While, a detailed analysis of temporal trends (monthly, day-of-the-week and hourly) are examined in a later section, it appeared that $PM_{2.5}$ concentrations fluctuated a lot during the monitoring period with no clear seasonal trends.

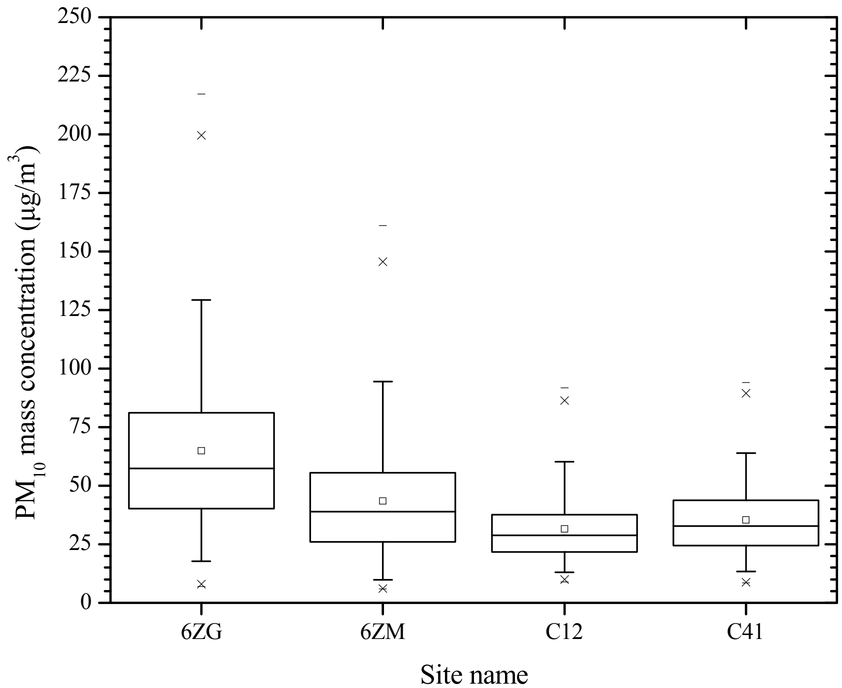

Figure 3-5. Box plots of 24-hr PM_{10} mass concentrations in Sunland Park, New Mexico and El Paso, Texas with TEOM.

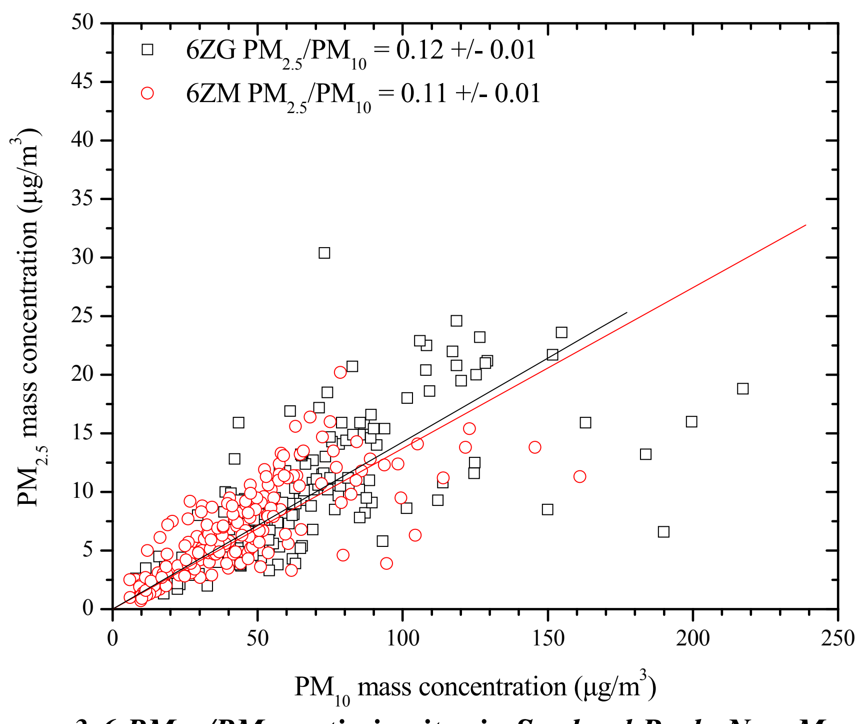

Figure 3-6 $PM_{2.5}/PM_{10}$ ratio in sites in Sunland Park, New Mexico

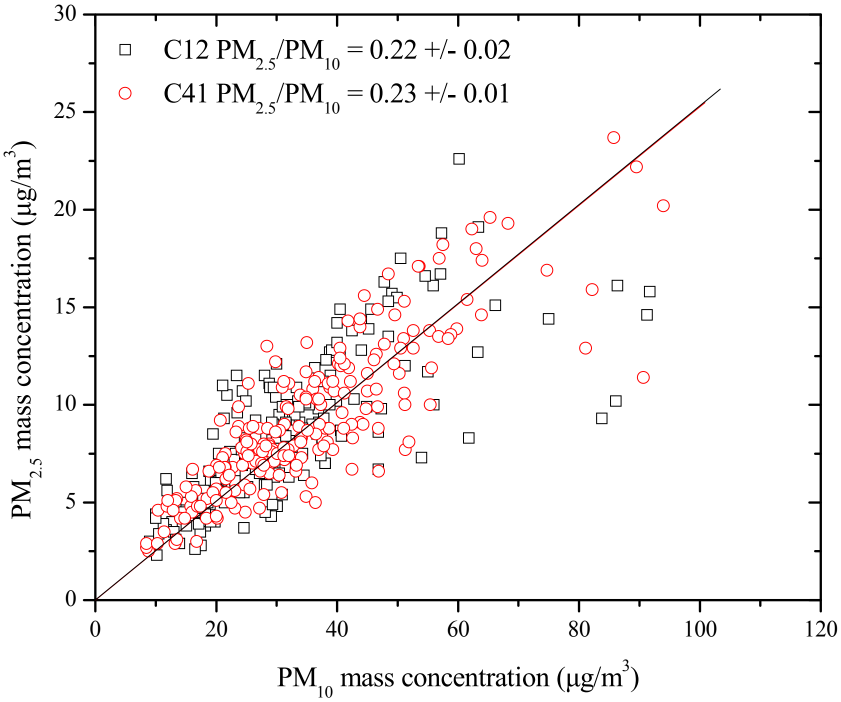

Figure 3-7 $PM_{2.5}/PM_{10}$ ratio in sites in El Paso, Texas

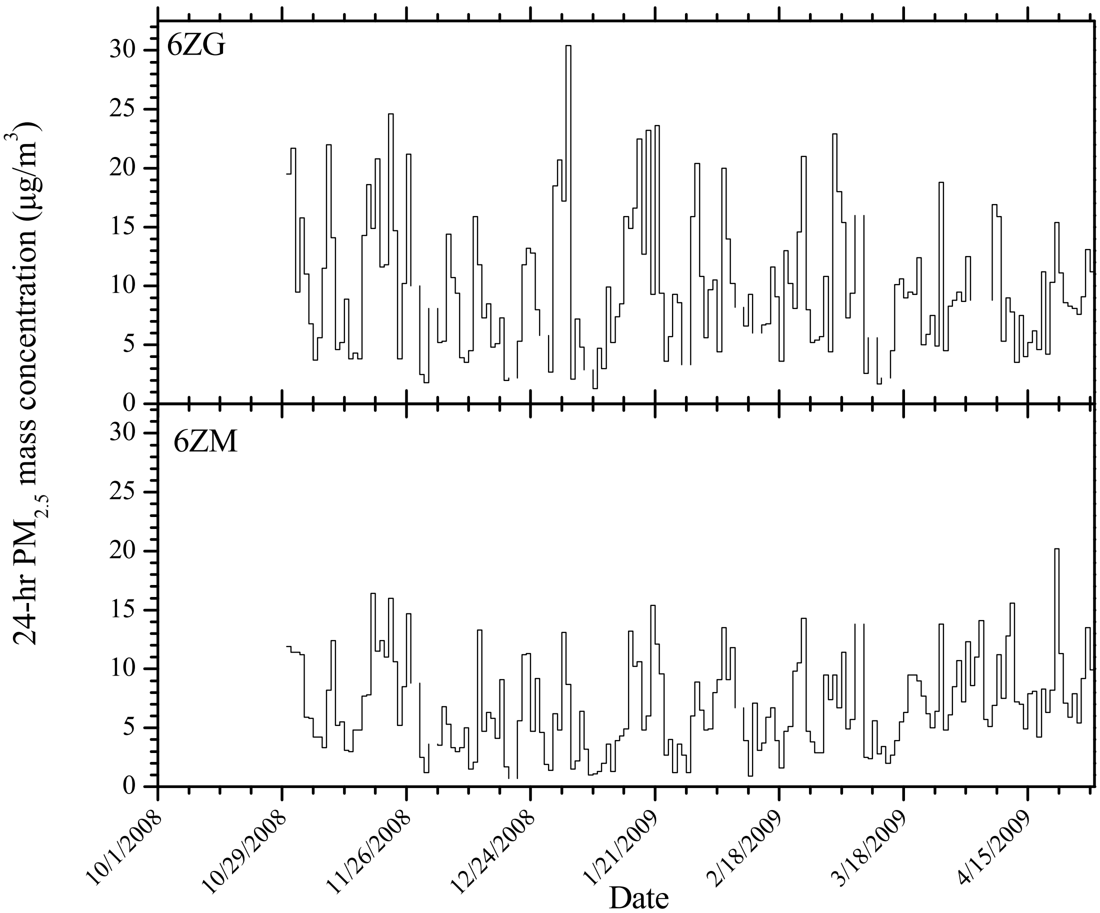

Figure 3-8. Time series of 24-hr $PM_{2.5}$ mass concentrations at the NMED sites as measured by TEOM

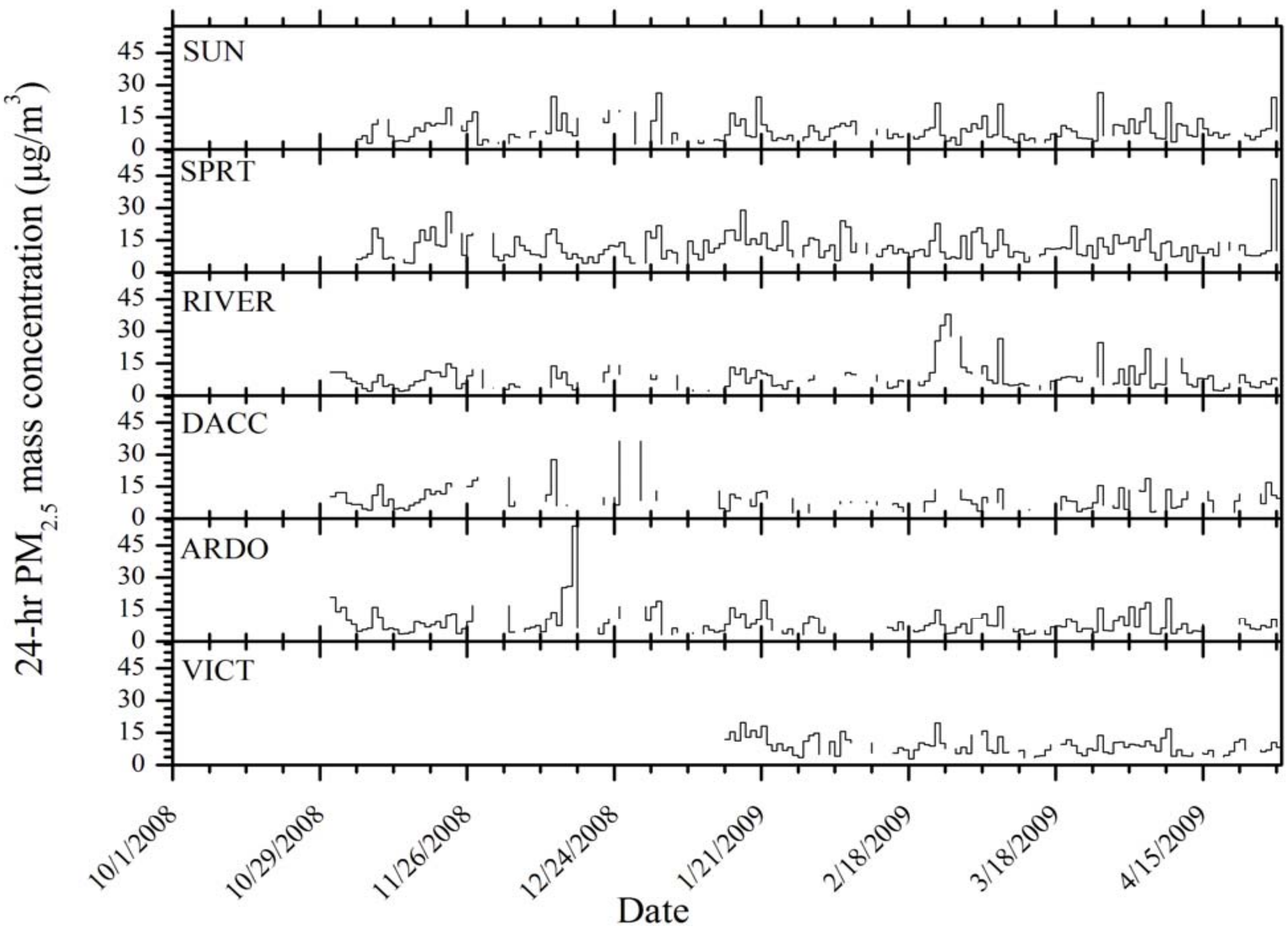

Figure 3-9. Time series of 24-hr $PM_{2.5}$ mass concentrations in New Mexico measured by the E-BAM

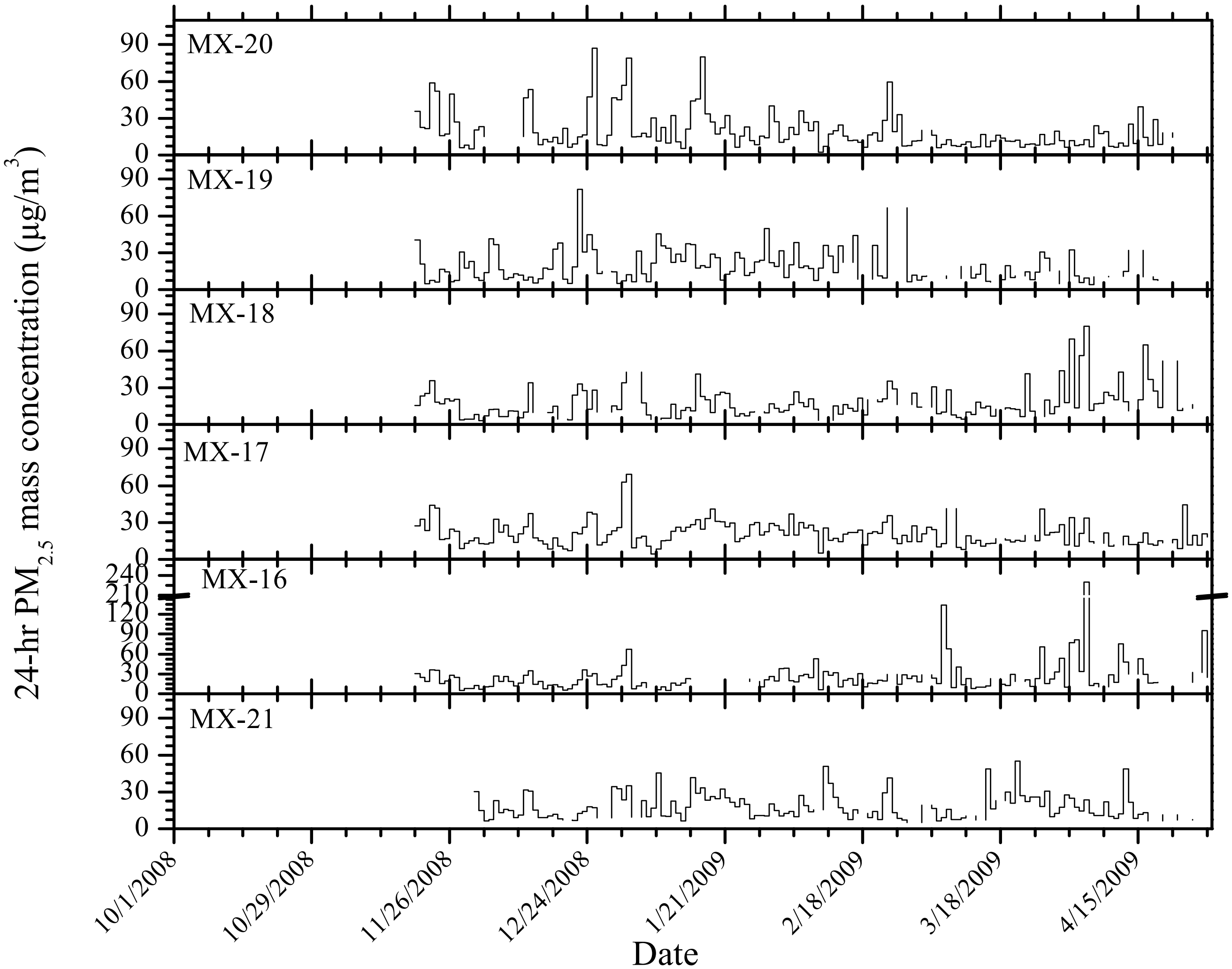

Figure 3-10. Time series of 24-hr $PM_{2.5}$ mass concentrations in Ciudad Juárez, Mexico measured by BAM

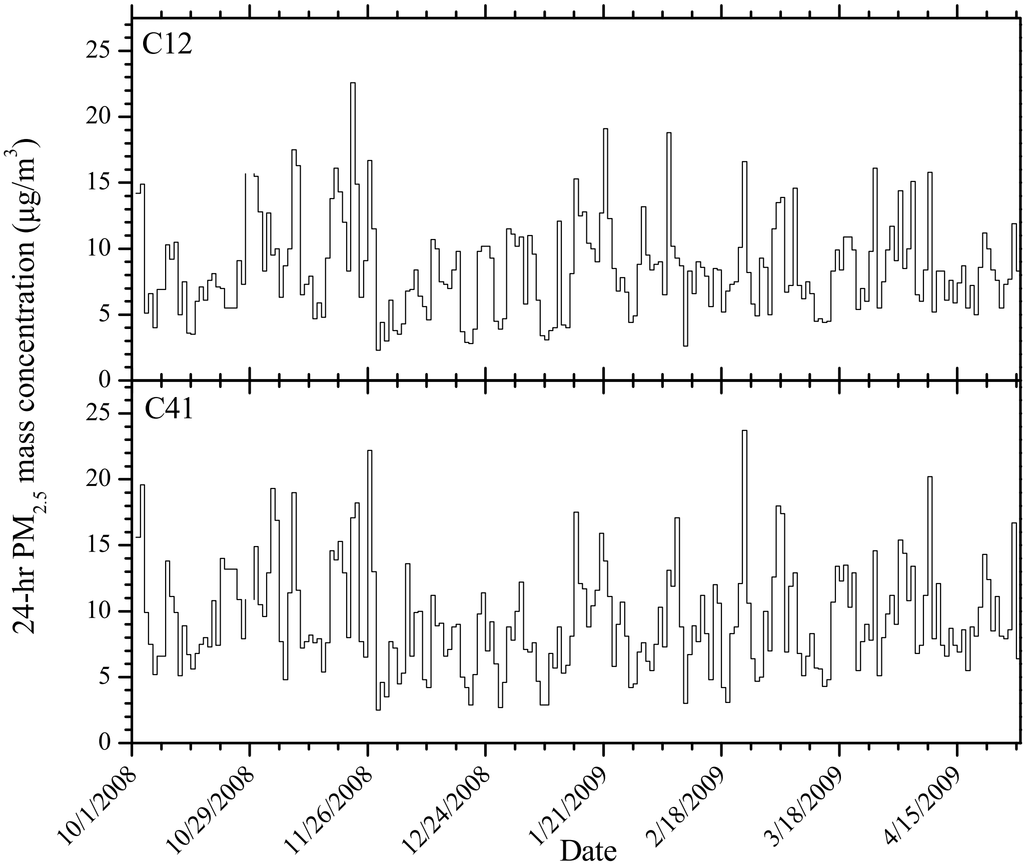

Figure 3-11. Time series of 24-hr $PM_{2.5}$ mass concentrations in El Paso, Texas, measured by TEOM

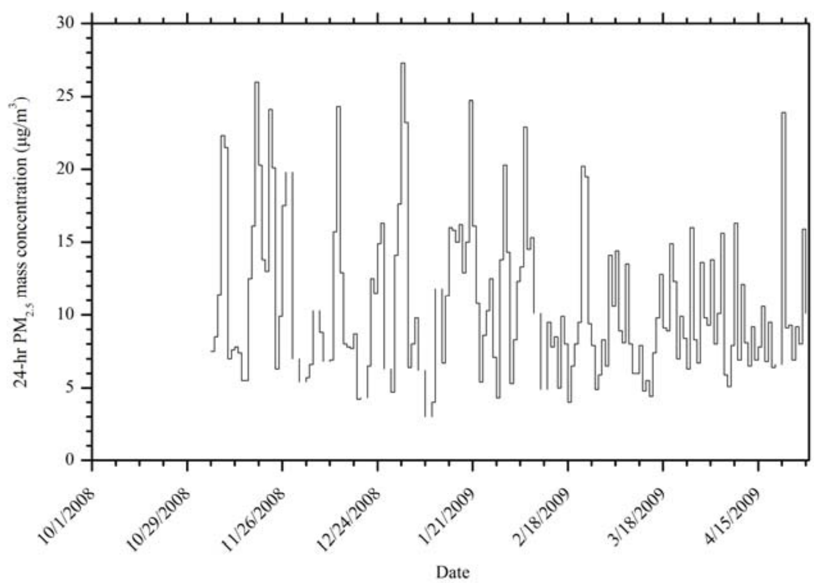

Figure 3-12. Time series of 24-hr $PM_{2.5}$ mass concentrations in El Paso, Texas, measured by E-BAM

3.2 Meteorological Conditions

During periods of stagnation, particulate concentrations are typically at their highest. Stagnations generally occur during high-pressure systems or anticyclones when the sinking air causes a subsidence inversion that can cover a whole region. At night, during conditions of clear skies, nocturnal radiative cooling may also occur and create substantial atmospheric stability. As a result of this stability, temperature inversions form and severely limit dispersions and wind flow. Stagnation conditions can occur over large areas, over distances as much as hundreds of kilometers. As the sun heats the ground, the stagnation condition is reduced by generating turbulent and convective motions that eventually break up the inversion. In some low elevation regions of the U.S., a forecast of stagnation conditions can be generated by the use of air temperatures at the 850 mb pressure height (Smith et al., 1996). A prediction of a warm layer aloft provides enough stability to create a lid to trap surface generated emissions. This method is successful because of the existence of elevated inversion layers that extends up to about 1500 m or at the 850 mb pressure level.
Surface topography plays an important role in determining wind transport directions, frequencies and magnitudes.

Air stagnation events are often correlated with high pressure at the surface and upper level ridges aloft. Figure 3-13 below shows the 500 mb geopotential heights with episodes noted in bold. These heights are indicative of the type of weather system over the area with larger numbers associated with upper level ridges and high pressure at the surface.

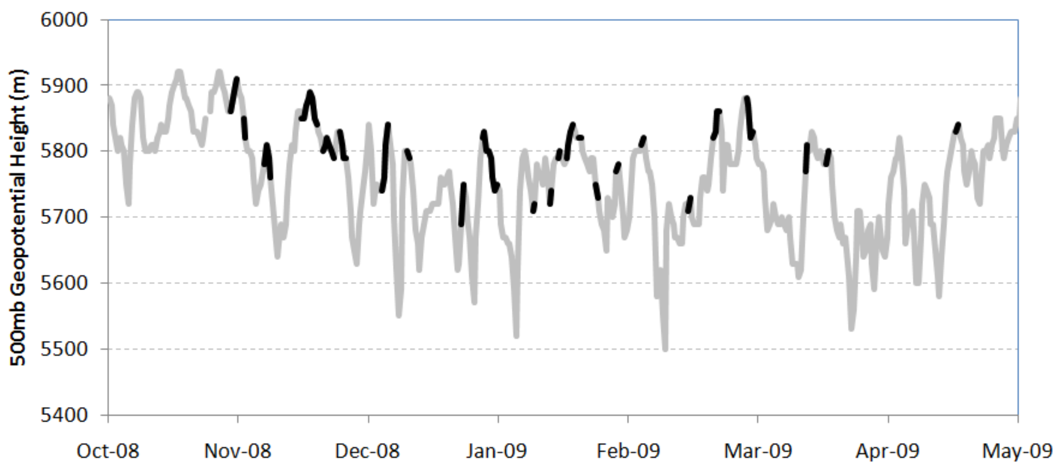

Figure 3-13. Time series of 500mb geopotential heights over the course of the study with episodes indicated in bold

These heights were extracted from radiosonde measurements taken at the Santa Teresa National Weather Service office near the Santa Teresa airport. These radiosonde observations were taken twice a day at 5 am and again at 5 pm. As expected all of the episodes visually occur at or near the peak 500 mb heights using the figure. As stated before, aloft temperatures can be used to find warm layers aloft and possible inversion layers over the area. To examine the efficacy of using geopotential heights and temperatures aloft to predict these high PM events, temperatures at the 700 mb pressure level and 500mb geopotential heights were compared with the hourly $PM_{2.5}$ concentatins at the 6GZ site. The 700 mb pressure height represents an approximate height of 10,000 feet above mean sea level or about 6000 feet above the ground. During stagnant conditions, a warm layer at this height could signal a temperature inversion. By comparing the temperature at this height we investigate this potential relationship. Figure 3-14 shows a summary of a regression analysis.

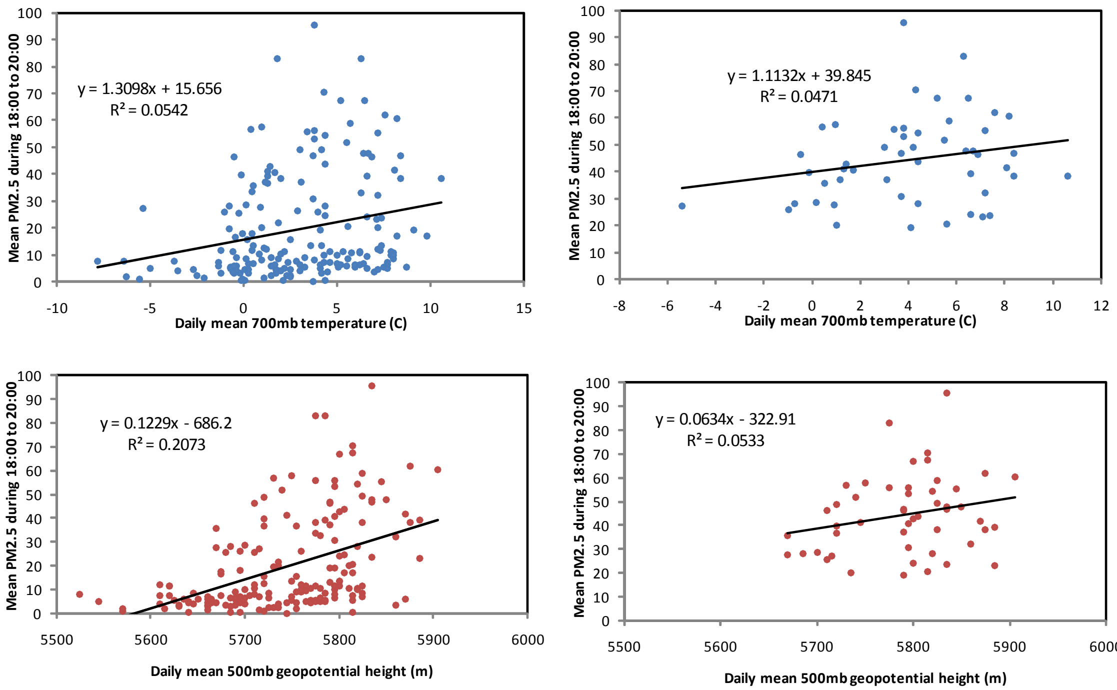

Figure 3-14. Regression plots of low wind PM events with 500mb heights and 700mb temperatures. Left plots are of all hours and the right hand side plots are for only days where an episode occurred.

To make the comparison, mean $PM_{2.5}$ concentrations over the hours from 18:00 to 20:00 MST were used in the calculations since most of the episodes occurred during those hours in the study. For those episodes with hourly $PM_{2.5}$ more than 30 $\mu g/m^3$, the median start hour was 18:00 MST and the median duration was 2 hours. Interestingly, low correlations were seen between $PM_{2.5}$ and both the temperature at 700 mb and 500 mb geopotential heights. Another predictor of high PM episodes is mixing height. Below shows how the mixing height varied throughout the study.

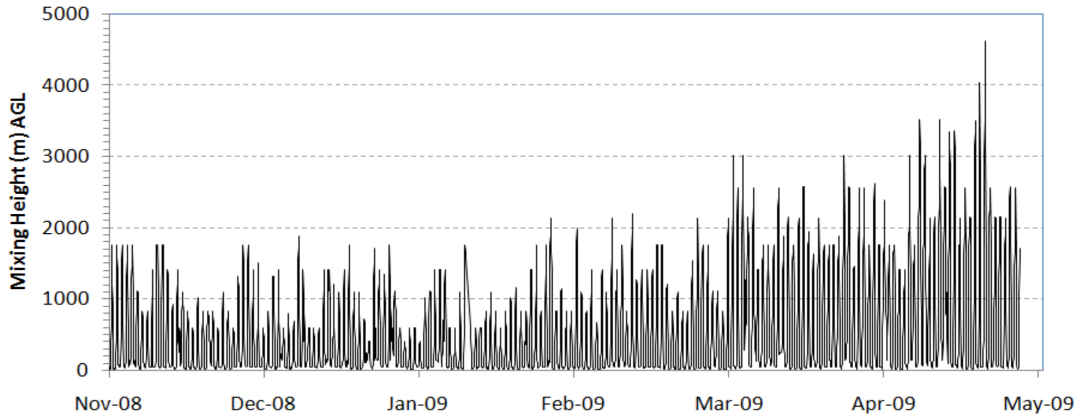

Figure 3-15. Time series of mixing heights during the study

The figure above shows the seasonal change of low mixing heights in the winter and increasing during the spring months. Mixing heights will be used in the episode analysis to offer an explanation of the high PM concentrations and indicate the stability.

3.2.1 Wind Patterns

In regions of complex terrain, such as mountains and valleys, orographic effects may dominate air transport conditions when synoptic flows are minimal. In mountainous areas predictable upslope and downslope winds are important physical phenomena that should be considered when interpreting short-term concentrations. During the night a shallow layer of cool air flows down toward lower elevation and during the day warmer less dense air flows up the mountain. These slope flows are strongest on cloudless days and minimal during overcast conditions. In valleys, circulations can be generated to cause wind that may flow up and down the valley axis or up and down from higher to lower elevations and vice versa. Nocturnal valley flows during clear nights may create a shallow inversion layer over the valley floor, trapping locally emitted pollutants.

The terrain surrounding that site has a major influence on the transport of pollutants to that site. Windroses in Figure 3-16 shows some of the terrain influences on winds. This figure shows only the sites in the northern portion of the study area and includes winds from all hours in the study.

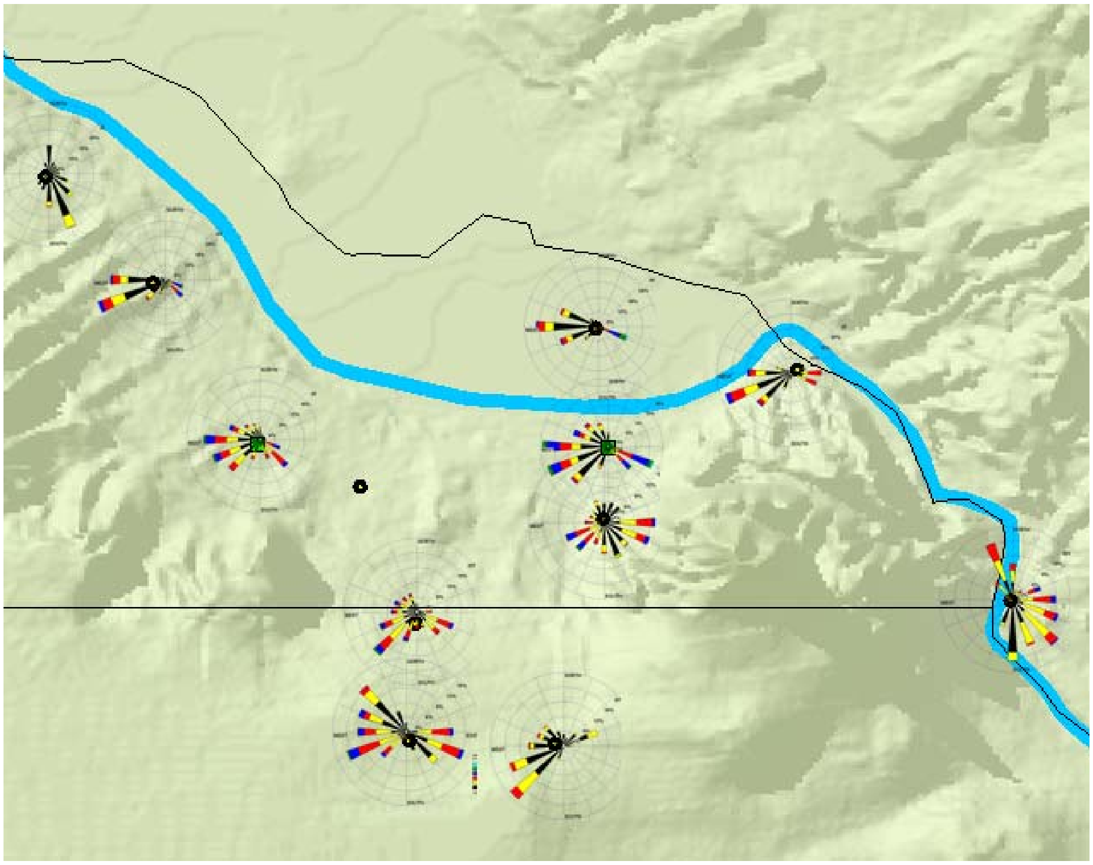

Figure 3-16. Windroses for E-BAM and NMED sites to the north of the study area

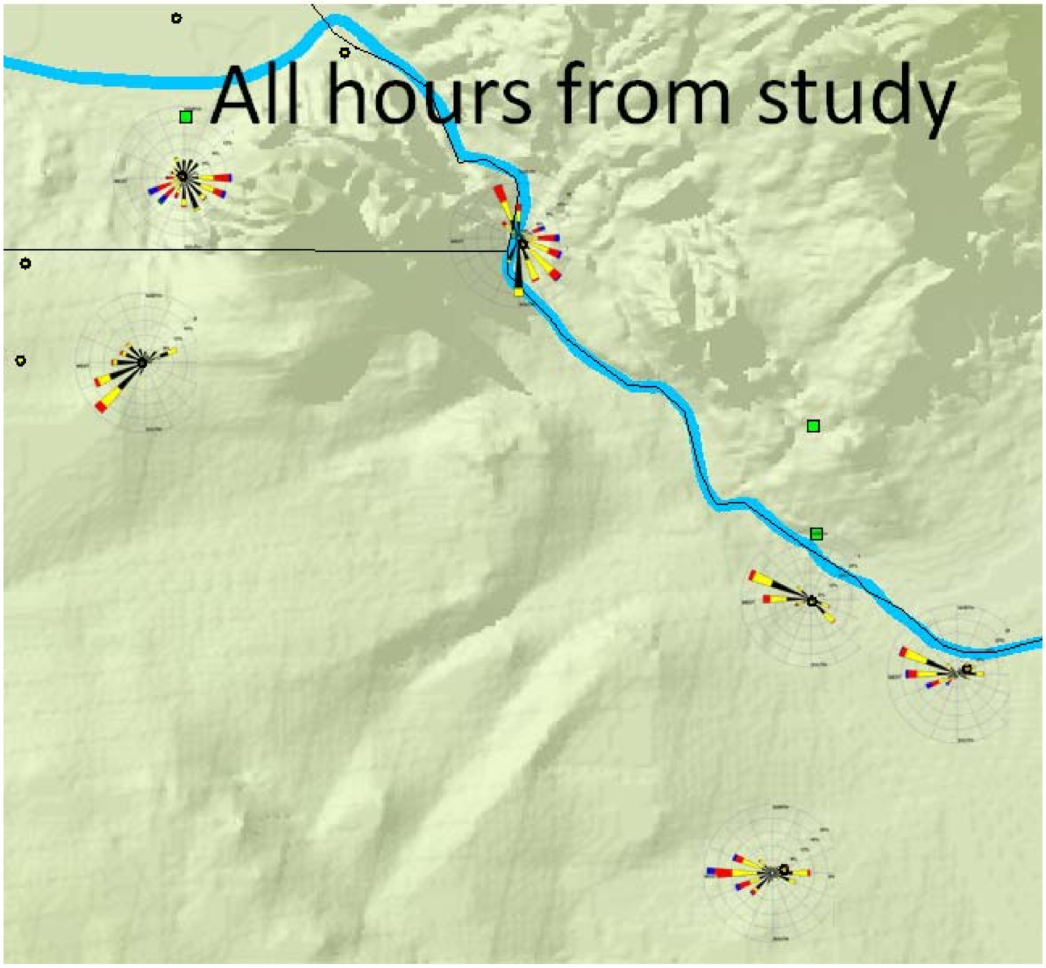

Figure 3-17. Windroses for E-BAM and Ciudad Juárez sites during the study

Overall the wind patterns look reasonable given the terrain surrounding each site. Sunland Park Elementary had no wind direction data so no wind rose was created. There were questionable winds from Riverside Elementary as seen on the windrose where there were low winds throughout the study. This probably is due to the location of the E-BAM and wind sensor on the roof of the building based on photos.

3.3 Episode Criteria

Episodes were based on the hourly $PM_{2.5}$ concentrations measured at the Sunland Park City Yard site, 6ZG from October 31, 2008 to April 30, 2009. Episodes were found by filtering the hourly data for concentrations greater than 30 $\mu g/m^3$ during low wind speeds of less than 2 miles per hour or 0.89 meters per second. Using that criteria there were 63 episodes of at least one hour in duration. The median starting hour was 18:00 and ended by 20:00 MST. Two of these episodes lasted 9 hours. The mean number of days between episodes was about 3 days (median 2 days). During these episodes the temperature difference between the 2 and 10 meter heights varied from near zero to more than 4 degrees C. A positive number shows that the temperature at the top of the 10 meter tower is warmer than the bottom, implying a stable atmosphere. These episodes are listed in

Appendix A showing the dates, maximum and mean $PM_{2.5}$ and mean lapse rate between 2 and 10 meters during that episode. Increasing the criteria to concentrations greater than 40 ug/m^3 and 2 mph, there were 49 episodes. Using 50 ug/m^3 and 2 mph there were 37 episodes of at least 1 hour in duration. These episodes typically started by 19:00 and ended by 20:00 MST and occurred on average every 4.8 days (median 2.3 days apart).

4 Discussion

This section presents the temporal variations of meteorological and air quality parameters, and the analysis of days with for all $PM_{2.5}$ mass concentrations.

4.1 Temporal Patterns

The diurnal and day-of-week patterns of local meteorology, and particulate matter are characterized to obtain a better understanding of direct emissions, mechanisms and pathways of fine particulate matter in the Paso del Norte. While traffic count information was not collected as part of this effort, previous studies determined that traffic patterns varied greatly by vehicle type, day of week, and the type of road (freeway vs. surface) (Fujita, et al. 2002) (Marr, Balck and Harley 2002). Based on studies in Atlanta, Georgia and central California, passenger and light-duty vehicle traffic increased from Monday to Friday and decreased by 15-30% during weekends. The intensity of diesel-powered heavy duty vehicles remains relatively unchanged during weekdays but drops as much as 80% during weekends (especially on Sundays). On a diurnal basis, a bimodal diurnal profile in the morning and evening commuting hours during weekdays is observed for light-duty vehicles on surface streets and highways, while a single mode peak in midday is observed for weekends. For heavy-duty vehicles, a bimodal distribution was observed on surface streets and a single-mode peaking late in the morning was observed on freeways and during weekdays.

4.1.1 Diurnal Variation

The diurnal variation of $PM_{2.5}$ mass concentration is shown in Figure 4-1 through Figure 4-17. To further identify the possible impacts of direct traffic emissions and secondary particulate matter, the hourly plots of NO and NO_2 for the 6ZM site were also plotted in Figure 4-18 and Figure 4-19, respectively. For NO, a bimodal temporal pattern with the first maximum in early morning (6-9 am) followed by a daytime minimum at noon and a second maximum in evening (20-22). This pattern is indicative of direct traffic emissions. For NO_2, a slight increase was observed in early morning because a fraction of NO_2 is directly emitted from traffic. The second peak started in early evening (17-18), reached its maximum at 22 and remained unchanged during night, due to the accumulation of oxidation reaction products. This is a typical trend for monitoring sites in or nearby urban areas.

For $PM_{2.5}$, a bimodal distribution was also observed for most of the sites, with the first maximum in early morning being attributable to traffic emissions for sites in Sunland

Park, New Mexico and El Paso, Texas, followed by a mid-day minimum. An increase of $PM_{2.5}$ mass concentrations was observed in late afternoon, reaching their maximum concentrations between 18:00 to 21:00, followed by a slight decrease during nighttime. For sites in Ciudad Juárez, Mexico, $PM_{2.5}$ mass concentrations increased in early morning, following by a progressive increase during the day and reaching heir maxima in late evening. The observed profile of $PM_{2.5}$ in late afternoon and evening exhibited many similarities to that observed for NO_2 at 6ZM site, indicating the possible contribution of secondary aerosol on $PM_{2.5}$ mass concentrations. At the MX sites this would be smoke from wood-burning heating stoves. In addition, the descent of the boundary layer height may also be responsible for elevated $PM_{2.5}$ concentrations during night.

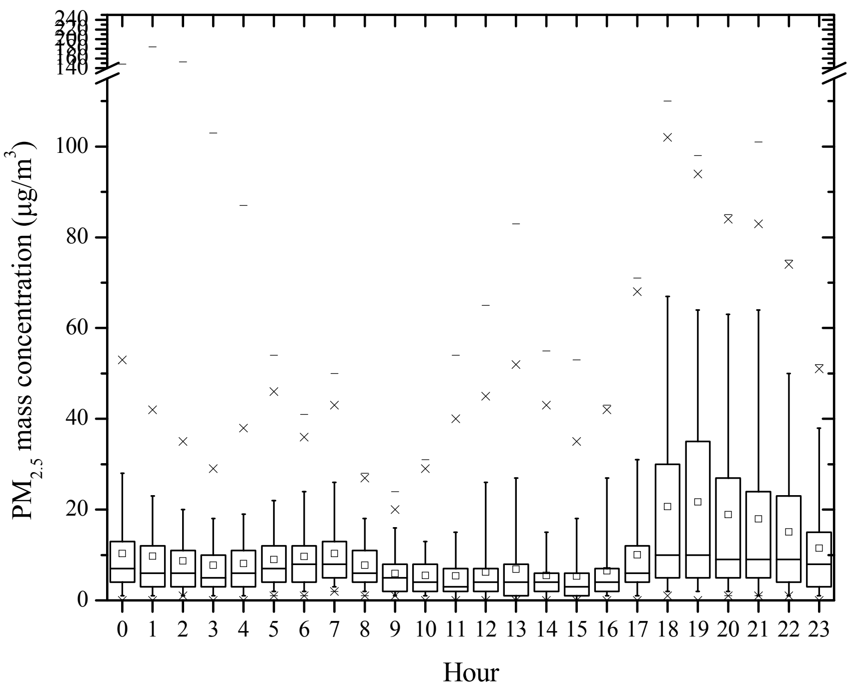

Figure 4-1. Hourly variation of $PM_{2.5}$ mass concentration at 6ZG

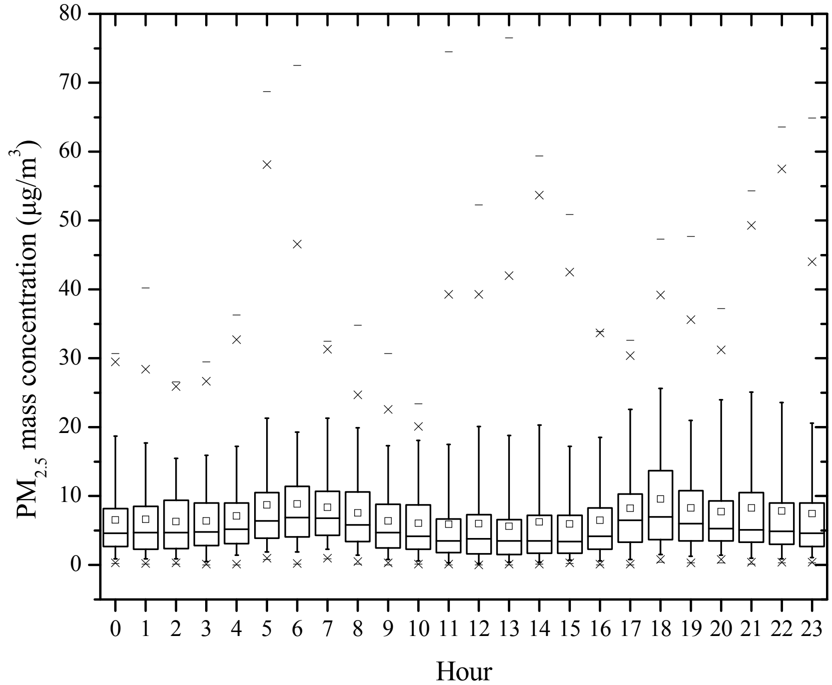

Figure 4-2. Hourly variation of $PM_{2.5}$ mass concentration at 6ZM site

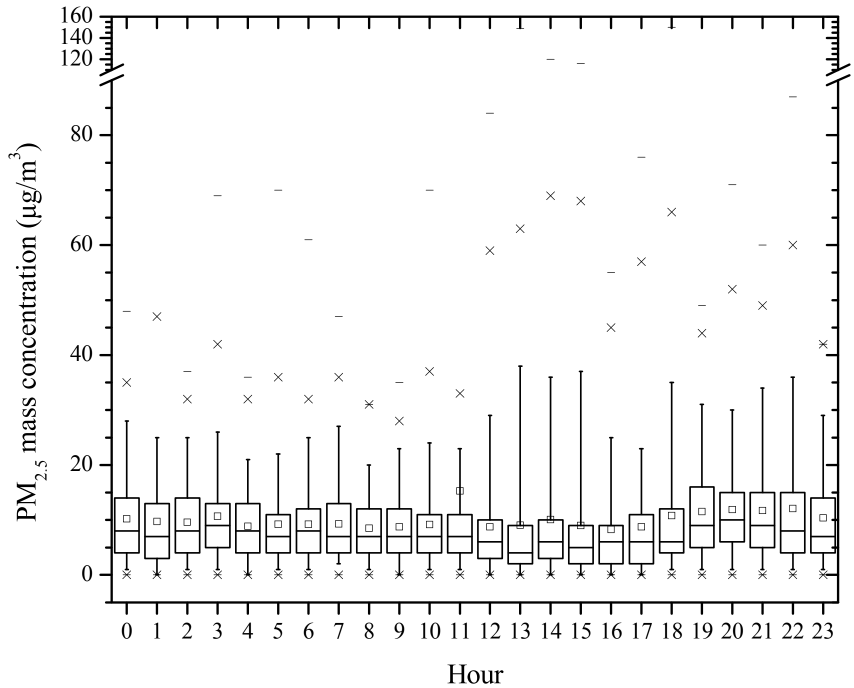

Figure 4-3. Hourly variation of $PM_{2.5}$ mass concentration at ARDO site

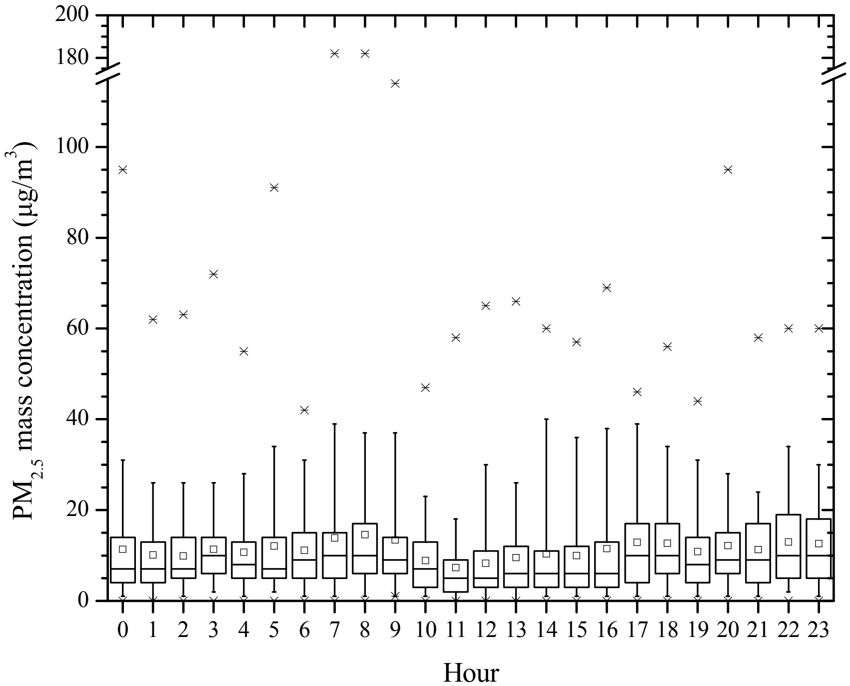

Figure 4-4. Hourly variation of $PM_{2.5}$ mass concentration at DACC site

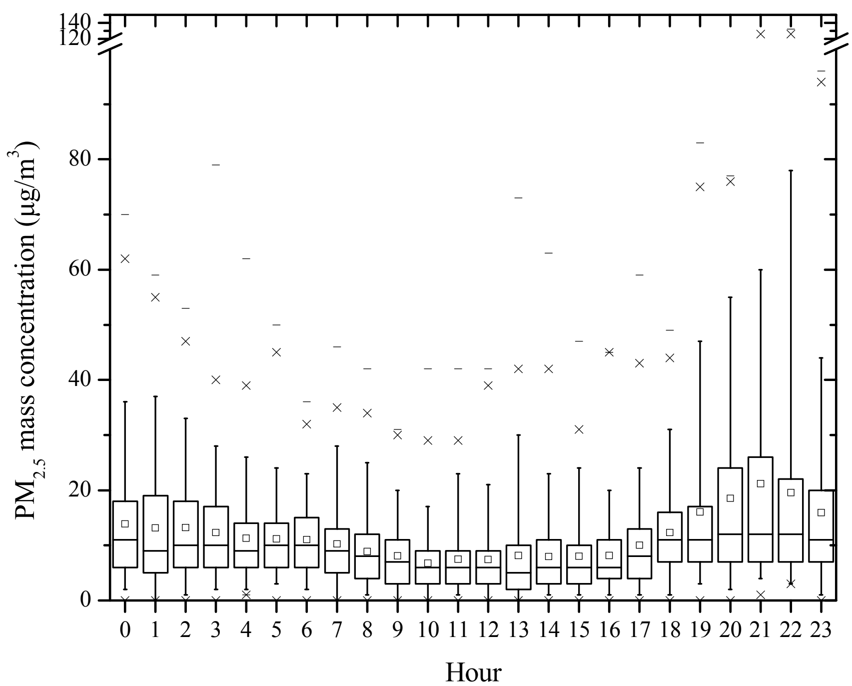

Figure 4-5. Hourly variation of $PM_{2.5}$ mass concentration at IBWC site

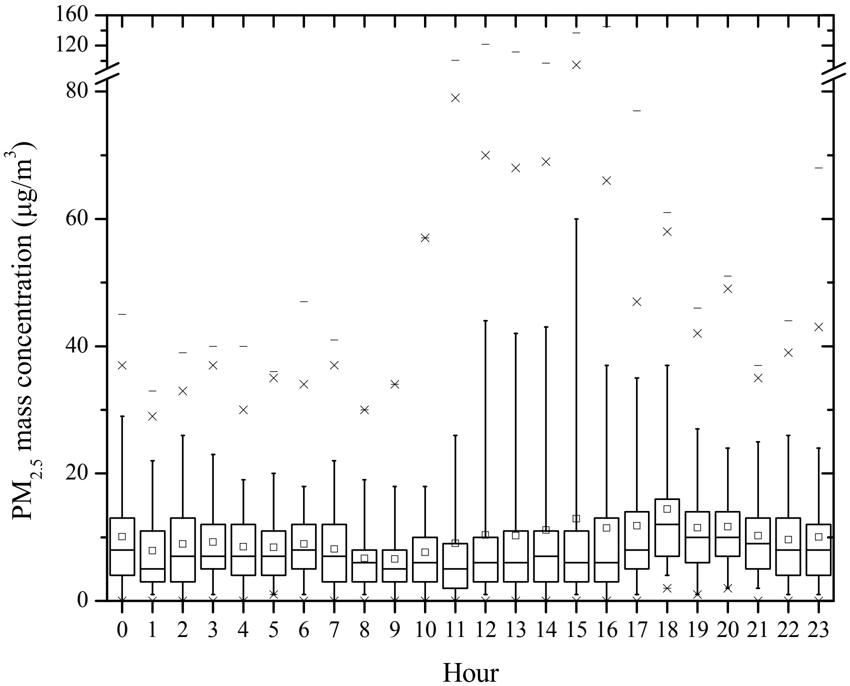

Figure 4-6. Hourly variation of $PM_{2.5}$ mass concentration at RIVER site

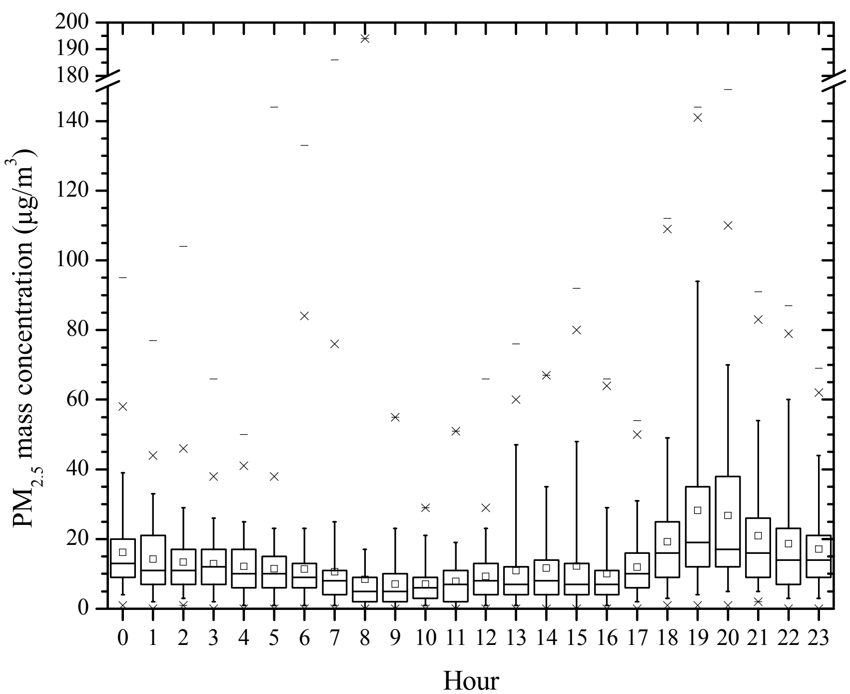

Figure 4-7. Hourly variation of $PM_{2.5}$ mass concentration at SPRT site

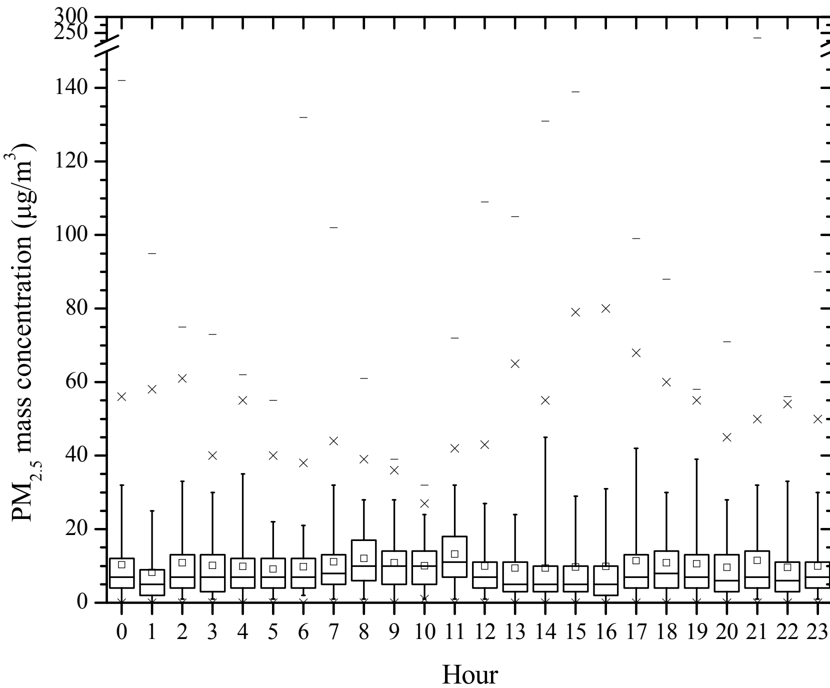

Figure 4-8. Hourly variation of $PM_{2.5}$ mass concentration at SUN site

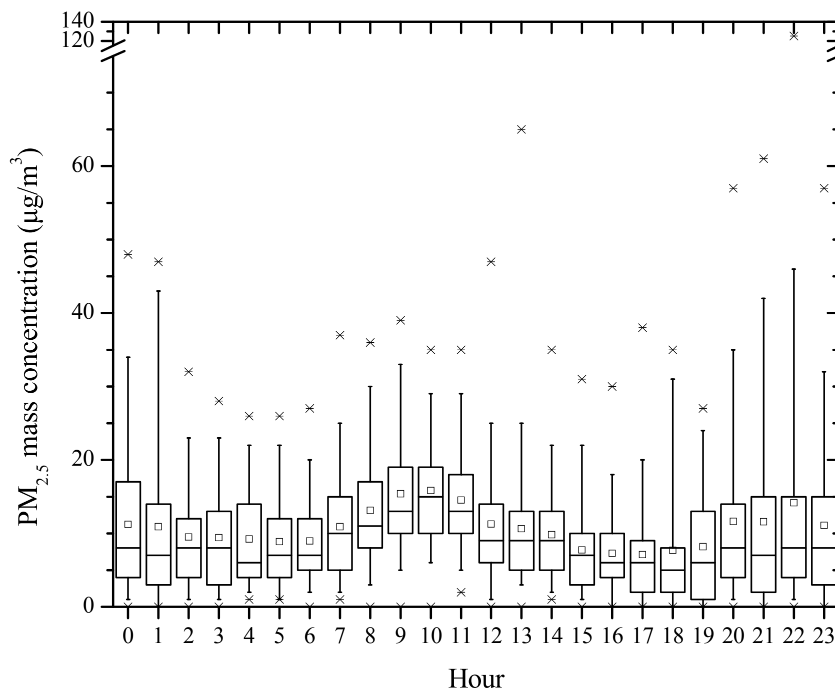

Figure 4-9. Hourly variation of $PM_{2.5}$ mass concentration at VICT site

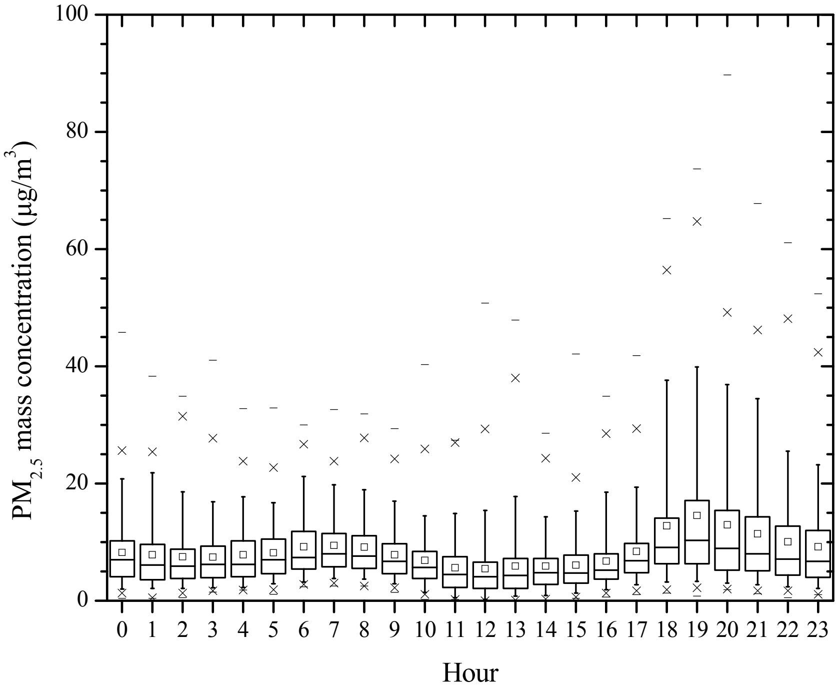

Figure 4-10. Hourly variation of PM$_{2.5}$ mass concentration at C12 site

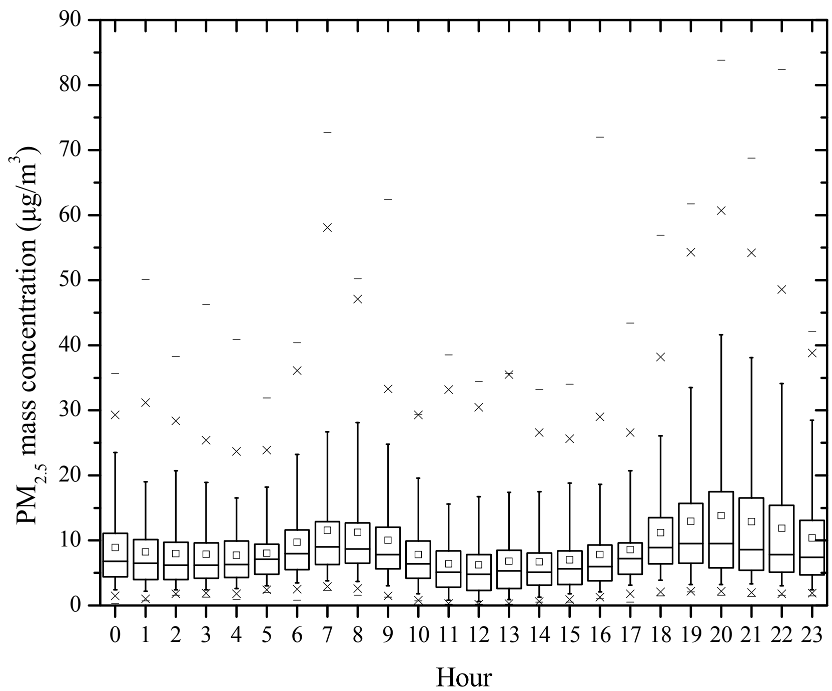

Figure 4-11. Hourly variation of PM$_{2.5}$ mass concentration at C41 site

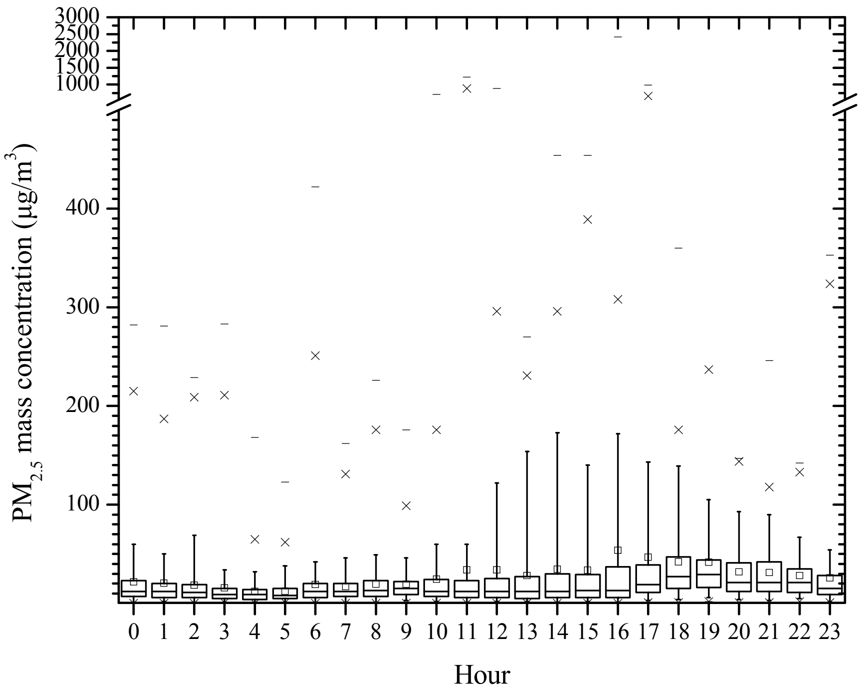

Figure 4-12. Hourly variation of $PM_{2.5}$ mass concentration at MX-16 site

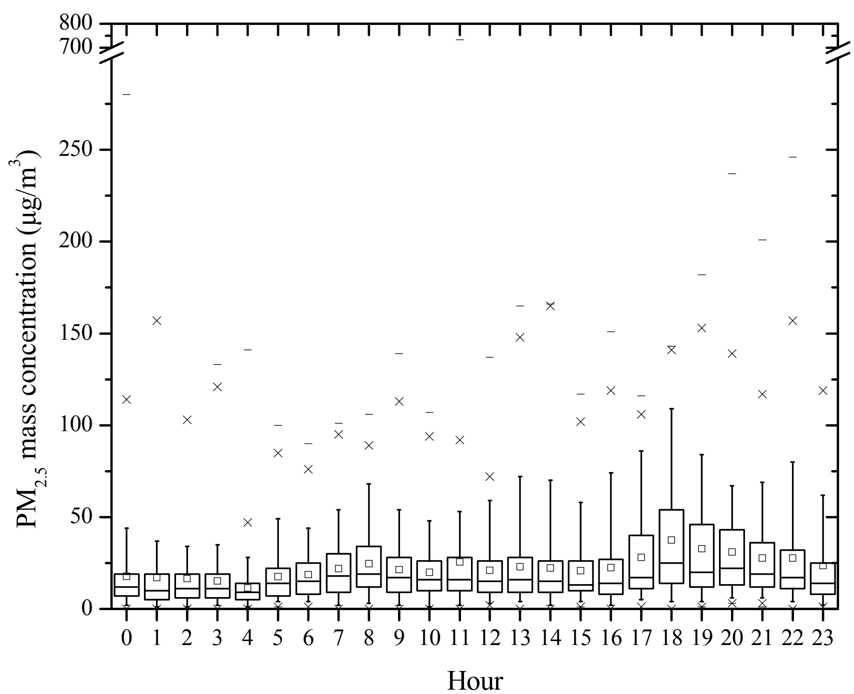

Figure 4-13. Hourly variation of $PM_{2.5}$ mass concentration at MX-17 site

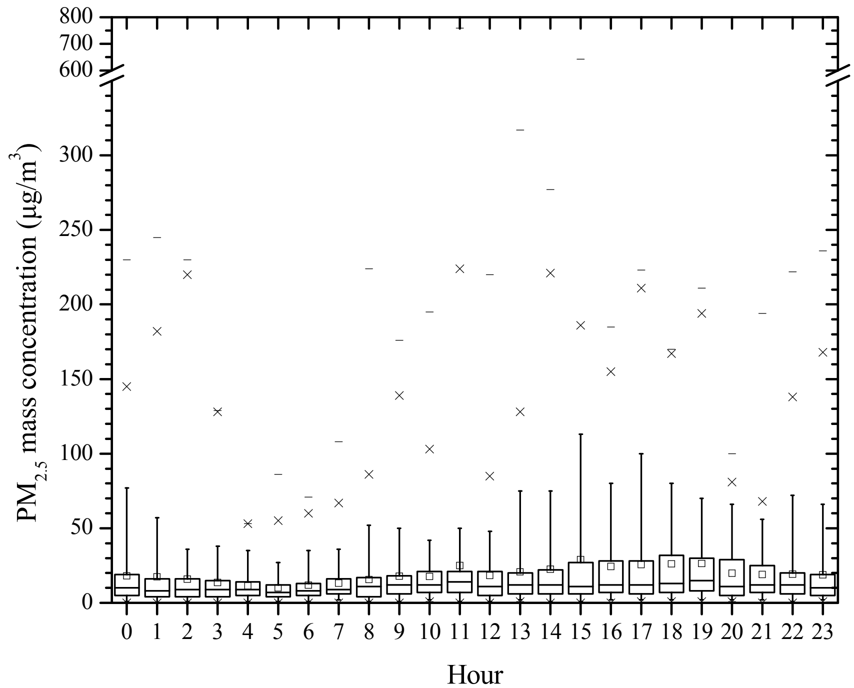

Figure 4-14. Hourly variation of $PM_{2.5}$ mass concentration at MX-18 site

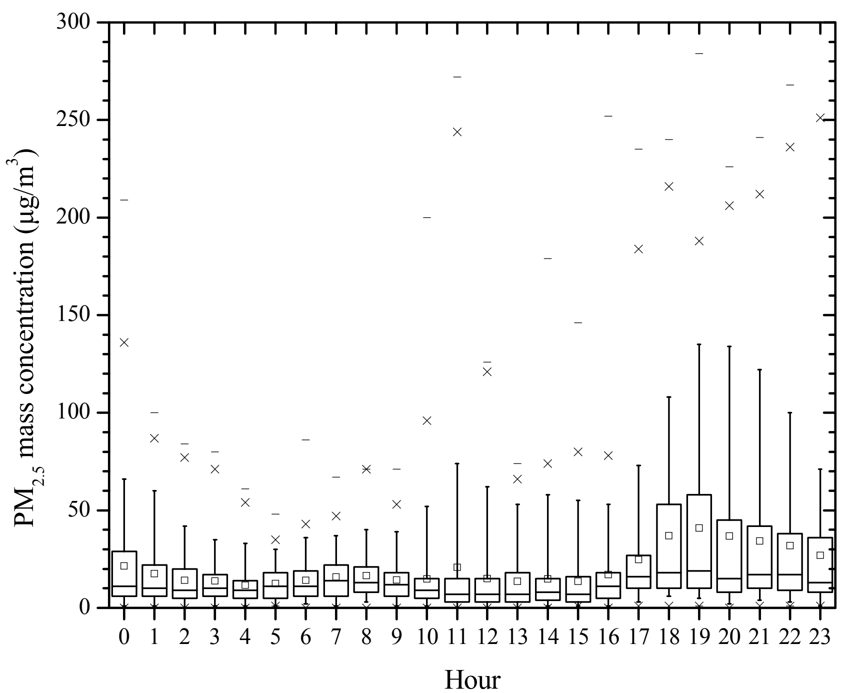

Figure 4-15. Hourly variation of $PM_{2.5}$ mass concentration at MX-19 site

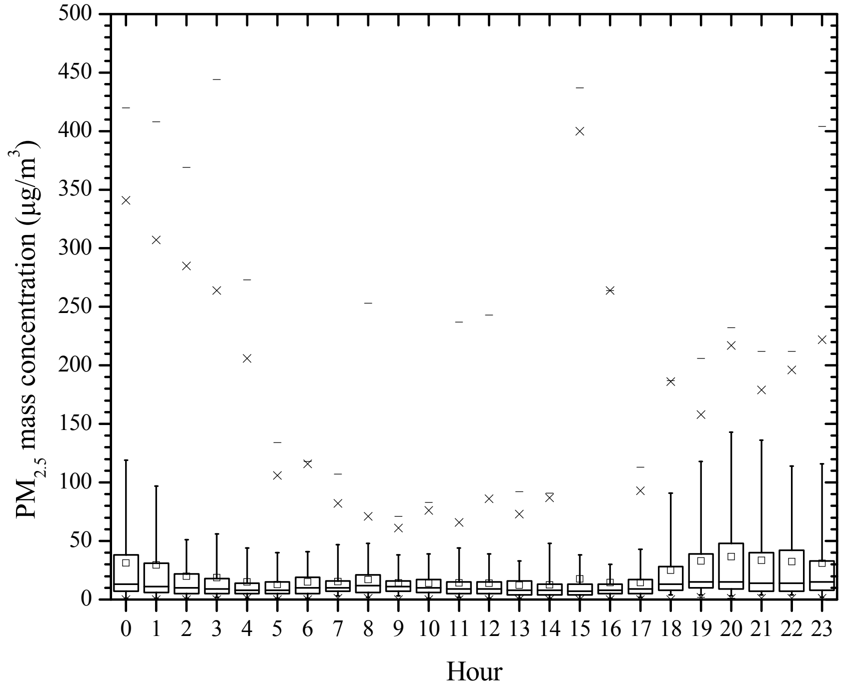

Figure 4-16. Hourly variation of PM$_{2.5}$ mass concentration at MX-20 site

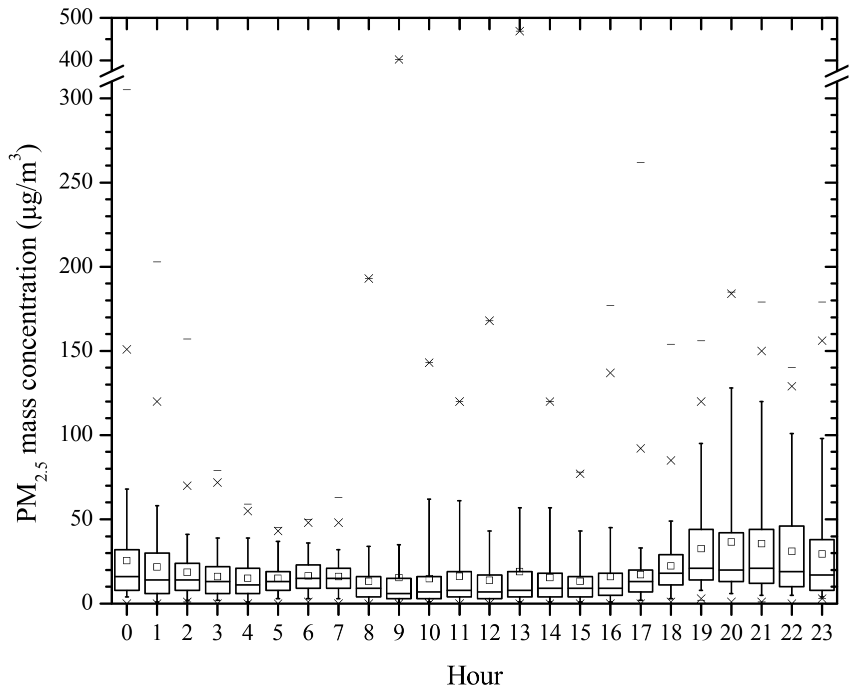

Figure 4-17. Hourly variation of PM$_{2.5}$ mass concentration at MX-21 site

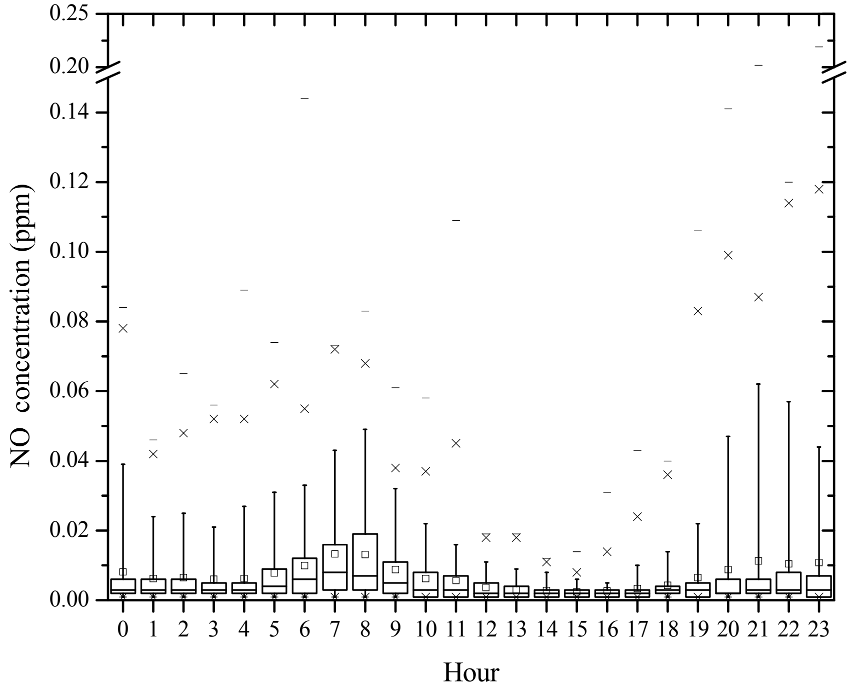

Figure 4-18. Hourly variation of NO concentration at 6ZM site

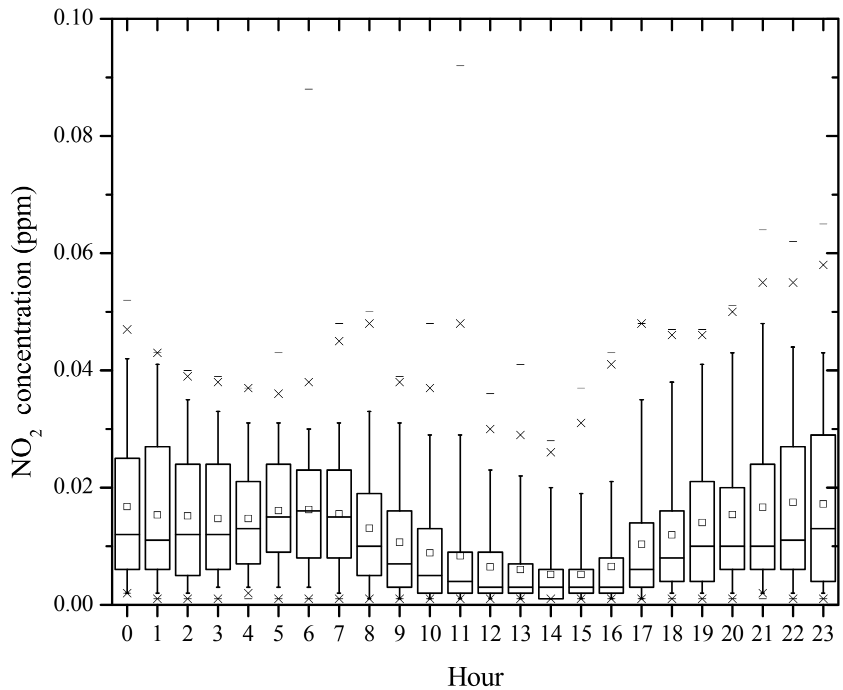

Figure 4-19. Hourly variation of NO_2 concentration at 6ZM site

4.1.2 Weekday/Weekend Variation

Figure 4-20 - Figure 4-36 show the weekday/weekend variation of $PM_{2.5}$ mass concentrations for each site. The day-of-week patterns of the $PM_{2.5}$ mass concentrations were characterized by a minimum on Sunday, increased sharply on Monday and remained relatively unchanged till Thursday. A slight decrease was observed on Friday, followed by an increase on Saturday. This “Monday effect” was also observed for $PM_{2.5}$ mass in the South Coast Air basin (Motallebi, et al. 2003). The observed profile is indicative of increased traffic emissions during commuting in weekdays (with the exception of Fridays). Low PM on Fridays and Mondays for sites MX 16, 17 and 21 reflect the fact that these days were job furlough days. Increased $PM_{2.5}$ concentrations in Saturday may also be related to traffic emissions, as residents do their shopping or other non-work related activities. One exception, at MX 19, may reflect less traffic due to the poor economy.

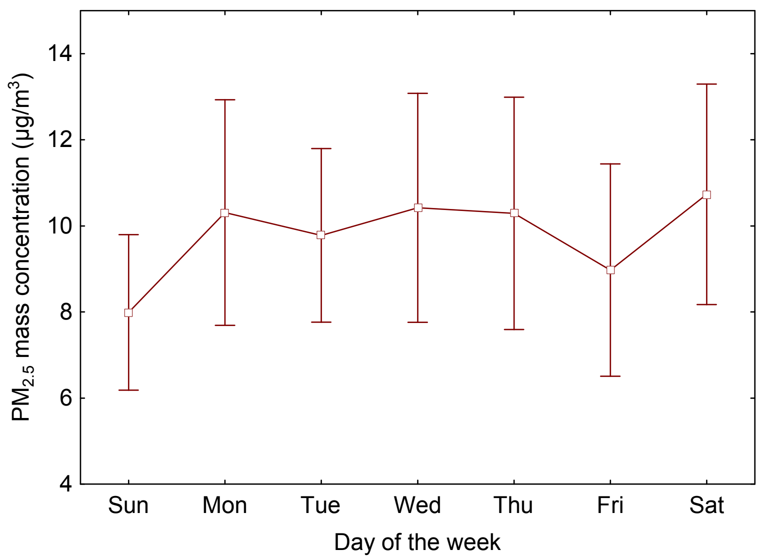

Figure 4-20. Day of the week variation of $PM_{2.5}$ mass concentration at 6ZG site

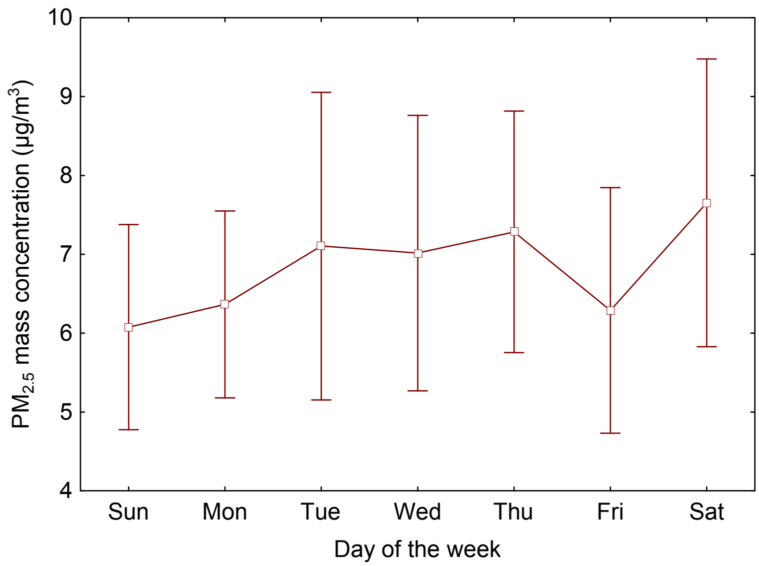

Figure 4-21. Day of the week variation of $PM_{2.5}$ mass concentration at 6ZM site

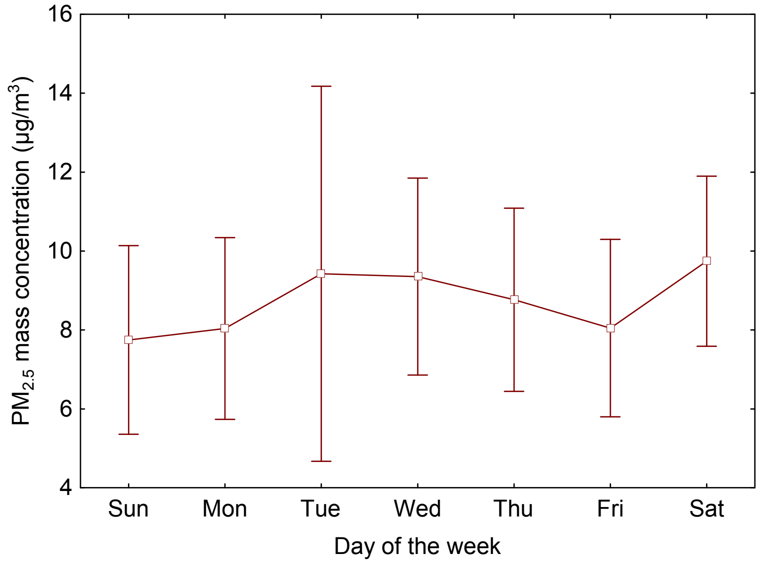

Figure 4-22. Day of the week variation of $PM_{2.5}$ mass concentration at ARDO site

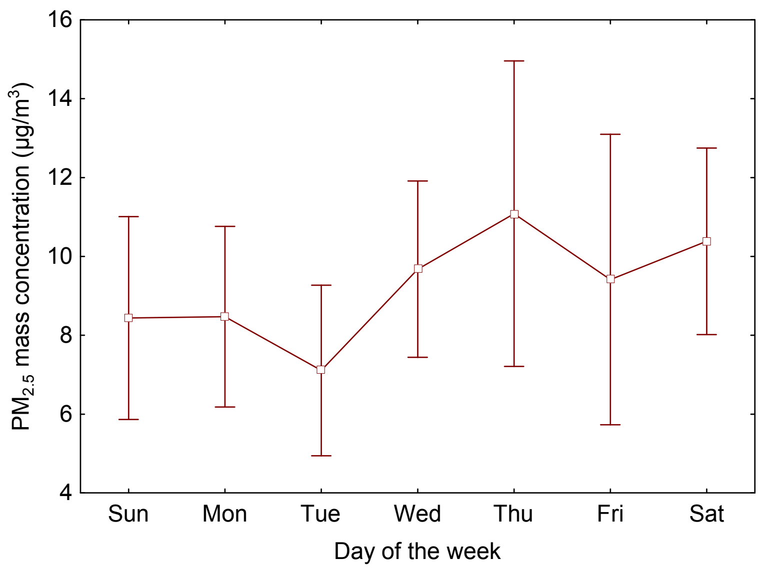

Figure 4-23. Day of the week variation of $PM_{2.5}$ mass concentration at DACC site

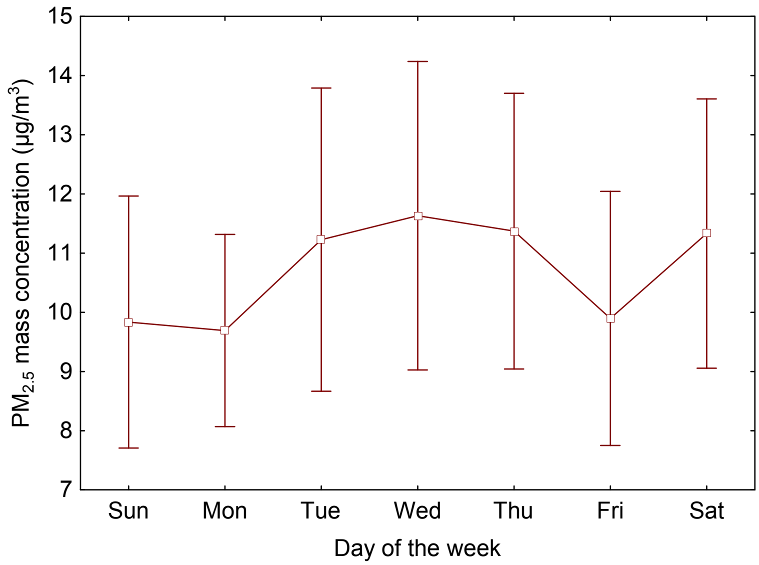

Figure 4-24. Day of the week variation of $PM_{2.5}$ mass concentration at IBWC site

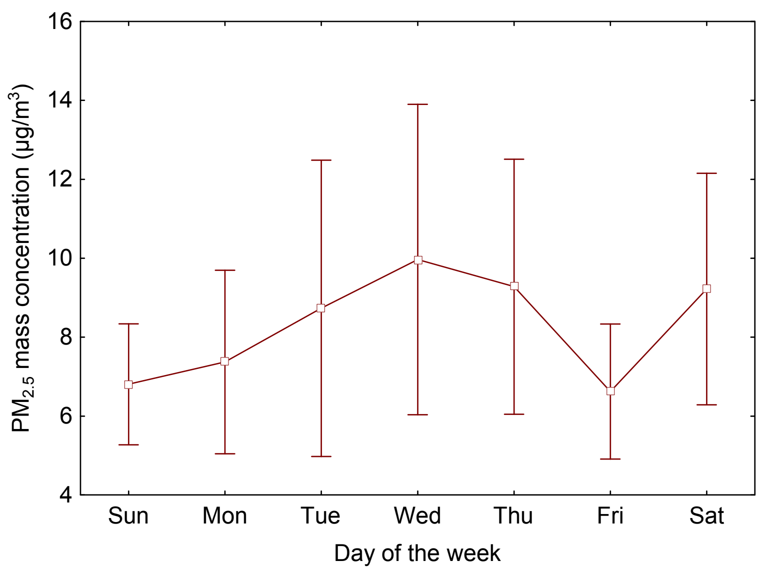

Figure 4-25. Day of the week variation of $PM_{2.5}$ mass concentration at RIVER site

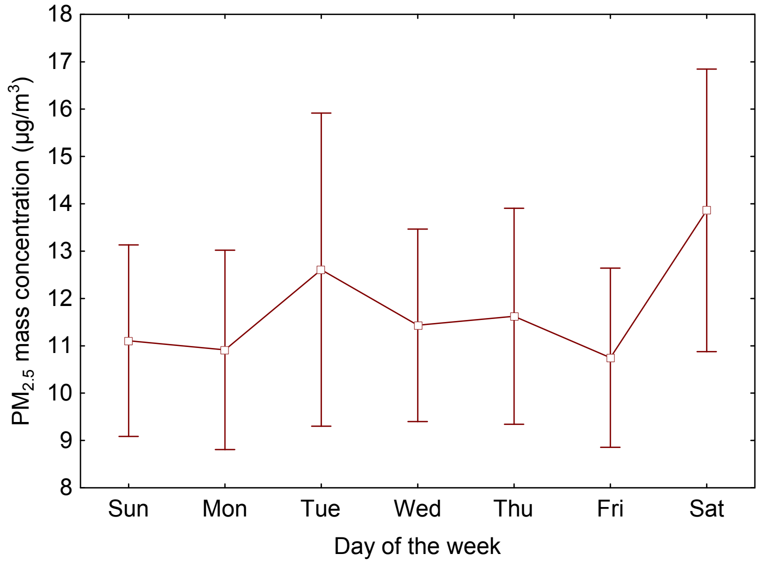

Figure 4-26. Day of the week variation of $PM_{2.5}$ mass concentration at SPRT site

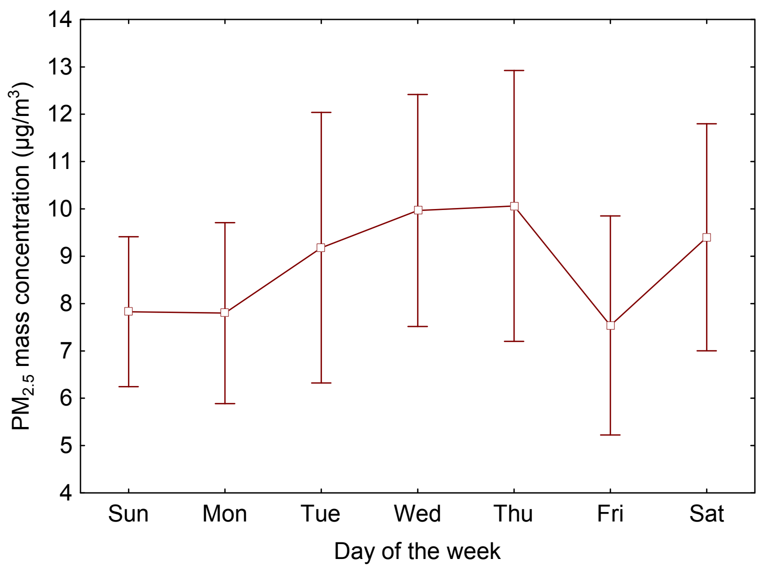

Figure 4-27. Day of the week variation of $PM_{2.5}$ mass concentration at SUN site

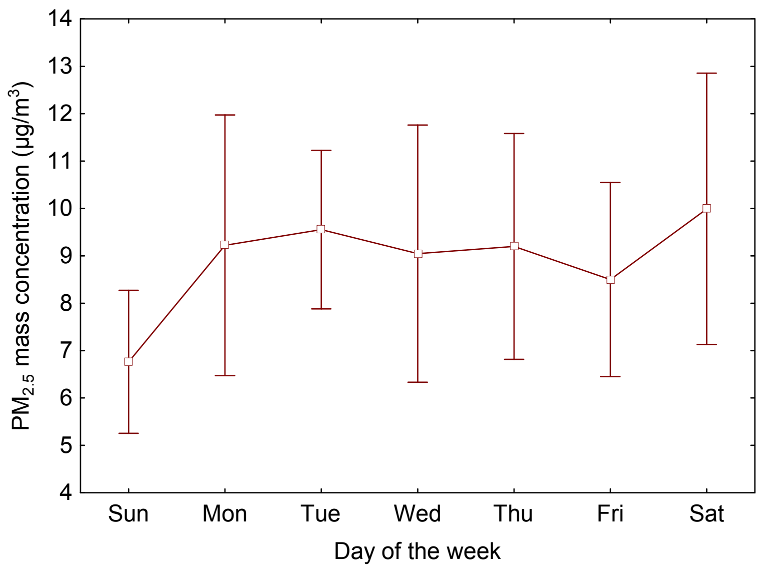

Figure 4-28. Day of the week variation of $PM_{2.5}$ mass concentration at VICT site

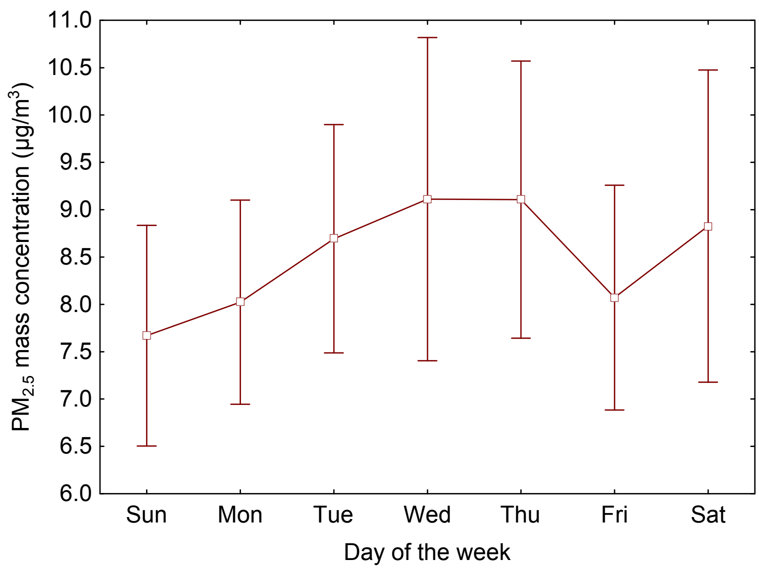

Figure 4-29. Day of the week variation of $PM_{2.5}$ mass concentration at C12 site

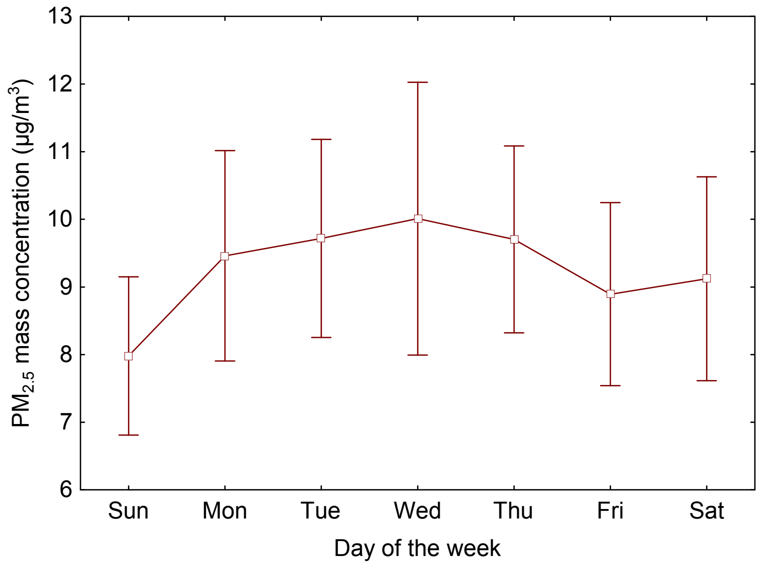

Figure 4-30. Day of the week variation of $PM_{2.5}$ mass concentration at C41 site

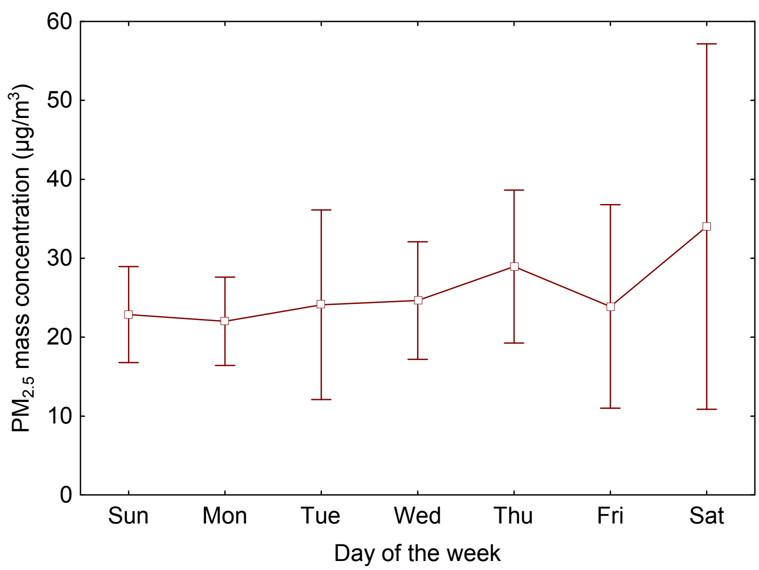

Figure 4-31. Day of the week variation of $PM_{2.5}$ mass concentration at MX-16 site

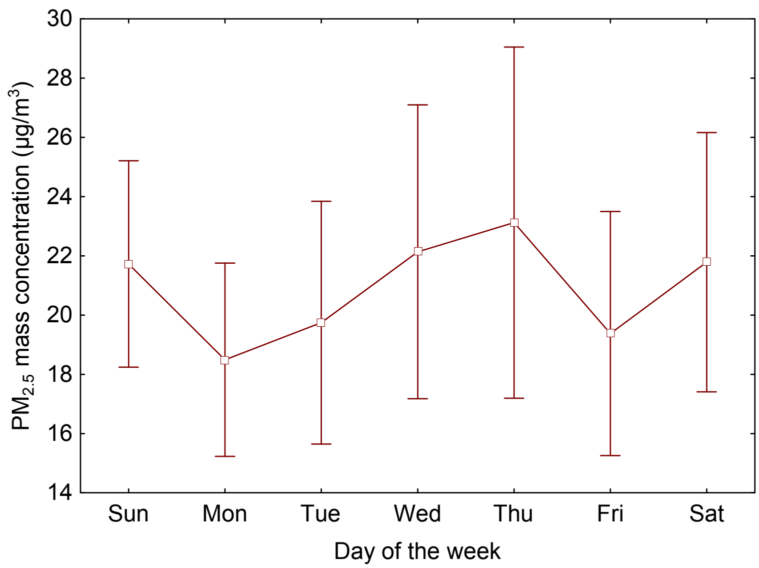

Figure 4-32. Day of the week variation of $PM_{2.5}$ mass concentration at MX-17 site

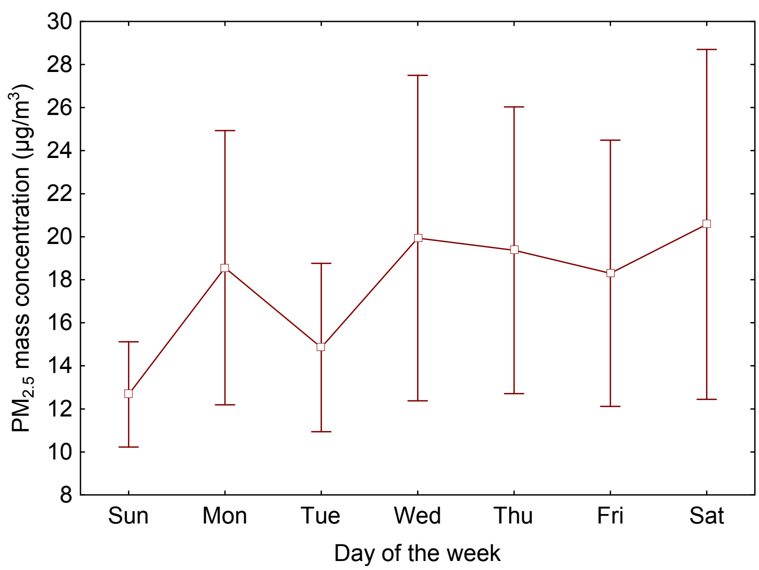

Figure 4-33. Day of the week variation of $PM_{2.5}$ mass concentration at MX-18 site

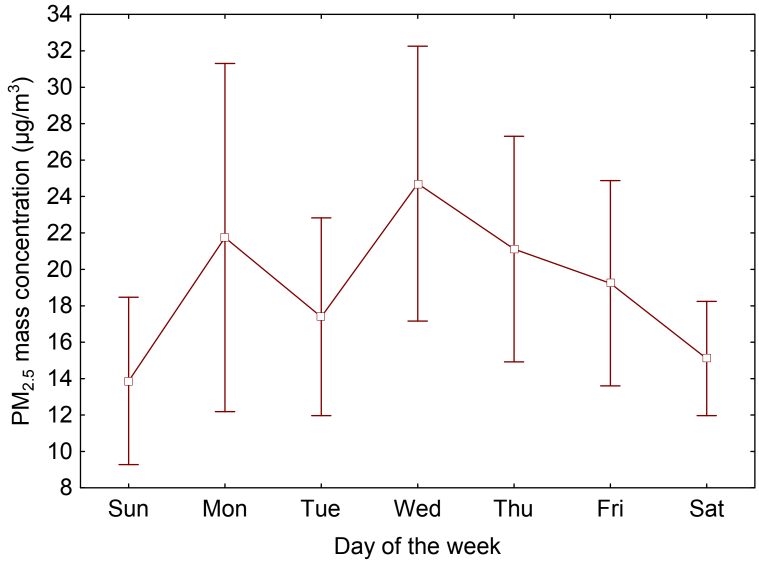

Figure 4-34. Day of the week variation of $PM_{2.5}$ mass concentration at MX-19 site

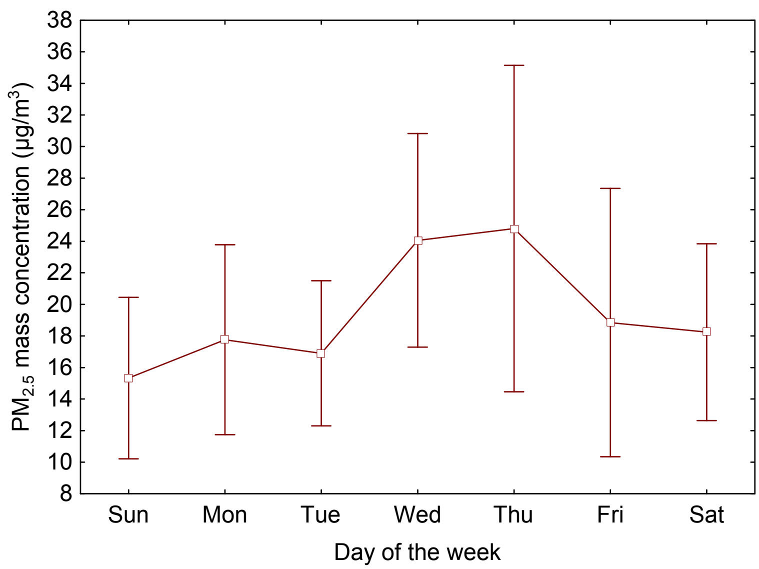

Figure 4-35. Day of the week variation of $PM_{2.5}$ mass concentration at MX-20 site

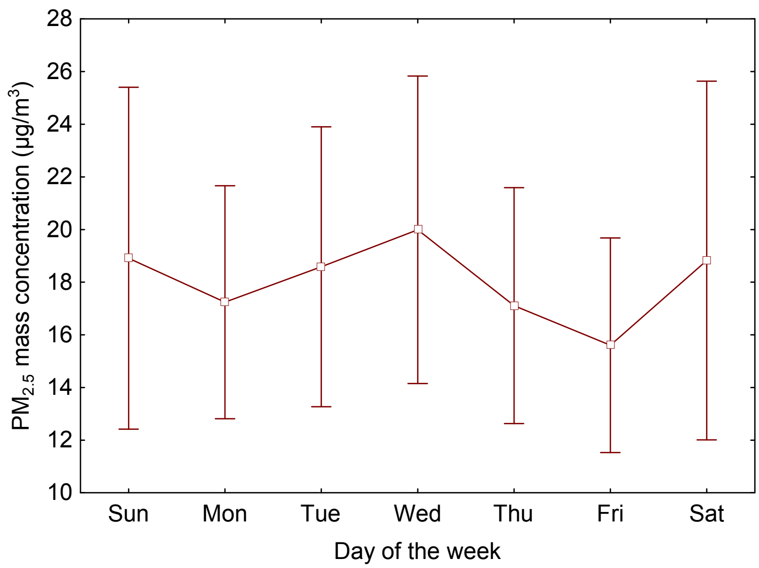

Figure 4-36. Day of the week variation of $PM_{2.5}$ mass concentration at MX-21 site

4.2 Spatial and Temporal Correlations

The purpose of this section is to determine the spatial and temporal characteristics of $PM_{2.5}$ using a set of data analysis tools. These include:

- the Spearman correlation coefficient (r) to determine whether there is a uniform temporal profile (concentrations decrease or increase simultaneously). Pearson's correlation reflects the degree of linear relationship between two variables. High (>0.70) correlation coefficients values indicate a positive linear relationship between variables, while negative values suggest a strong anti-correlation.
- the absolute (ΔC) and the relative difference ($\%\Delta C/Ref$) of 24-hr paired concentration differences between two sites. The relative difference was computed as the percentage of the absolute concentration difference to the reference site concentration. For the needs of this study, we used 6ZG as a reference site for air toxics because of its central location with respect to the other sites. Positive values indicate that air toxics concentrations at the site were higher than those measured at 6ZG. Median absolute and relative differences provided an indication of systematic differences between the sites, whereas site-to-site variation was quantified using the standard deviation
- The coefficient of divergence (COD) was used to assess the spatial uniformity of measurements with respect to the concentration levels. The COD was estimated as follows:

$$COD = \sqrt{\frac{1}{p} \cdot \sum_{i=1}^{p} \left(\frac{C_{ij} - C_{ik}}{C_{ij} + C_{ik}} \right)^2}$$

where p is the total number of paired measurements, and C_{ij} and C_{ik} are the measured concentrations at the reference and comparison sites on the i-th day, respectively. The COD was computed using 1hr and 24-hr concentrations at 6ZG for the reference values. COD values vary from 0 to 1, with COD values close to unity being indicative of strong spatial variation.

Table 4-1 shows the correlation coefficients of 24-hr $PM_{2.5}$ measurements among the sites in Sunland Park in New Mexico, El Paso in Texas and Ciudad Juárez in Mexico. Stronger correlations (>0.55) were observed among sites in New Mexico and Texas. For sites in Mexico, correlations were lower while MX-19 showed negative correlations with all the other sites. These correlations indicated that $PM_{2.5}$ concentrations followed comparable daily profiles in New Mexico and Texas, probably influenced by traffic emissions, while a stronger site-to-site variation was observed for Mexico.

Table 4-2 shows the distribution (median and standard deviation) of the 24-hour absolute (ΔC) and relative differences ($\%\Delta C/Ref$), between measurements for all sites. In general, median ΔC values were low for sites in New Mexico and El Paso, indicating a rather uniform spatial pattern on a day-to-day basis. High 24-hour $PM_{2.5}$ ΔC values were more commonly associated with sites in Mexico where $PM_{2.5}$ levels were substantially higher than those measured at New Mexico and Texas. The rather uniform spatial pattern of daily $PM_{2.5}$ concentrations was demonstrated by the low COD values for New Mexico and Texas site, while strong spatial variation was observed for monitoring sites in Ciudad Juárez. The analysis of the site-to-site variation of $PM_{2.5}$ concentrations, expressed by the standard deviation of $\%\Delta C/Ref$ values, further confirmed the differences between sites in New Mexico/Texas and Mexico.

To further examine temporal differences between the sites, we plotted the relative difference as a function of the time of day for each site (Figure 4-37 - Figure 4-39). There are unique profiles for each site (or group of sites). More specifically, for sites in El Paso, Texas, the relative difference increased during morning and late afternoon probably because of increased emissions from traffic. An early morning peak was also observed for VICT site. However, for the rest of sites in New Mexico, the relative differences were quite variable and site-dependent with two peaks (for most of the sites) in the early morning (6:00-7:00) and late in the evening (18:00 - 22:00) which may be related to changes in meteorology and air circulation (e.g boundary layer). For sites in Ciudad Juárez, Mexico, the relative differences were also quite variable but higher during midday and decreased in evening and night. Traffic during midday may also be responsible for increased levels in Mexico (as compared to New Mexico sites).

Table 4-1. Spearman correlation coefficients over all hours

	6ZM	**ARDO**	**DACC**	**IBWC**	**RIVER**	**SPRT**	**SUN**	**VICT**	**C12**	**C41**	**MX-16**	**MX-17**	**MX-18**	**MX-19**	**MX-20**	**MX-21**
6ZG	0.65	0.69	0.47	0.83	0.53	0.83	0.58	0.85	0.83	0.74	0.54	0.65	0.44	-0.02	0.63	0.47
6ZM		0.68	0.72	0.69	0.72	0.55	0.84	0.57	0.69	0.66	0.61	0.46	0.74	-0.14	0.33	0.29
ARDO			0.67	0.77	0.64	0.68	0.78	0.75	0.78	0.62	0.48	0.46	0.55	-0.08	0.46	0.39
DACC				0.61	0.75	0.50	0.71	0.47	0.57	0.46	0.56	0.42	0.50	-0.14	0.46	0.39
IBWC					0.61	0.78	0.71	0.81	0.85	0.76	0.54	0.67	0.48	-0.04	0.65	0.52
RIVER						0.49	0.70	0.55	0.62	0.51	0.56	0.53	0.61	-0.10	0.35	0.25
SPRT							0.58	0.77	0.76	0.71	0.50	0.63	0.41	0.02	0.56	0.59
SUN								0.58	0.67	0.60	0.56	0.51	0.66	-0.08	0.44	0.32
VICT									0.82	0.71	0.26	0.62	0.26	0.17	0.59	0.41
C12										0.79	0.65	0.64	0.54	-0.05	0.56	0.55
C41											0.57	0.53	0.49	-0.12	0.48	0.51
MX-16												0.59	0.53	-0.10	0.30	0.31
MX-17													0.47	0.10	0.53	0.42
MX-18														-0.14	0.34	0.23
MX-19															0.02	0.01
MX-20																0.40

Table 4-2. Absolute (ΔC) and relative (%ΔC/Fixed) differences (median and σ) of daily concentrations of $PM_{2.5}$ mass concentrations and mean COD

	Median ΔC	σ (ΔC)	Median % $\Delta C/C_{ref}$	σ (%ΔC)	COD
6ZM	-1.7	4.6	-25.9	38.4	0.283
ARDO	-1.4	6.5	-18.7	100.3	0.230
DACC	-1.6	6.7	-17	64.2	0.270
IBWC	1.3	3.8	15.6	50.5	0.195
RIVER	-1.8	6.7	-19	86.5	0.290
SPRT	1.8	4	23.3	95.6	0.214
SUN	-0.9	5.2	-12	56.8	0.249
VICT	-0.8	2.7	-10.5	32.7	0.148
C12	-0.6	3.6	-7.4	43.5	0.179
C41	0.5	4.2	5.3	51.3	0.204
MX-16	9.9	18	150	249	0.483
MX-17	10.5	7.6	153.2	150.5	0.446
MX-18	4.9	11.2	68.1	166.6	0.369
MX-19	6.9	14.5	94.2	407.5	0.457
MX-20	6.9	13.1	94.8	170.5	0.387
MX-21	5.7	10.3	87.5	351	0.378

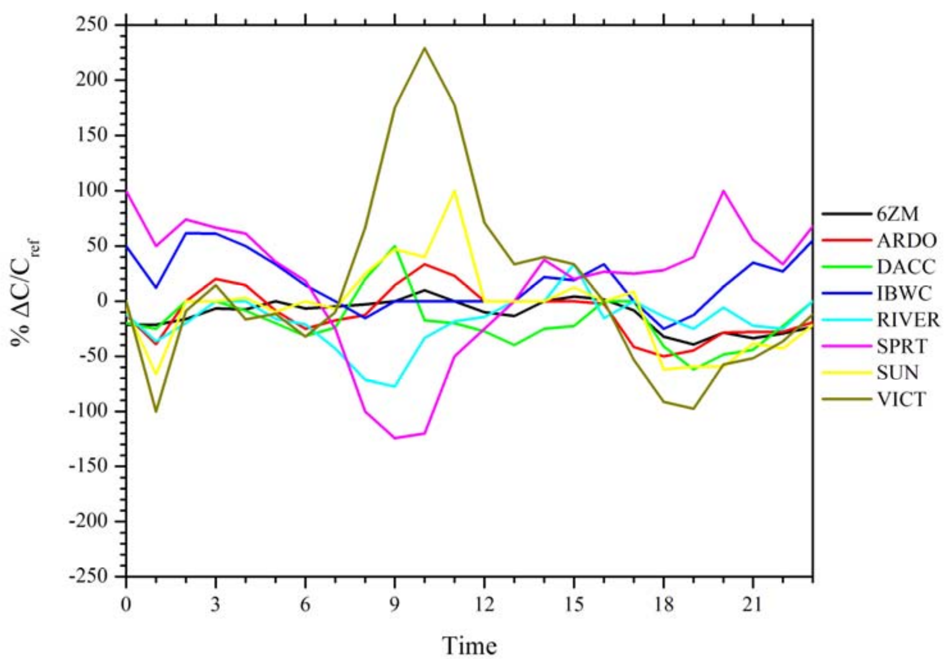

Figure 4-37. Diurnal profile of the relative difference for sites in US E-BAM network (Reference site: 6ZG)

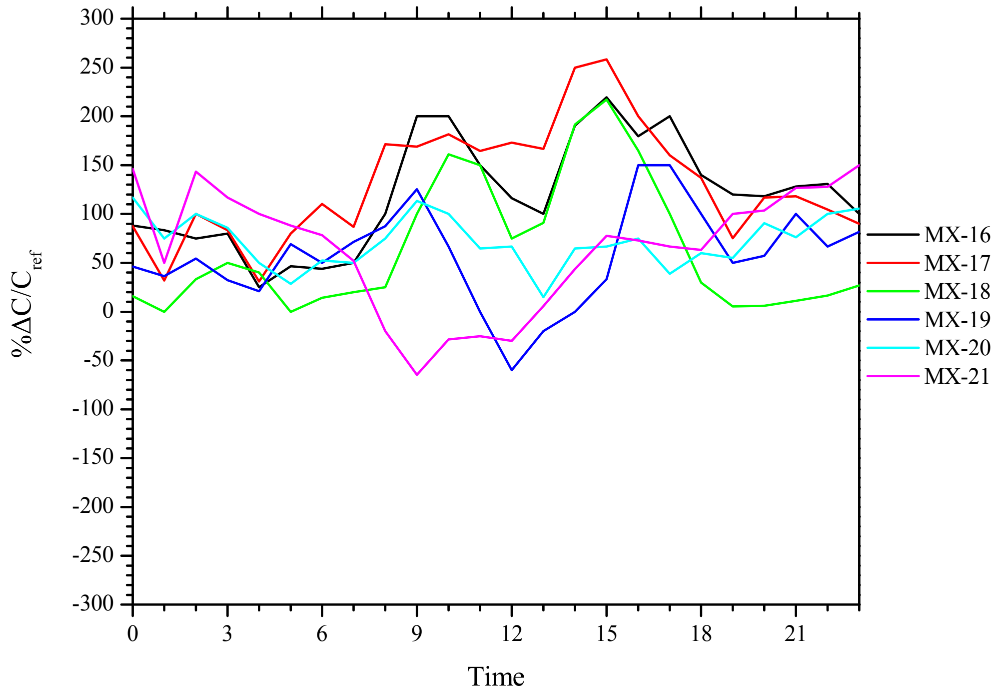

Figure 4-38. Diurnal profile of the relative difference for sites in Ciudad Juárez, Mexico (Reference site: 6ZG)

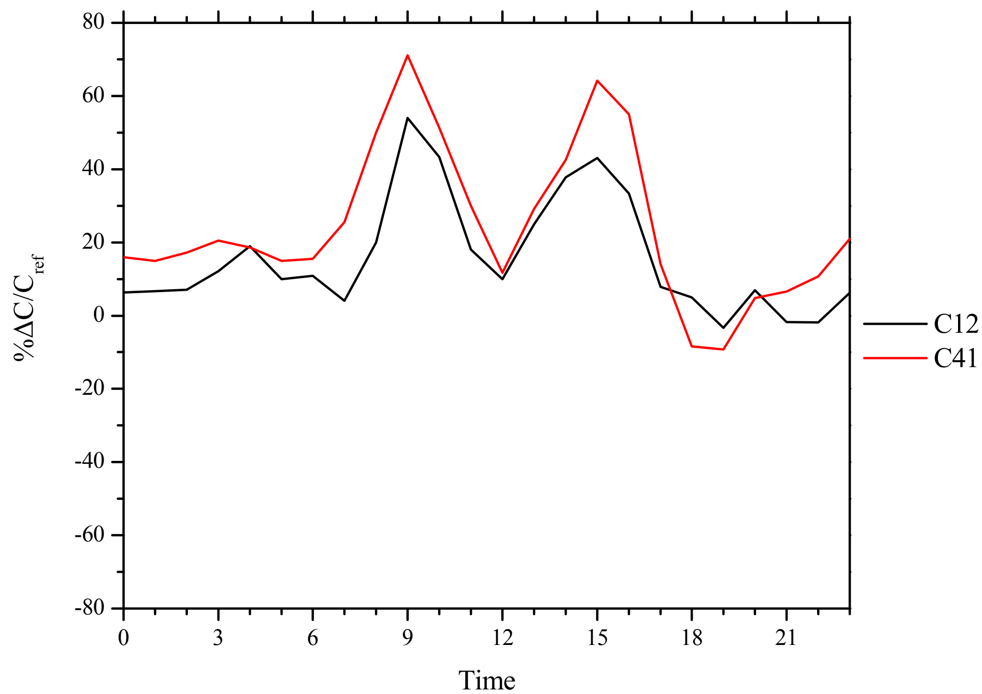

Figure 4-39. Diurnal profile of the relative difference for sites in El Paso, Texas (Reference site: 6ZG)

4.3 Episode Analysis

Episodes were chosen based on their severity with highest hourly $PM_{2.5}$ concentrations and in duration. Six case studies were chosen that represent episodes throughout the study from the fall (November 11, 2008) to spring (March 2, 2009). The analysis in this section provides details on the hourly $PM_{2.5}$ concentrations at each site, how they varies from site to site spatially and any details on the weather patterns that influenced the episode. Tables of the hourly $PM_{2.5}$ leading up to and during the episode are provided.

Spatial maps showing hourly concentrations showed that on several occasions, the MX-17 site appeared to see the onset of the low wind spike the first before other sites. This however does not happen in all cases. The MX-17 site is located in the midst of a grid of unpaved roads and surrounded by residential homes. Based on aerial photos, the landuse is similar at the MX-16 site just to the east.

Backward trajectories with a resolution of one hour and going back three hours were generated for Sunland Park for each of the six cases at 1-hour intervals using the NOAA HYSPLIT trajectory model version 4.9 (Draxler and Hess, 1995; 1997). We generated backtrajectories using the 12-kilometer North American Model (NAM) as well as from winds from the 6ZG station as inputs. Starting heights were 10 m above ground level. The residence time, defined as the fraction of the total time of back trajectories that the airmass was over a given area of 0.05 degree latitude by 0.05 degree longitude, or about 900 by 900 meters was computed. Hourly end points were used in ArcInfo to calculate the residence time maps. Mixing height was calculated using the HYSPLIT model for each hour of the study. The mixing heights were based on the 12-km NAM model vertical profiles of potential temperature.

4.3.1 Episode 1: New Years, December 31, 2008

The New Year episode occurred during the evening of December 31, 2008 to January 1, 2009. This episode was the longest in duration and recorded the highest $PM_{2.5}$ concentrations at the Sunland Park City Yard site of all the episodes in the study.

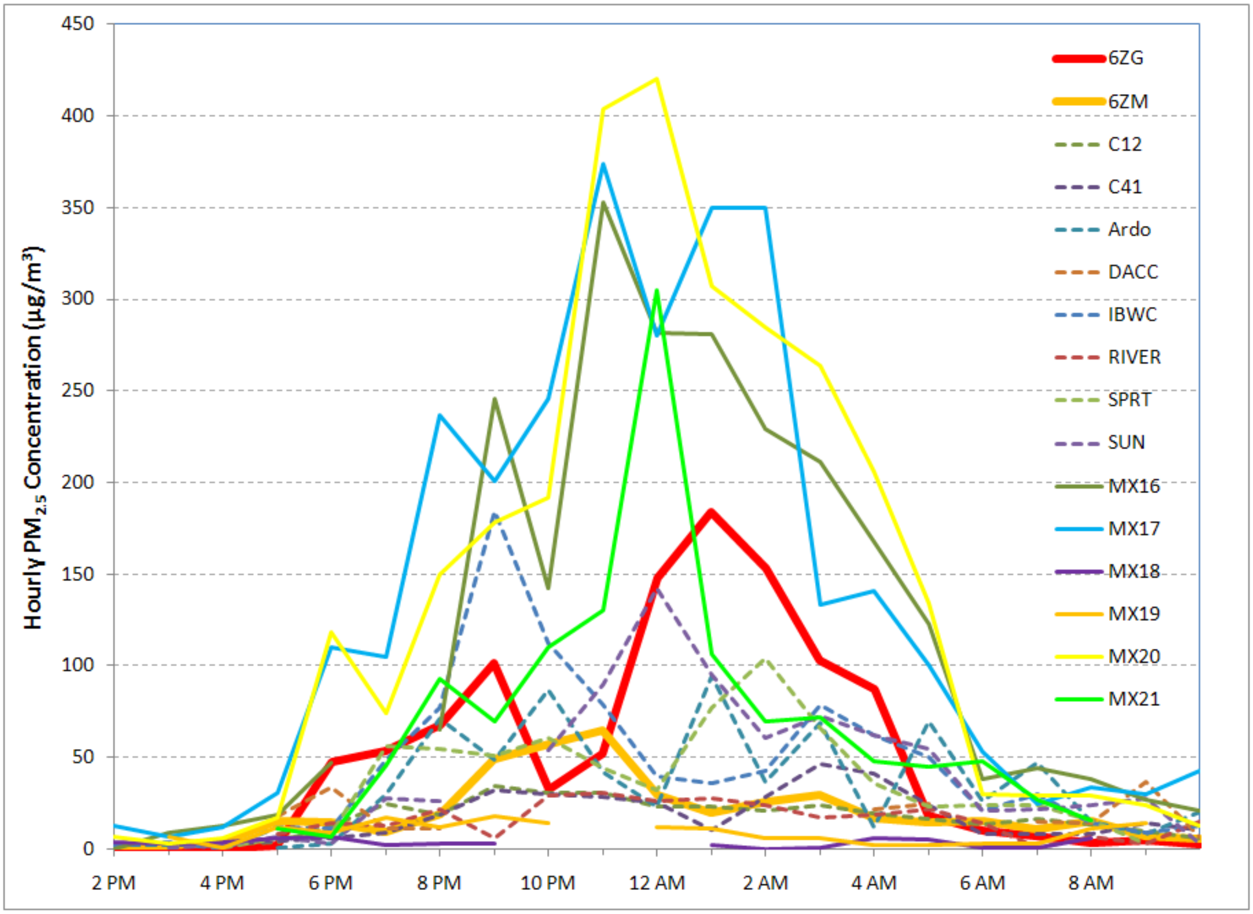

Figure 4-40. The New Year episode showing $PM_{2.5}$ from all sites. The two NMED sites are shown as the thick lines. New Mexico E-BAM sites are indicated by dashed lines and Mexican E-BAM sites are thin continuous lines.

The table below provides the concentration values during the episode with hours meeting the criteria for the 50 ug/m^3 threshold concentration in bold.

Table 4-3. Hourly $PM_{2.5}$ concentrations during the New Years episode

Time (MST)	6ZG	6ZM	C12	C41	Ardo	DACC	IBWC	RIVER	SPRT	SUN	VICT	MX16	MX17	MX18	MX19	MX20	MX21
12/31/2008 17:00	2	15	4	4	1	18	12	8	6	7		19	31	6	12	17	11
12/31/2008 18:00	47	15	12	6	3	34	11	14	8	3		47	110	7	9	118	7
12/31/2008 19:00	53	10	25	9	30	11	49	13	56	28			105	2	17	74	46
12/31/2008 20:00	67	19	19	19	71	11	77	22	55	26		65	237	3	12	150	93
12/31/2008 21:00	101	49	34	32	49		184	6	51			246	201	3	18	178	70
12/31/2008 22:00	32	57	30	30	87		112	29	61	54		142	246		14	192	110
12/31/2008 23:00	52	65	30	29	42		79	31	44	90		353	374	8		404	130
1/1/2009 0:00	148	29	24	26	23		40	26	32	142		282	280		12	420	305
1/1/2009 1:00	184	20	23	11	94		36	28	77	95		281	350	2	11	307	106
1/1/2009 2:00	153	26	21	28	37	63	43	24	104	61		229	350	0	6	285	70
1/1/2009 3:00	103	29	24	46	69		79	17	66	73		211	133	1	6	264	72
1/1/2009 4:00	87	17	20	41	12	22	62	19	36	62		168	141	6	2	206	48
1/1/2009 5:00	18	15	17	24	70	25	50	22	23	55		123	100	5	2	134	45
1/1/2009 6:00	10	15	13	8	26		21	14	24	21		38	53	1	3	30	48
1/1/2009 7:00	7	11	16	8	47	15	30	1	24	22		44	25	1	3	29	27

Earlier in the day on the 31st a cold front passed on the area.

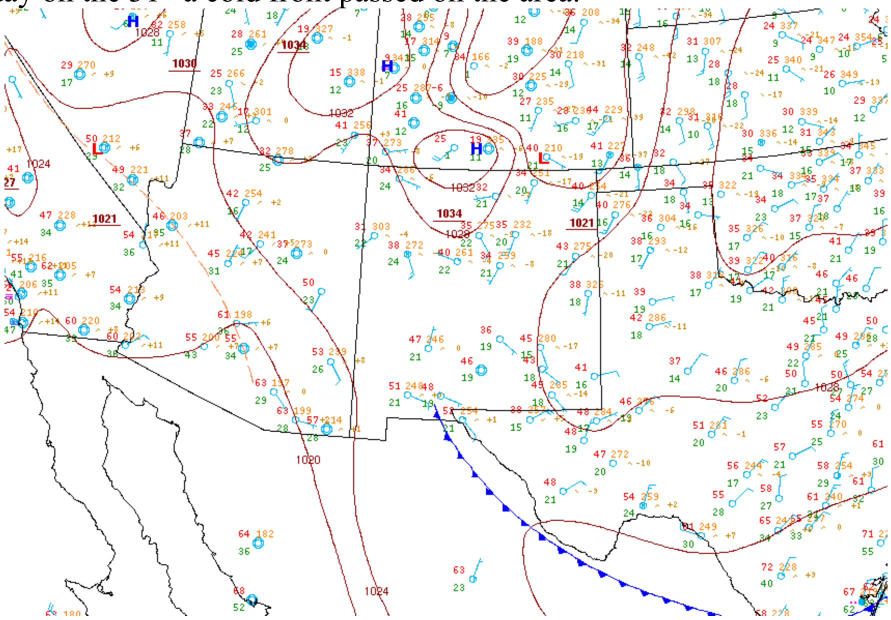

Figure 4-41. Surface weather map for 11 am (18 UTC) on December 31, 2008.

Mixing heights during this time showed a typical diurnal cycle with low heights in the morning and evening and a peak in the afternoon. Mixing heights were low in the evening hours of December 31 reaching a minimum of 52 meters by midnight. During the day mixing heights climbed to 600 meters on the 30th and 31st.

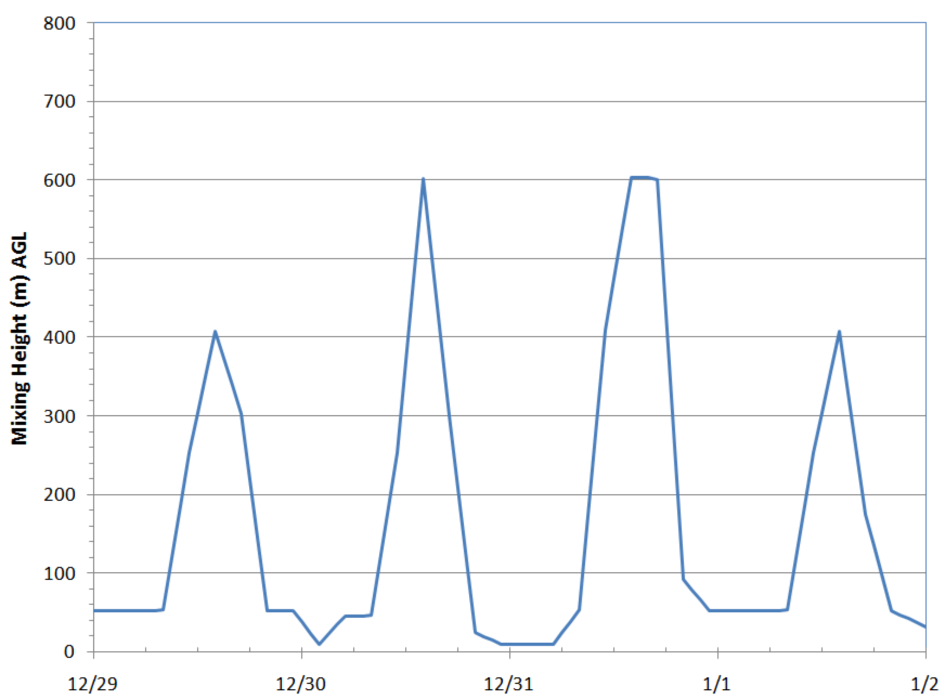

Figure 4-42. Sunland Park mixing heights from the NAM-12km model

Backtrajectories based on the NAM model revealed easterly winds early in the episode with a gradual shift in winds toward the south in the early morning hours. Backtrajectories based on single station (6ZG) winds indicate a westerly to southwesterly flow throughout the episode. The figure below shows trajectories generated every hour from 8 pm on December 31 to 4 am on January 1st.

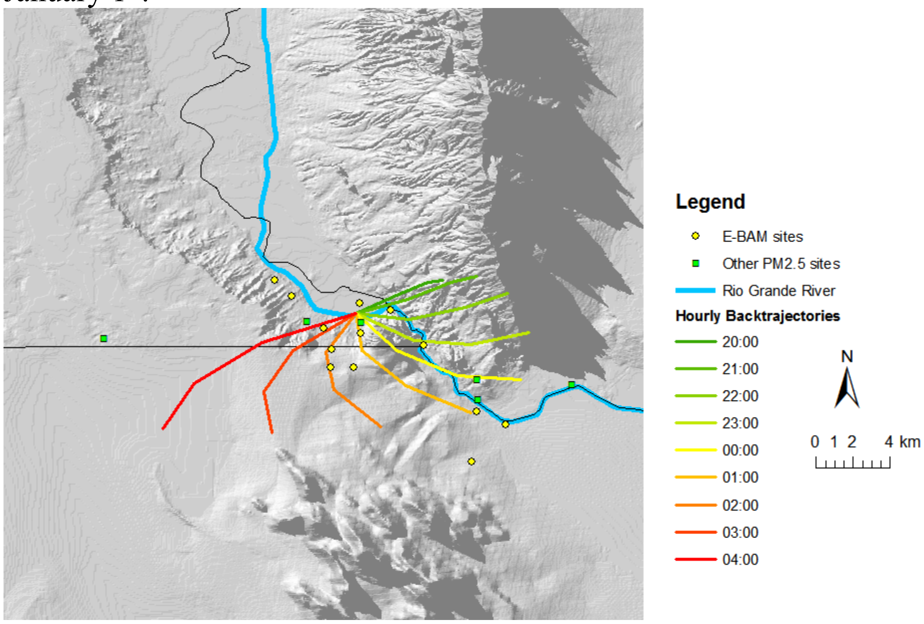

Figure 4-43. Backtrajectories during the episode generated using the 12-km NAM model

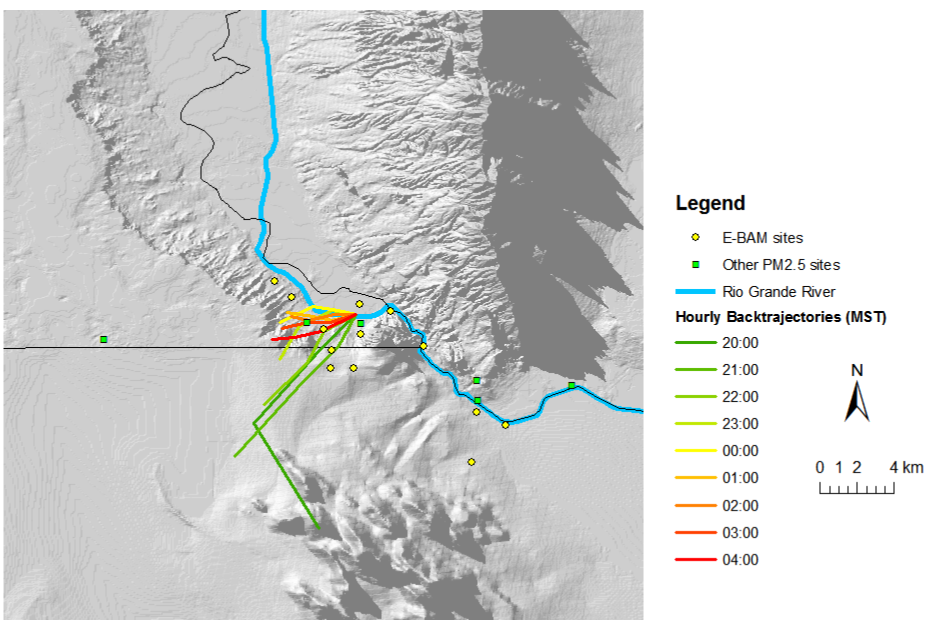

Figure 4-44. Backtrajectories during the episode generated using hourly 6ZG wind data

The following figure shows spatial plots of hourly $PM_{2.5}$ during the episode.

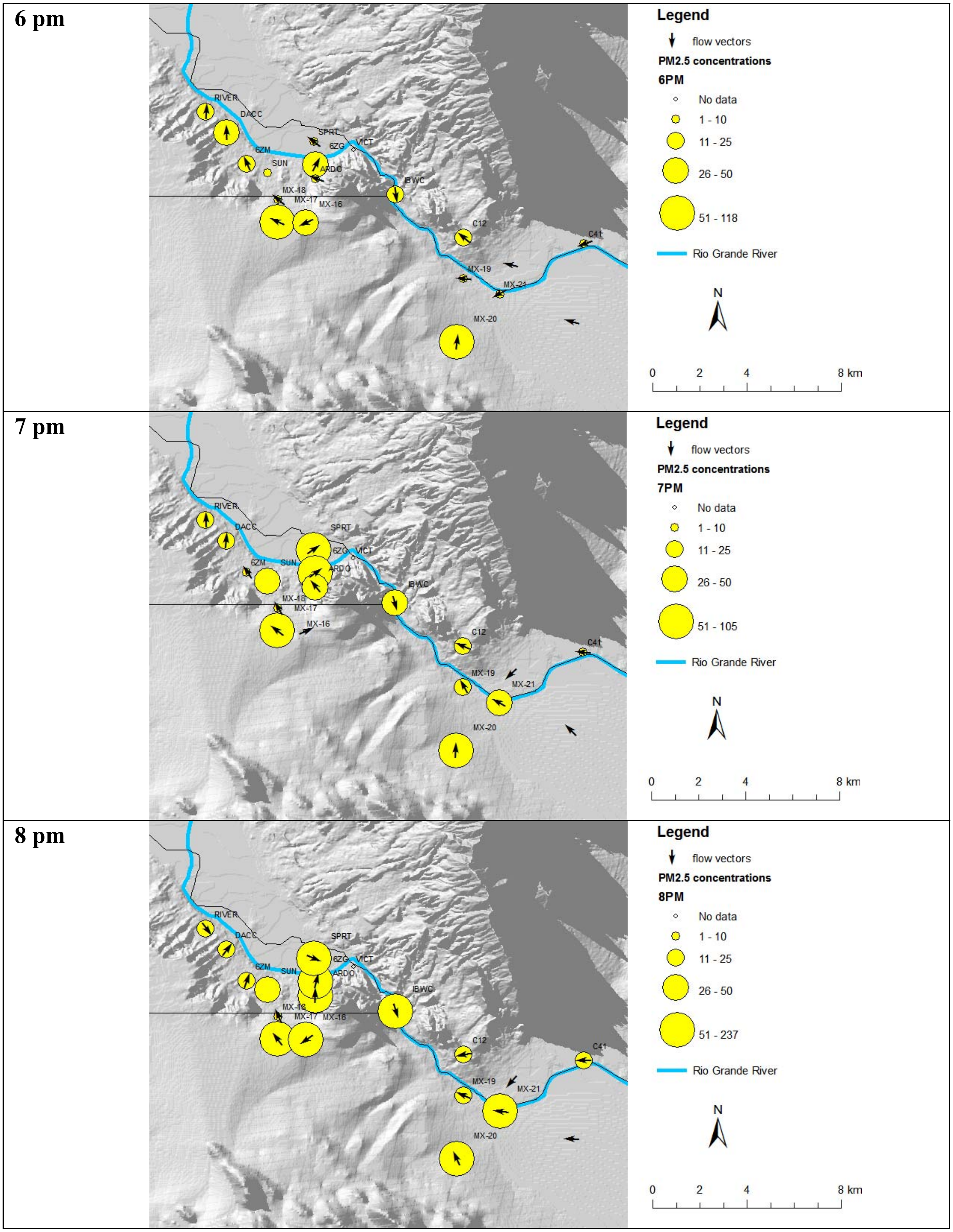

Figure 4-45. Spatial plots of hourly $PM_{2.5}$ during the episode from 6 to 8 pm

9 pm

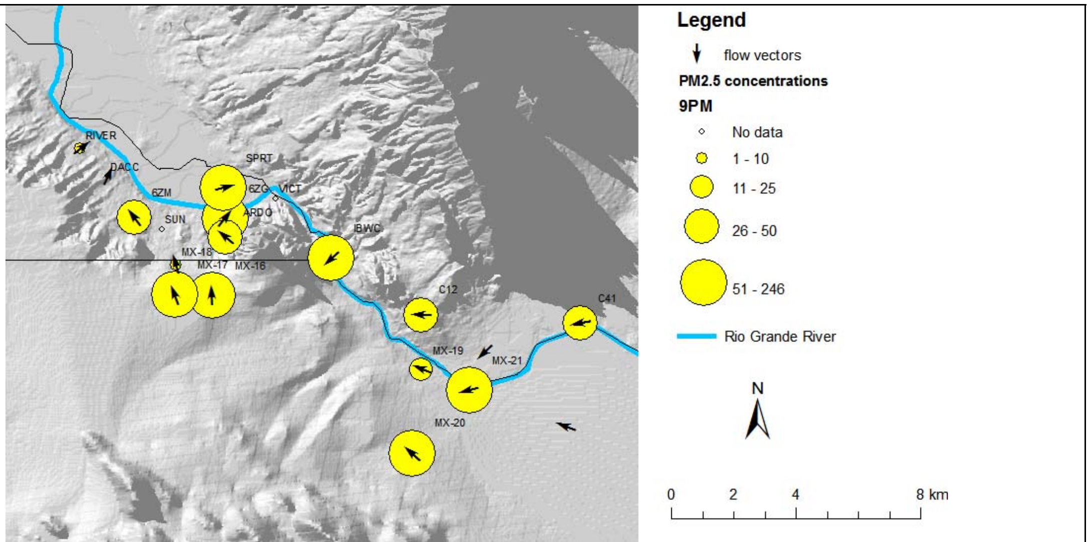

10 pm

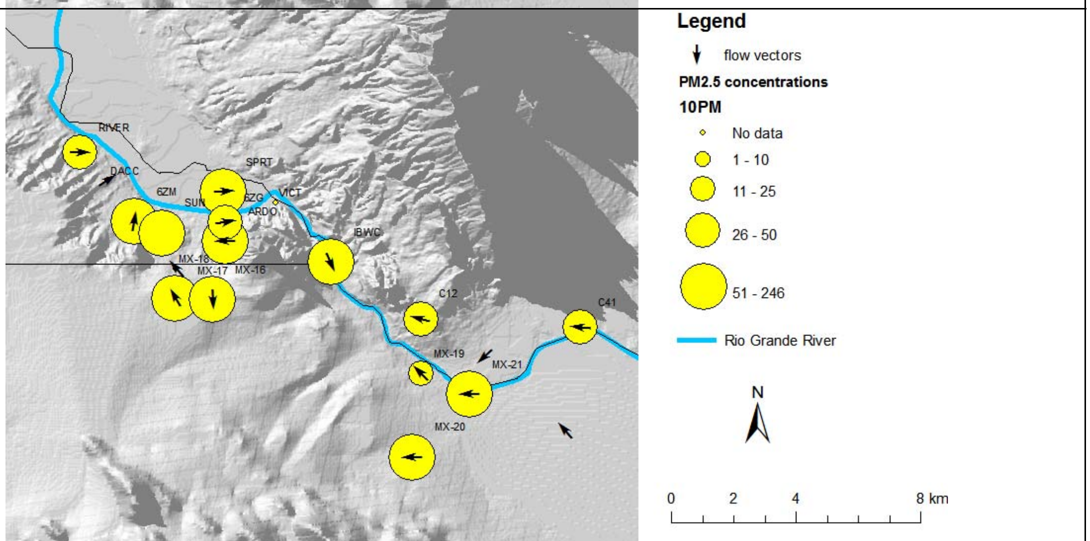

11 pm

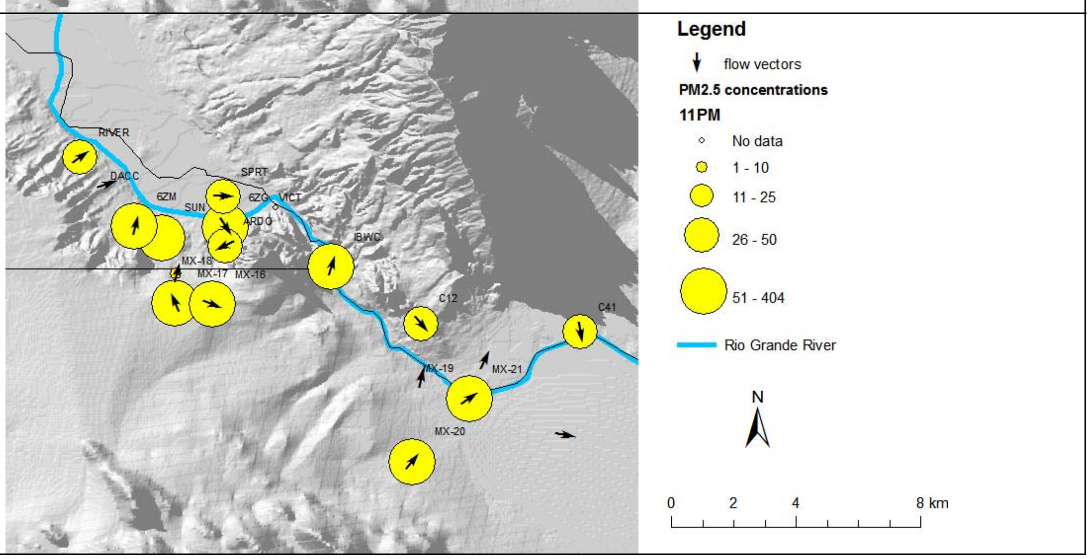

Figure 4-46. Spatial plots of hourly $PM_{2.5}$ during the episode from 9 to 11 pm

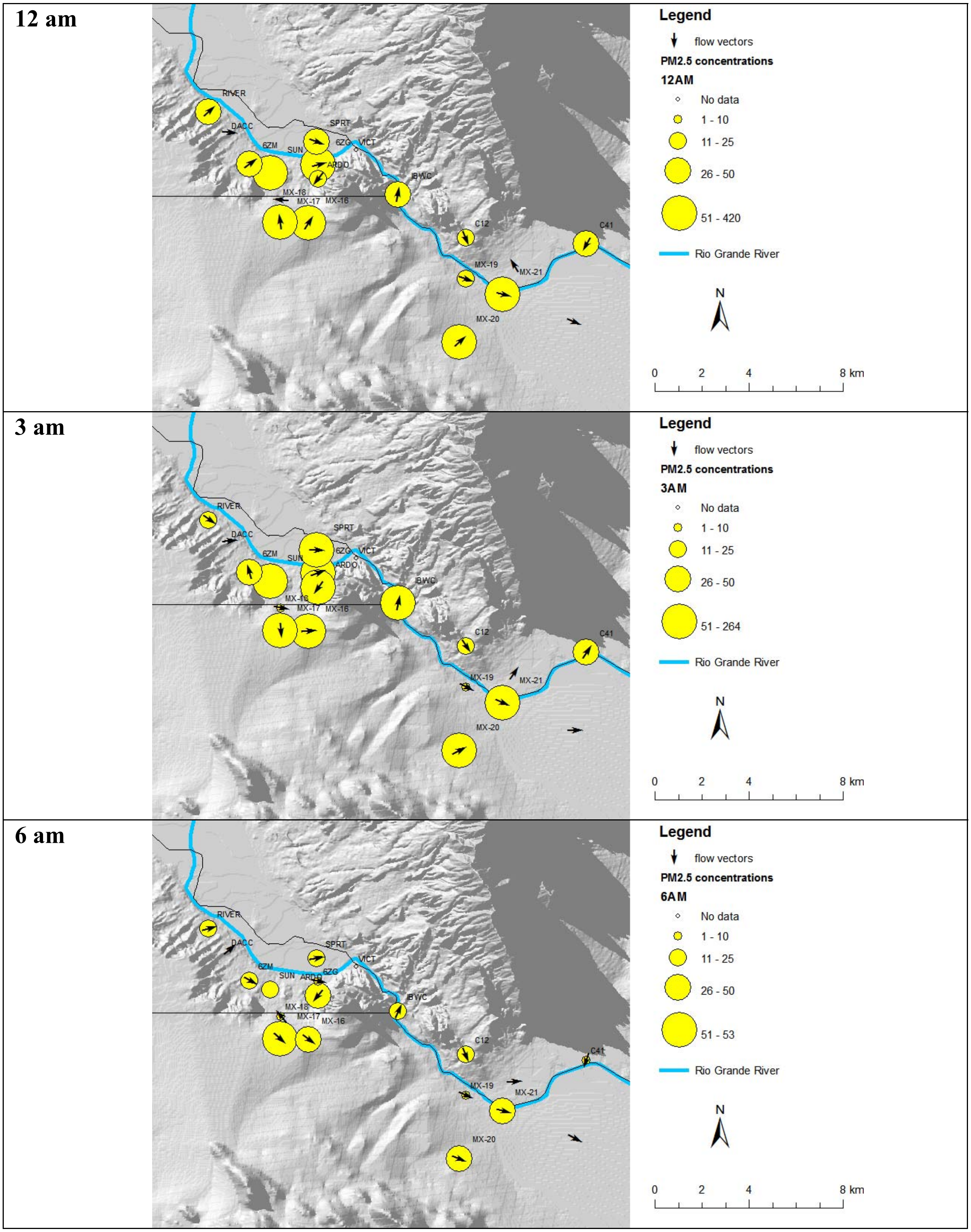

Figure 4-47. Spatial plots of hourly $PM_{2.5}$ during the episode from 12 to 6 am

4.3.2 Episode 2: November 22, 2008

This episode occurred during the evening of November 22, 2008 and continued to the next morning. Peak hourly $PM_{2.5}$ at the Sunland Park City Yard site occurred at 6 pm and remained above 50 µg/m^3 throughout the evening until after midnight. This was one of the longest episodes observed during the study at 9 hours long. The MX-20 site recorded very high $PM_{2.5}$ during this episode reaching hourly concentrations in excess of 200 µg/m^3 during two hours. It is noteworthy that the Desert View Elementary site 6ZM also recorded high concentrations near 30 µg/m^3 on this date.

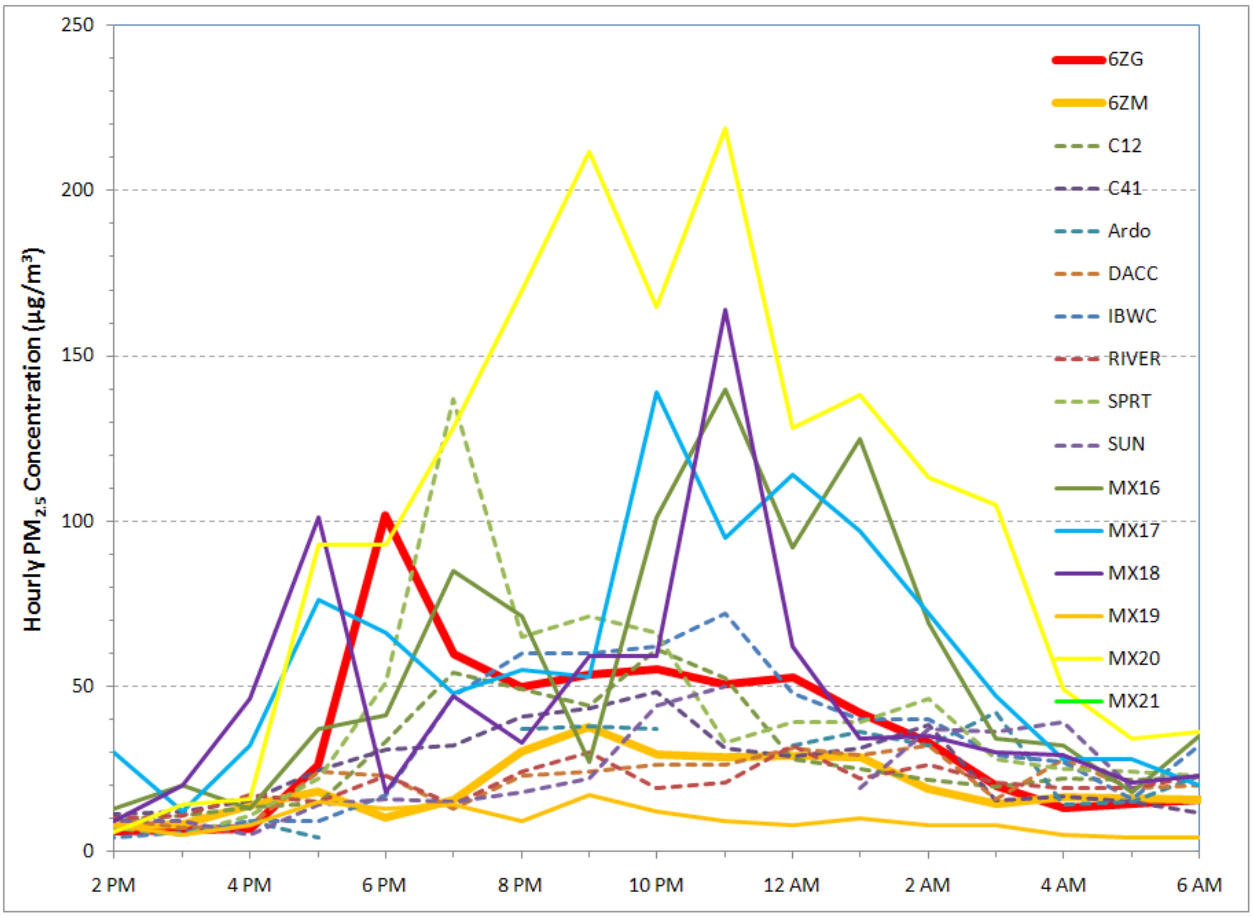

Figure 4-48. Hourly $PM_{2.5}$ during the November episode. The two NMED sites are shown as the thick lines. New Mexico E-BAM sites are indicated by dashed lines and Mexican E-BAM sites are thin continuous lines.

Table 4-4. $PM_{2.5}$ data during the November 22, 2008 episode

Time (MST)	6ZG	6ZM	C12	C41	Ardo	DACC	IBWC	RIVER	SPRT	SUN	VICT	MX16	MX17	MX18	MX19	MX20	MX21
11/22/2008 11:00	8	11	7	9	17	17	13		14	35		29	60	34	6	12	
11/22/2008 12:00	7	10	13	11	16		10	10	13	19		24	2	20	3	19	
11/22/2008 13:00	7	9	9	12	9	12	12	0	13	11		20	29	19		17	
11/22/2008 14:00	6	8	9	11		10	4	10	7	9		13	30	9	8	6	
11/22/2008 15:00	6	8	11	12		7	6	11	5	9		20	12	20	5	14	
11/22/2008 16:00	7	14	13	15	9	8	9	17	11	5		13	32	46	8	16	
11/22/2008 17:00	26	18	15	25	4	24	9	15	22	14		37	76	101	15	93	
11/22/2008 18:00	102	10	33	31		23	17	23	51	16		41	66	18	13	93	
11/22/2008 19:00	60	16	54	32		13	47	14	137	15		85	48	47	14	128	
11/22/2008 20:00	50	30	49	41	37	23	60	24	65	18		71	55	33	9	170	
11/22/2008 21:00	54	38	44	43	38	24	60	30	71	22		27	53	59	17	212	
11/22/2008 22:00	55	29	61	48	37	26	62	19	66	44		101	139	59	12	165	
11/22/2008 23:00	51	28	52	31		26	72	21	33	50		140	95	164	9	219	
11/23/2008 0:00	53	29	28	29	32	31	48	32	39			92	114	62	8	128	
11/23/2008 1:00	42	28	25	31	36	29	40	22	39	19		125	97	34	10	138	
11/23/2008 2:00	33	19	22	38	32	32	40	26	46	37		69	72	35	8	113	
11/23/2008 3:00	20	14	20	15	42	16	29	21	28	36		34	47	30	8	105	
11/23/2008 4:00	13	17	22	17	14	28	27	19	25	39		32	28	29	5	49	
11/23/2008 5:00	14	16	22	15	15	19	16	19	24	19		18	28	21	4	34	
11/23/2008 6:00	16	16	22	12	23	20	32	23	23			35	20	23	4	36	
11/23/2008 7:00	22	16	23	25	27	23	35	16	28	7		38	73	38	9	65	
11/23/2008 8:00	18	21	26	22	17	18	11	8	13	21		37	74	2	12	46	
11/23/2008 9:00	16	17	24	11	26	20	16	26	13	16		37	60	17		47	
11/23/2008 10:00	11	14	23	22	0	22	22	18	12	32		43	58	28	7	43	
11/23/2008 11:00	4	5	6	15	19	18	20	14	7	28		31	30	23	0	57	

Mixing heights were very low in the morning the day of the episode reaching a minimum of 10 meters by 5 am on November 22. During the day mixing heights climbed no more than around 600 meters by 2 pm. During the episode the mixing height began at 288 m at 6 pm and diminished to 47 m by midnight.

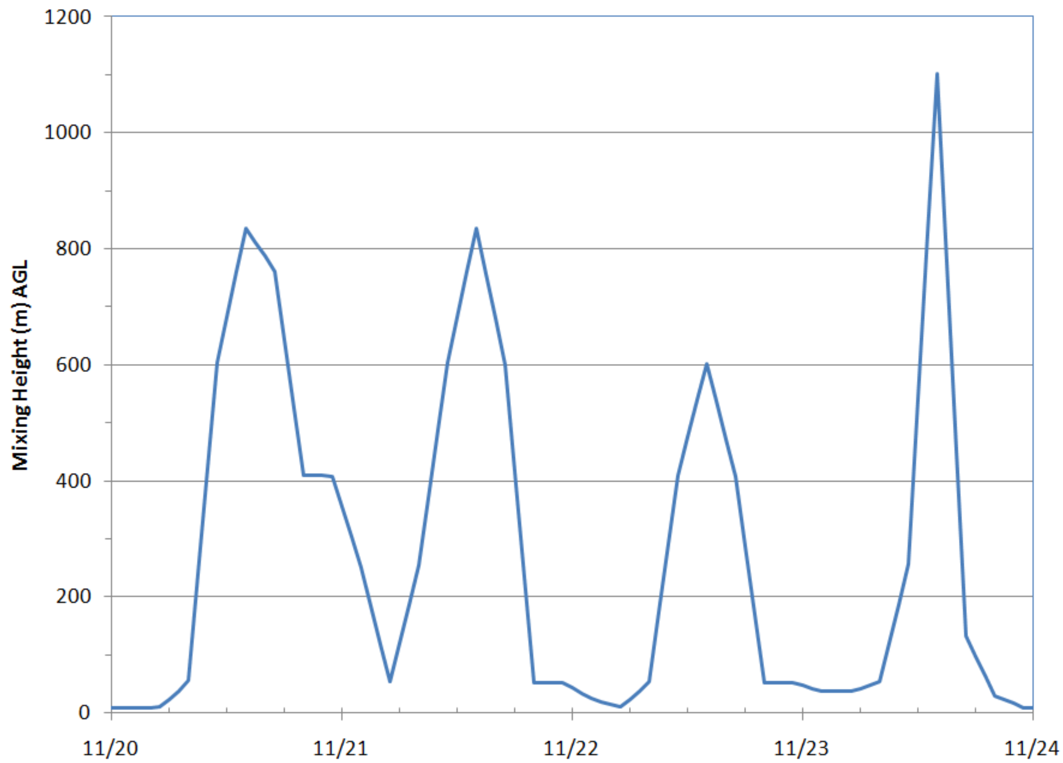

Figure 4-49. Mixing heights during the November episode

Backtrajectories revealed easterly winds early in the episode with a gradual shift in winds toward the south in the early morning hours.

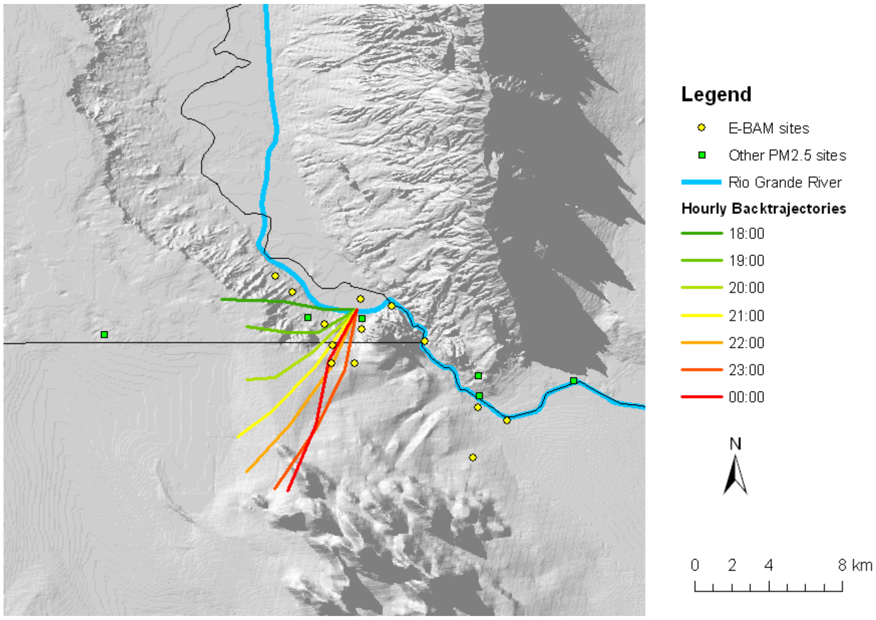

Figure 4-50. Backtrajectories during this episode based on the 12-km NAM model

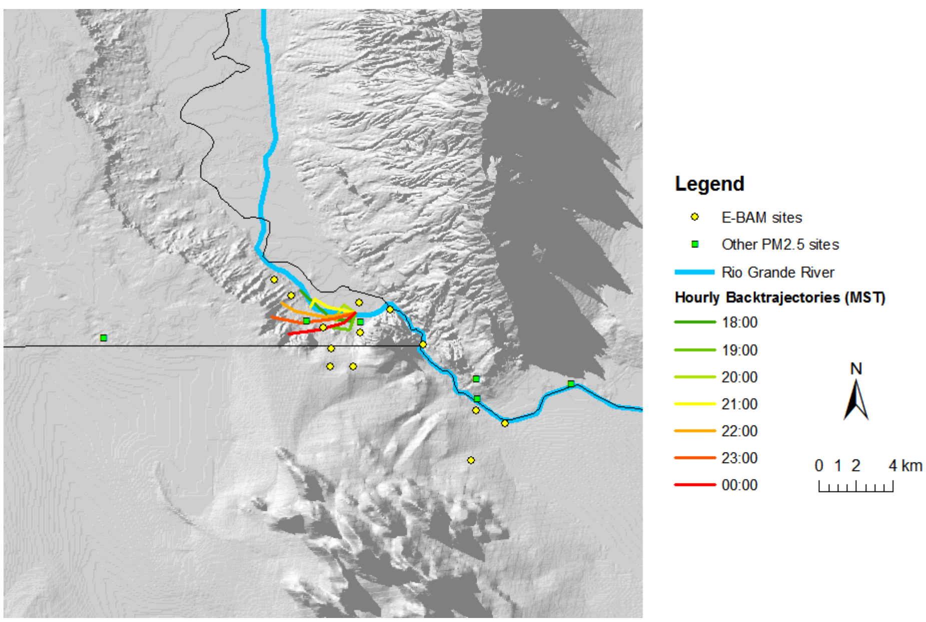

Figure 4-51. Backtrajectories during this episode based on winds from 6ZG

Spatial plots of hourly $PM_{2.5}$ during the episode are shown in the following figures.

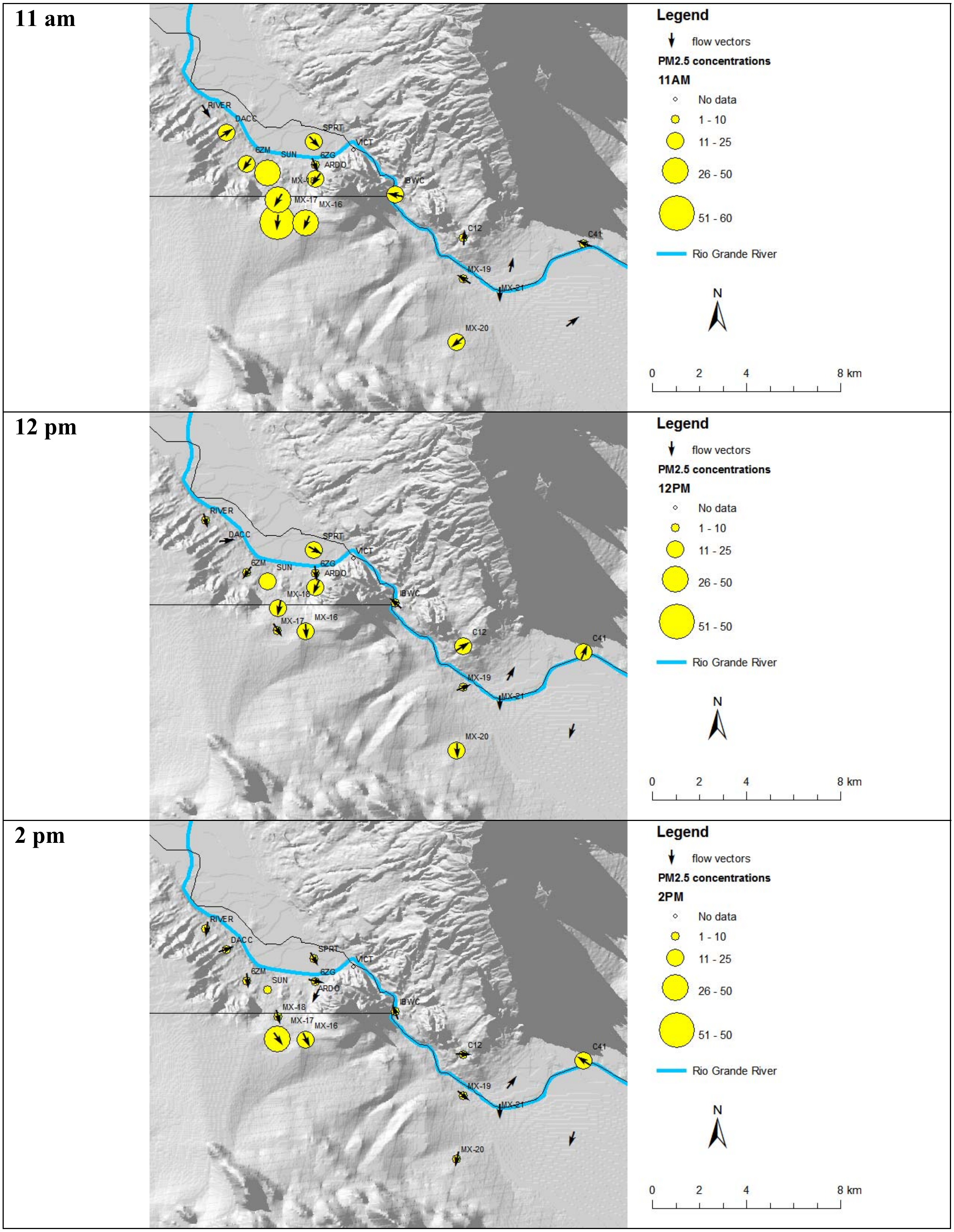

Figure 4-52. Spatial plots of hourly $PM_{2.5}$ during this episode from 11 am to 2 pm

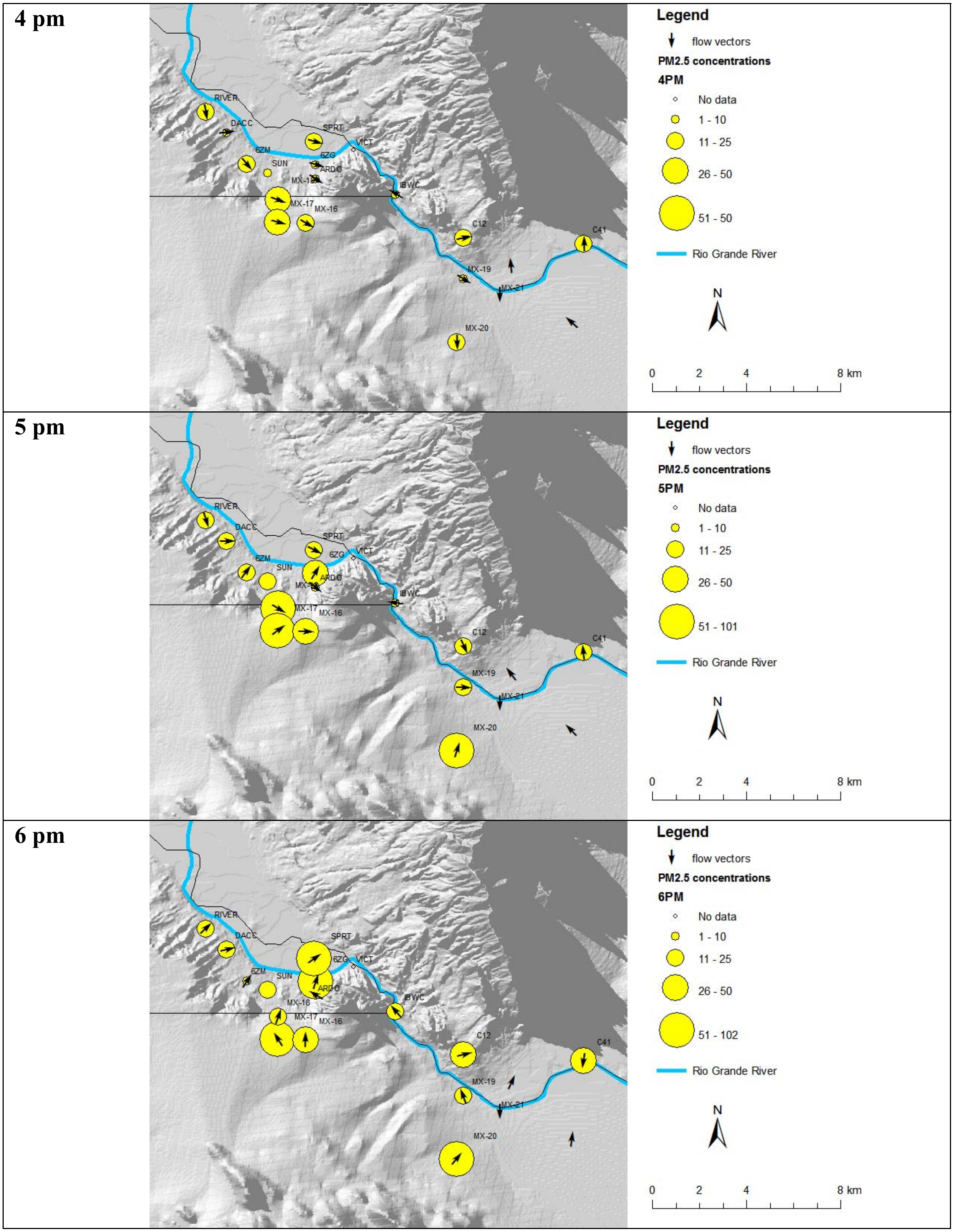

Figure 4-53. Spatial plots of hourly $PM_{2.5}$ during this episode from 4 pm to 6 pm

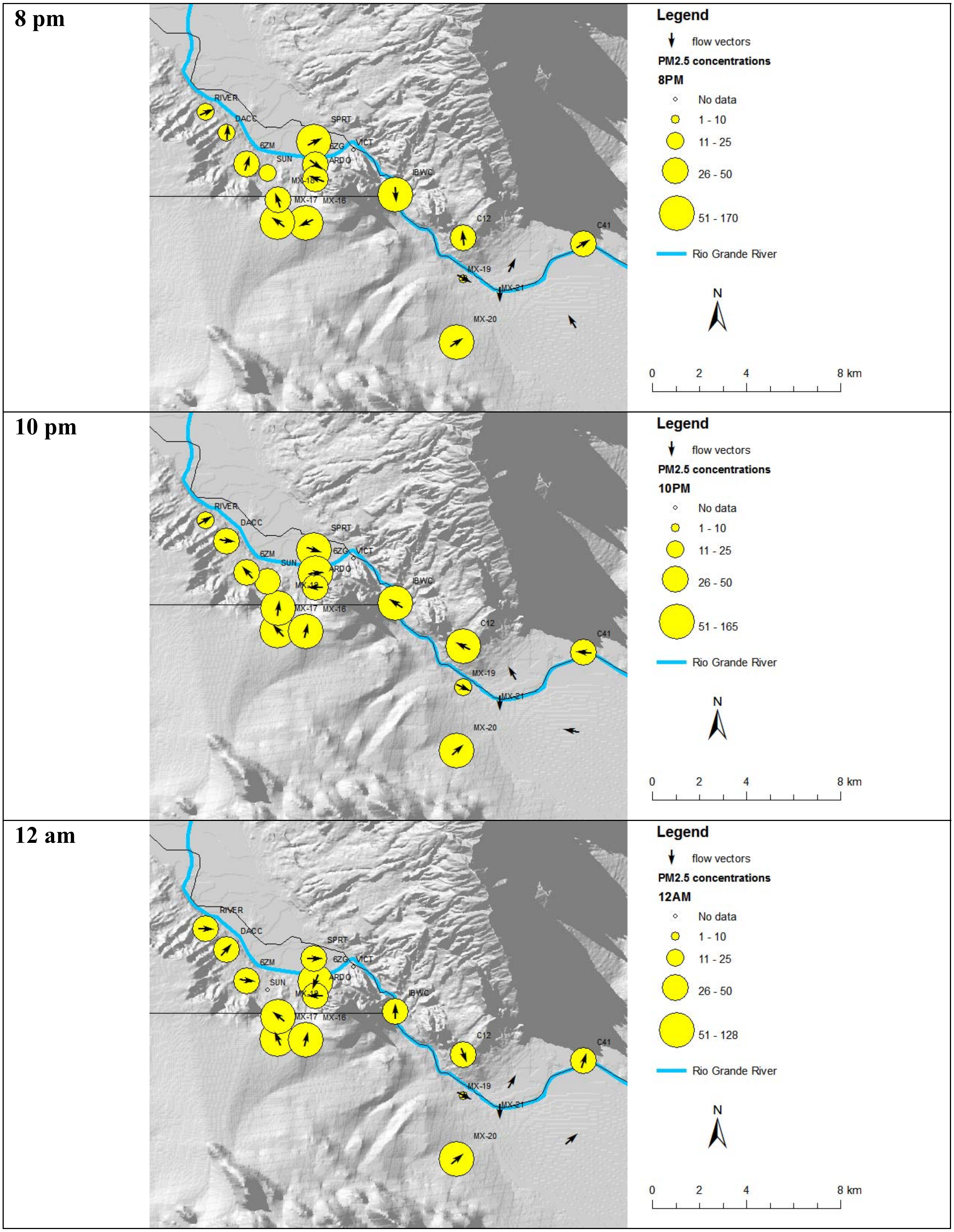

Figure 4-54. Spatial plots of hourly $PM_{2.5}$ during this episode from 8 pm to 12 am

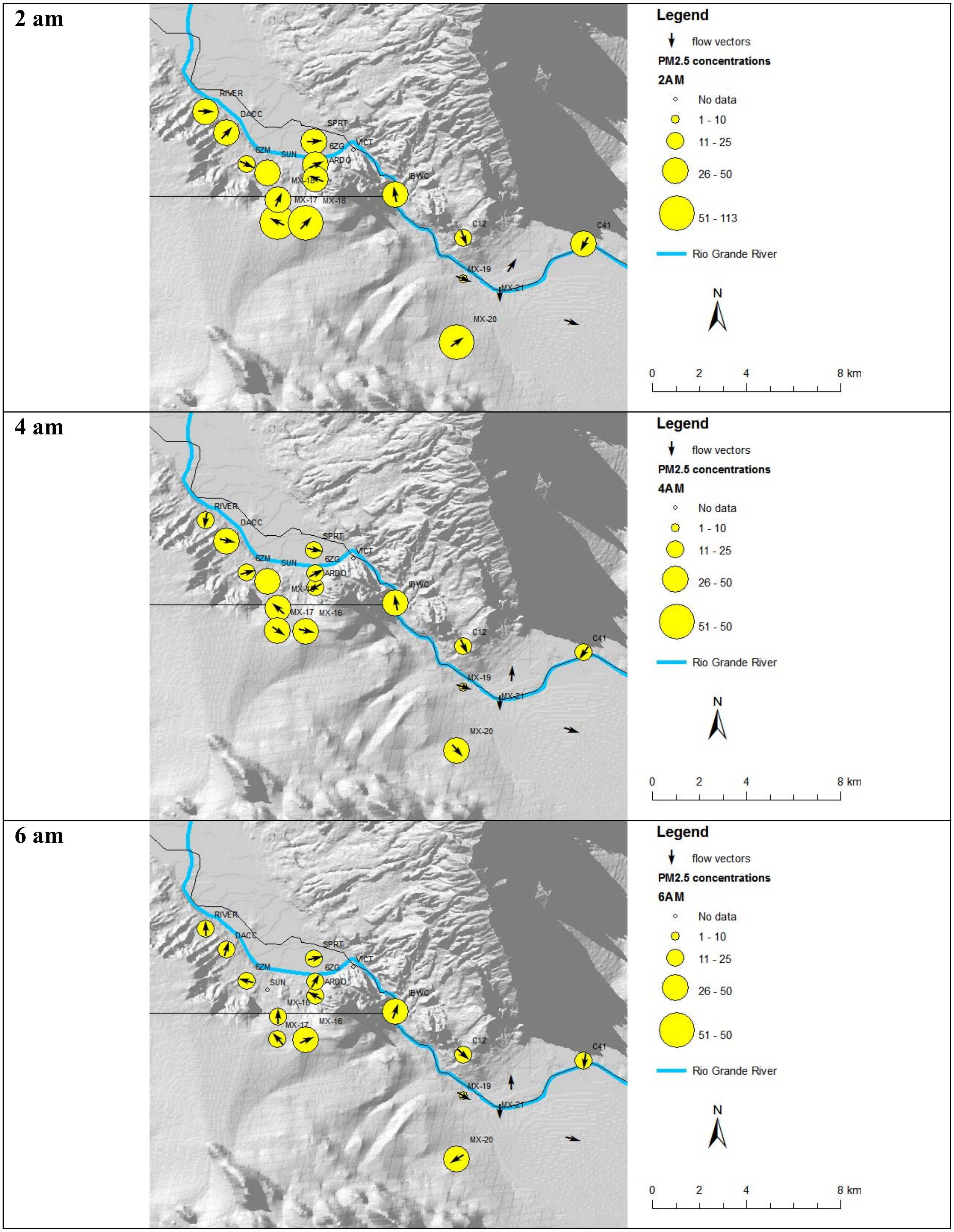

Figure 4-55. Spatial plots of hourly $PM_{2.5}$ during this episode from 2 am to 6 am

4.3.3 Episode 3: December 29, 2008

This episode occurred during the evening of December 29, 2008 and continued to the next morning. Peak hourly $PM_{2.5}$ at the Sunland Park City Yard site occurred at 8 pm and rose to the 50 µg/m^3 level from 8 to 11 pm.

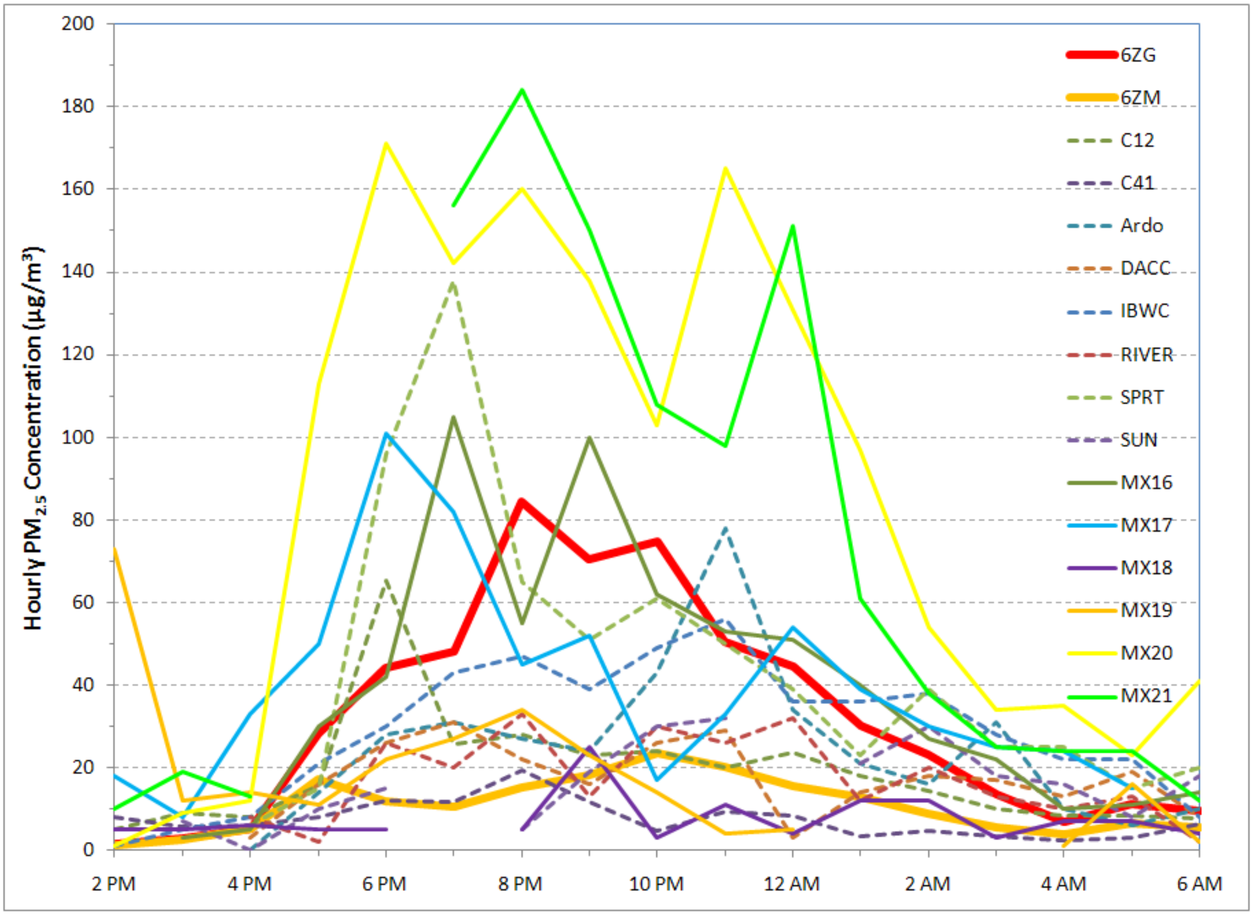

Figure 4-56. Hourly $PM_{2.5}$ during the December 29 episode. The two NMED sites are shown as the thick lines. New Mexico E-BAM sites are indicated by dashed lines and Mexican E-BAM sites are thin continuous lines.

Table 4-5 $PM_{2.5}$ concentrations leading to, during and after the episode

Date	LocalTime	6ZG	6ZM	C12	C41	Ardo	DACC	IBWC	RIVER	SPRT	SUN	VICT	MX16	MX17	MX18	MX19	MX20	MX21
12/29/2008	12/29/2008 14:00	1	1	5	8			1	8	0				18	5	73	1	10
12/29/2008	12/29/2008 15:00	3	2	9	6			5			7		3	8	5	12	9	19
12/29/2008	12/29/2008 16:00	5	5	8	6	0	3	8	8	6	0		5	33	6	14	12	13
12/29/2008	12/29/2008 17:00	28	17	16	8	14	16	21	2	15	10		30	50	5	11	113	
12/29/2008	12/29/2008 18:00	44	12	65	12	28	26	30	26	96	15		42	101	5	22	171	
12/29/2008	12/29/2008 19:00	48	11	26	12	31	31	43	20	138			105	82		27	142	156
12/29/2008	12/29/2008 20:00	84	15	28	19	27	22	47	33	65	5		55	45	5	34	160	184
12/29/2008	12/29/2008 21:00	70	18	23	12	24	16	39	13	51	19		100	52	25	23	138	150
12/29/2008	12/29/2008 22:00	75	24	24	5	43	26	49	30	61	30		62	17	3	14	103	108
12/29/2008	12/29/2008 23:00	51	20	20	9	78	29	56	26	50	32		53	33	11	4	165	98
12/30/2008	12/30/2008 0:00	44	15	24	8	34	3	36	32	39			51	54	4	5	131	151
12/30/2008	12/30/2008 1:00	30	13	18	3	21	14	36	12	23	21		40	39	12		97	61
12/30/2008	12/30/2008 2:00	23	9	14	5	16	18	38	20	39	30		27	30	12	15	54	38
12/30/2008	12/30/2008 3:00	13	5	10	3	31	17	28	13	25	18		22	25	3		34	25
12/30/2008	12/30/2008 4:00	7	4	8	2	10	13	22	10	25	16		10	24	7	1	35	24
12/30/2008	12/30/2008 5:00	11	6	8	3	6	19	22	13	15	8		11	15	7	16	23	24
12/30/2008	12/30/2008 6:00	9	6	8	6	10	8	8	2	20	18		14		4	2	41	12

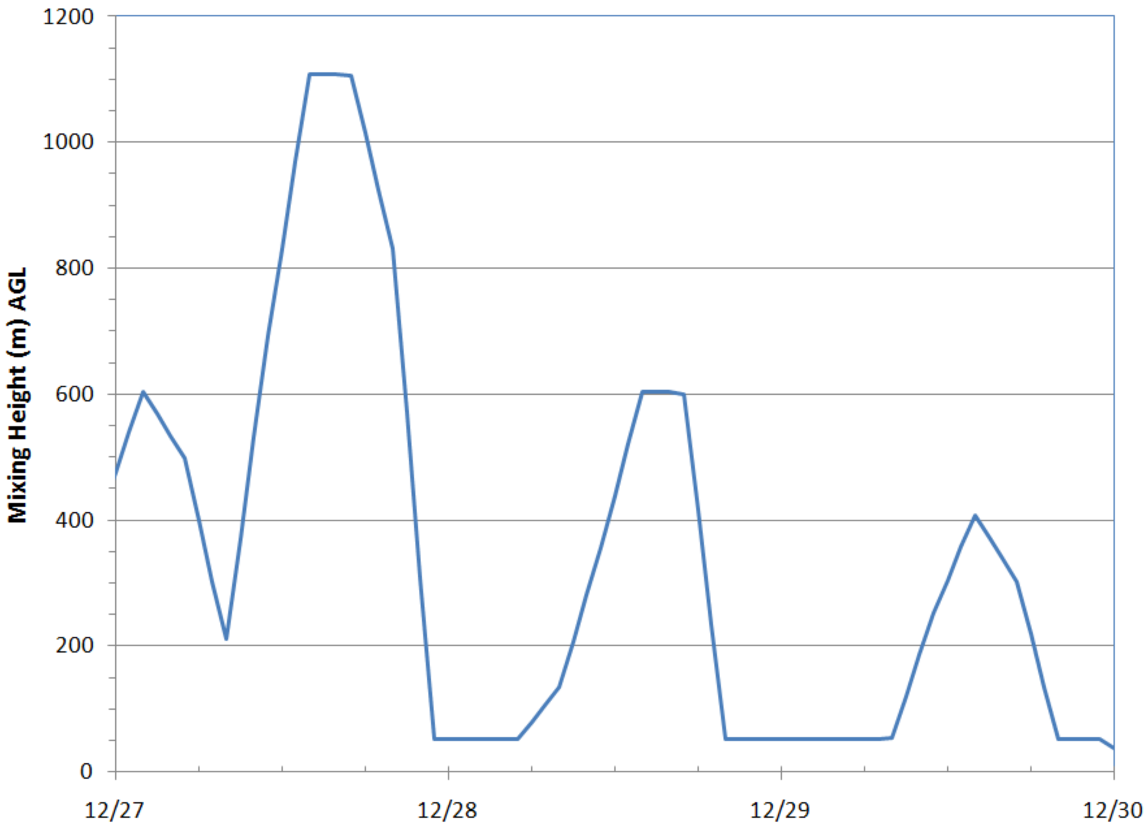

Figure 4-57. Mixing heights leading up to and during the episode based on the 12-km NAM model

Backtrajectories from the 12-km NAM model produced winds from the north to northeast sector throughout the episode.

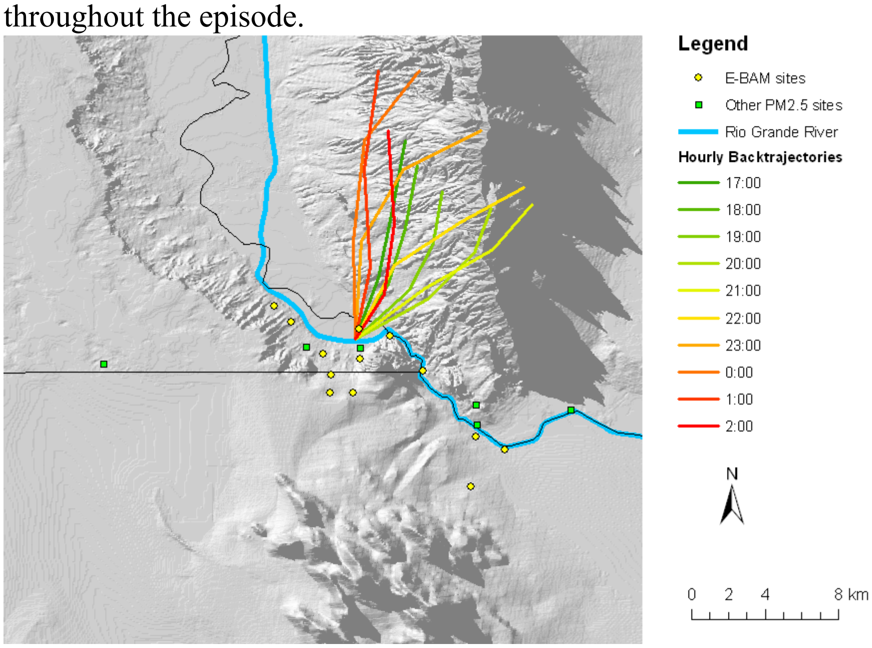

Figure 4-58. Backtrajectories during the December 29 episode based on the 12-km NAM

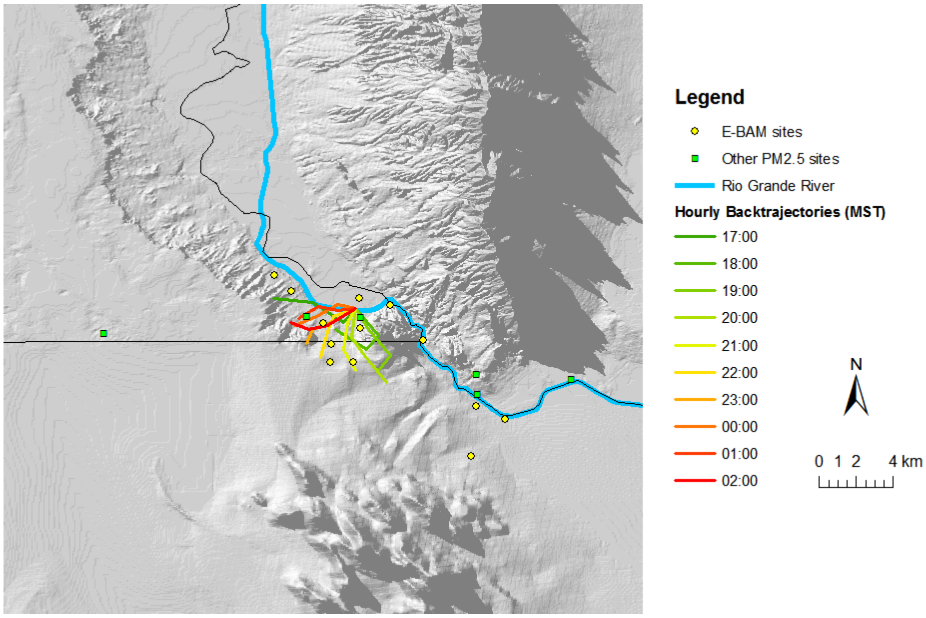

Figure 4-59. Backtrajectories during the December 29 episode based on 6ZG winds

However, winds from the model were considerably different from the winds observed at the SPCY and E-BAM monitoring sites. The map below sheds light on why the model trajectories are in error. Winds near the river valley were complicated and are terrain following while the winds outside of the Paso del Norte have an northeasterly component. This figure shows wind flow vectors at 8 pm and indicates some downslope winds where the winds flow from higher to lower terrain elevations.

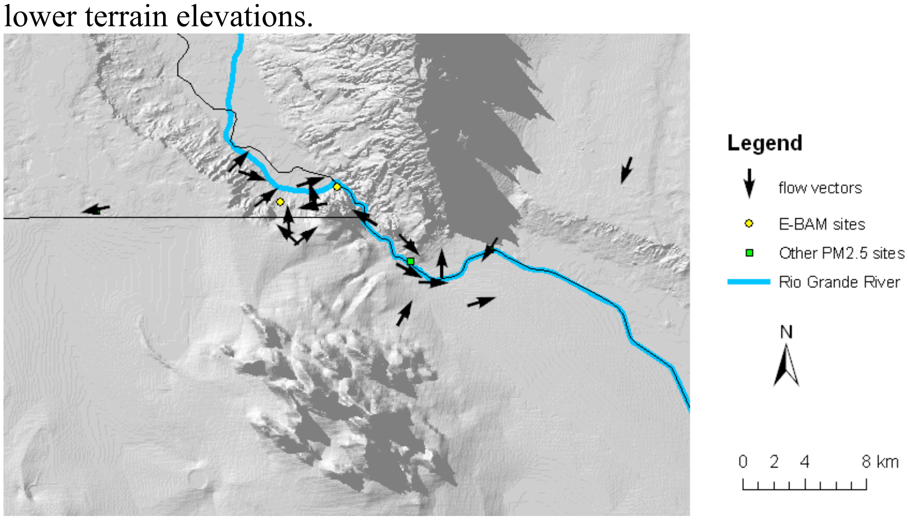

Figure 4-60. Flow vectors at 8 pm on December 29, 2008

Because of the low winds and the terrain effects, the NAM model does capture this episode well. The radar wind profiler located on the UTEP campus and collocated with the C12 site, does not capture the detailed downslope winds at the surface. The profiler shows light northeast winds at the lowest levels and southerly winds aloft at 1 km above the surface.

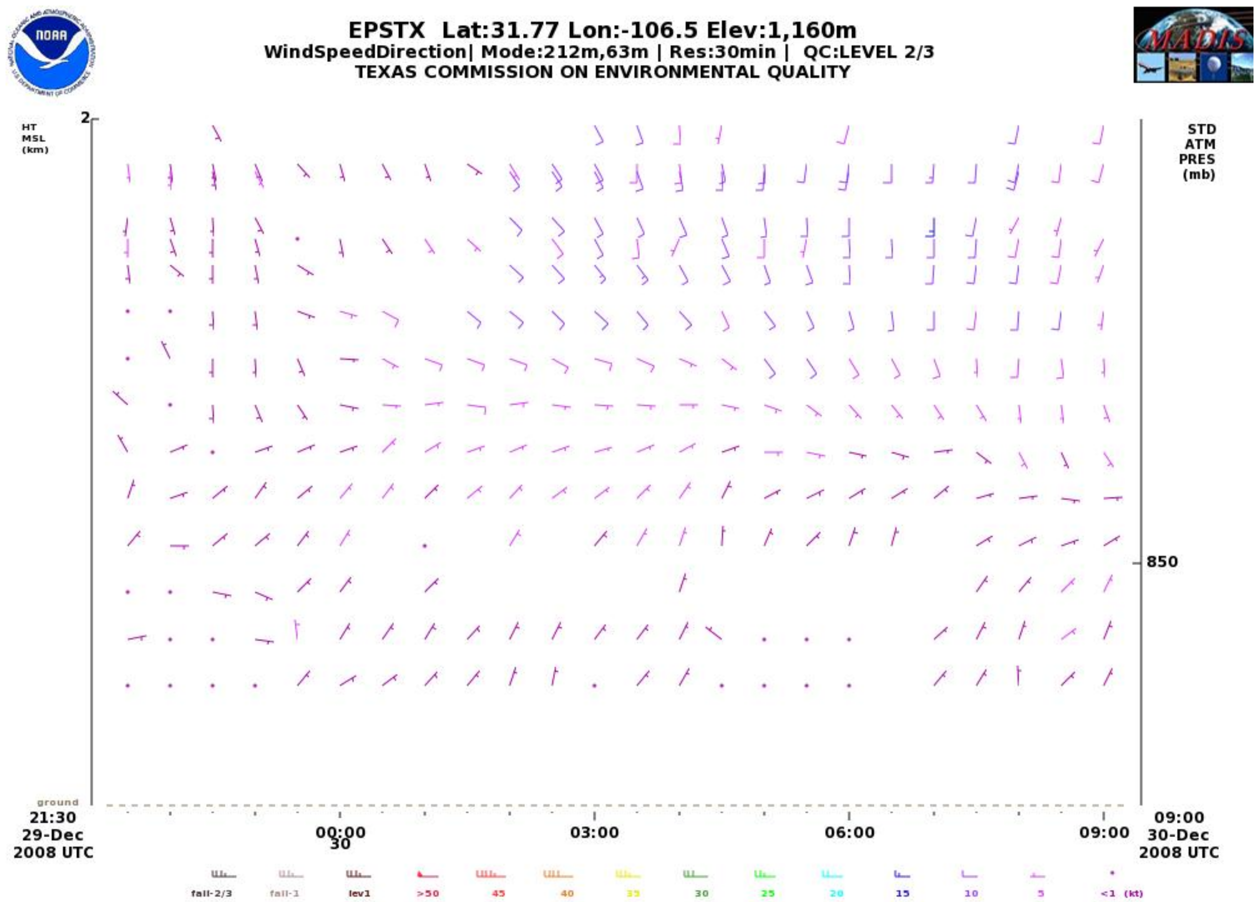

Figure 4-61. TCEQ radar wind profiler collocated with C12 site from 21:30 to 09:00 UTC

An important observation here with the profiler is that these low-wind patterns in the Paso del Norte are located in a very shallow layer that are not captured by routine forecast models.

Spatial plots of hourly $PM_{2.5}$ during the episode are shown in the following figures.

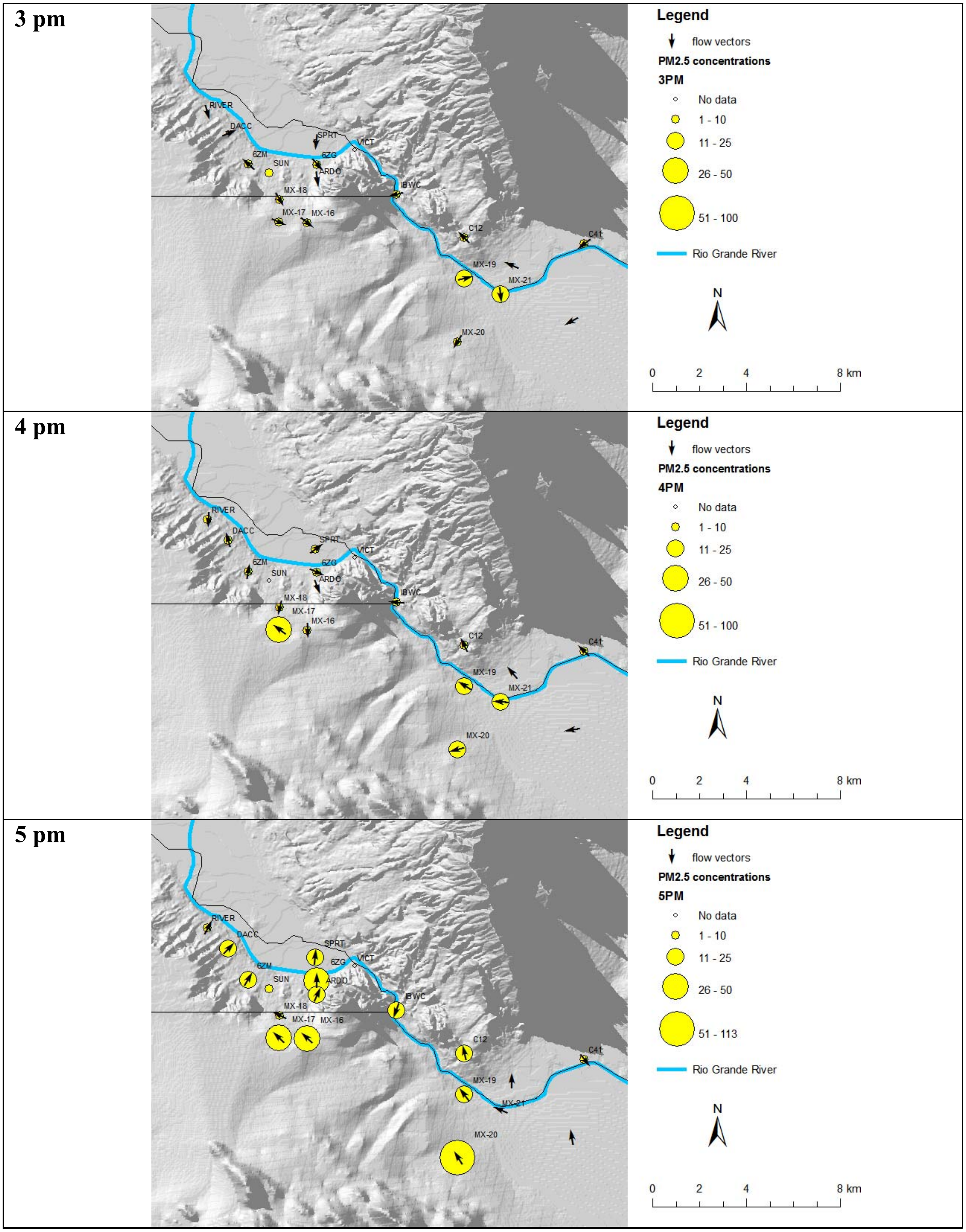

Figure 4-62. Spatial plots of hourly $PM_{2.5}$ during this episode from 3 pm to 5 pm

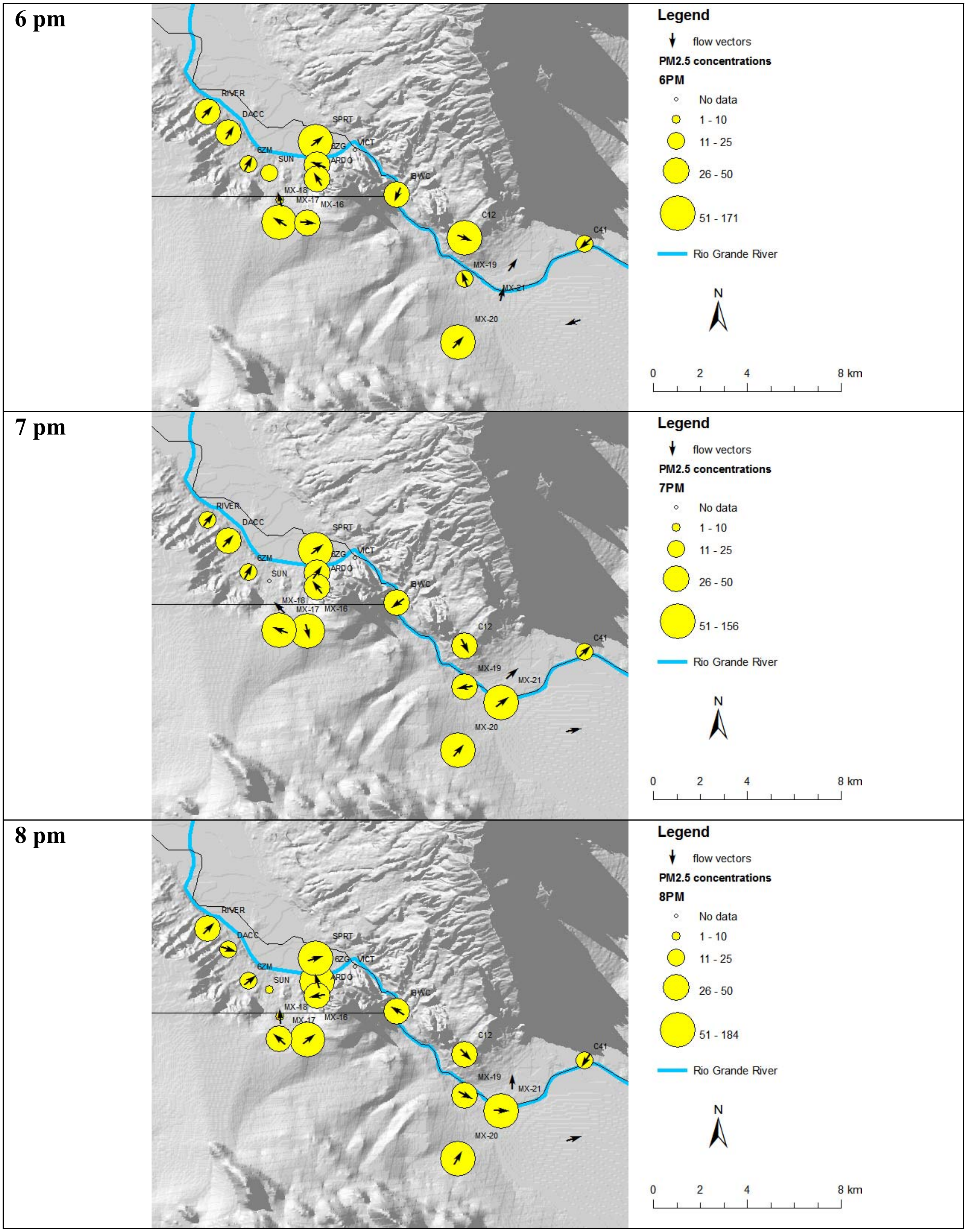

Figure 4-63. Spatial plots of hourly $PM_{2.5}$ during this episode from 6 pm to 8 pm

9 pm

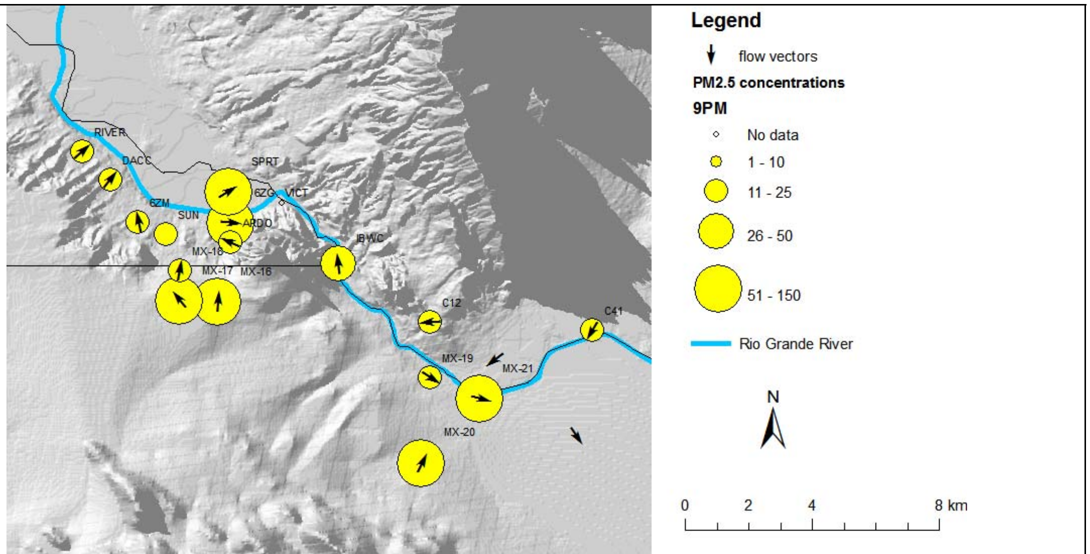

11 pm

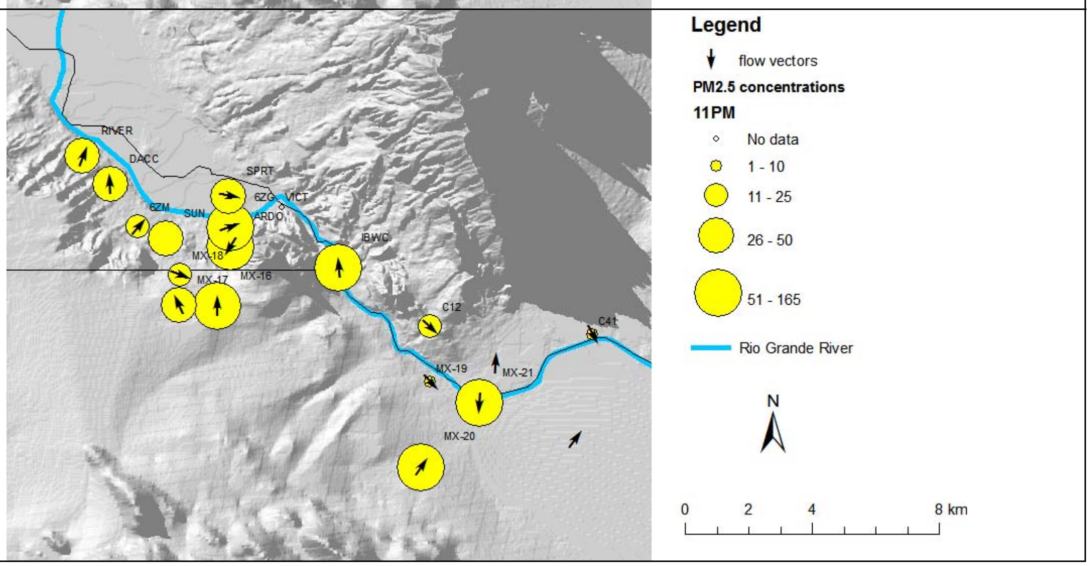

Figure 4-64. Spatial plots of hourly $PM_{2.5}$ during this episode from 9 pm to 11 pm

4.3.4 Episode 4: January 19, 2009

This episode occurred during the late afternoon and evening of January 19, 2009. A peak hourly PM2.5 of 110 µg/m^3 at the Sunland Park City Yard site occurred at 6 pm and remained above the 50 µg/m^3 level till 10 pm. This episode was unique in that the SPCY site recorded some of the highest PM2.5 concentrations within the network.

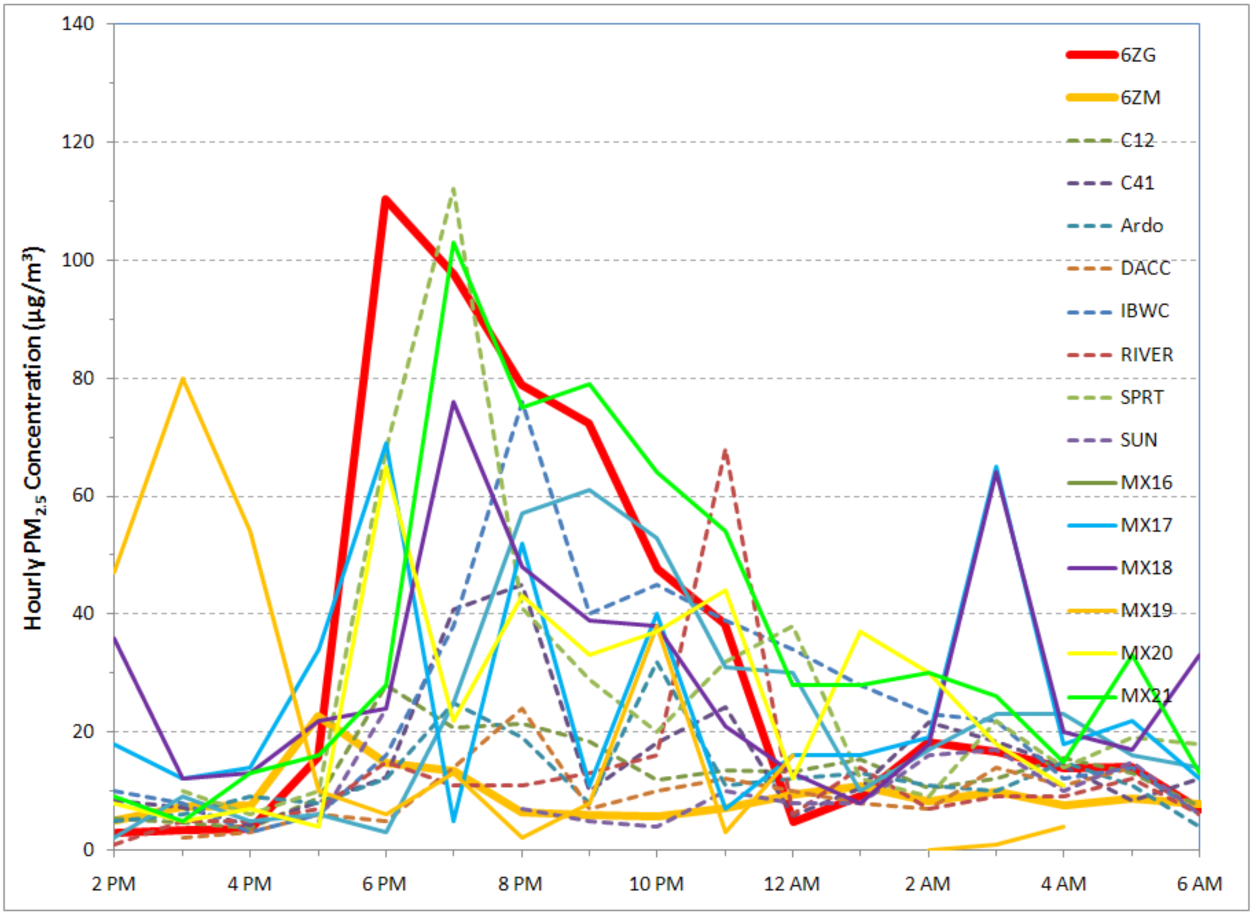

Figure 4-65. Hourly $PM_{2.5}$ concentrations during the January 19 episode. The two NMED sites are shown as the thick lines. New Mexico E-BAM sites are indicated by dashed lines and Mexican E-BAM sites are thin continuous lines.

There was no data for site MX-16 during this episode.

Table 4-6. $PM_{2.5}$ concentrations during the January 19 episode. Highlighted area shows episode defined for 6ZG concentrations greater than 50 $\mu g/m^3$. No data for site MX-16 was available during this episode

Time	6ZG	6ZM	C12	C41	Ardo	DACC	IBWC	RIVER	SPRT	SUN	VICT	MX16	MX17	MX18	MX19	MX20	MX21
1/19/2009 14:00	3	5	5	8	5		10	1			2		18	36	47	8	9
1/19/2009 15:00	3	7	5	7	6	2	8	5	10	8	9		12	12	80	5	5
1/19/2009 16:00	4	8	4	4	9	3	3	5	6		5		14	13	54	7	13
1/19/2009 17:00	16	23	9	8	8	6	6	7	10	5	6		34	22	10	4	16
1/19/2009 18:00	110	15	28	12	12	5	16	15	68	24	3		69	24	6	65	28
1/19/2009 19:00	98	13	21	41	25	14	38	11	112		25		5	76	13	22	103
1/19/2009 20:00	79	6	21	45	19	24	76	11	41	7	57		52	48	2	43	75
1/19/2009 21:00	72	6	19	10	8	7	40	13	29	5	61		11	39	8	33	79
1/19/2009 22:00	48	6	12	18	32	10	45	16	20	4	53		40	38	38	37	64
1/19/2009 23:00	38	7	13	24	11	12	39	68	32	10	31		7	21	3	44	54
1/20/2009 0:00	5	9	13	6	12	10	34	6	38	8	30		16	13	16	12	28
1/20/2009 1:00	9	11	15	11	13	8	28	14	12	8	10		16	8		37	28
1/20/2009 2:00	18	8	11	22	11	7	23	7	9	16	17		19	18	0	30	30
1/20/2009 3:00	17	10	12	18	10	14	22	9	22	17	23		65	64	1	18	26
1/20/2009 4:00	14	8	16	14	15	11	12	9	14	10	23		18	20	4	11	15
1/20/2009 5:00	14	9	13	8	11	14	14	12	19	15	16		22	17			33

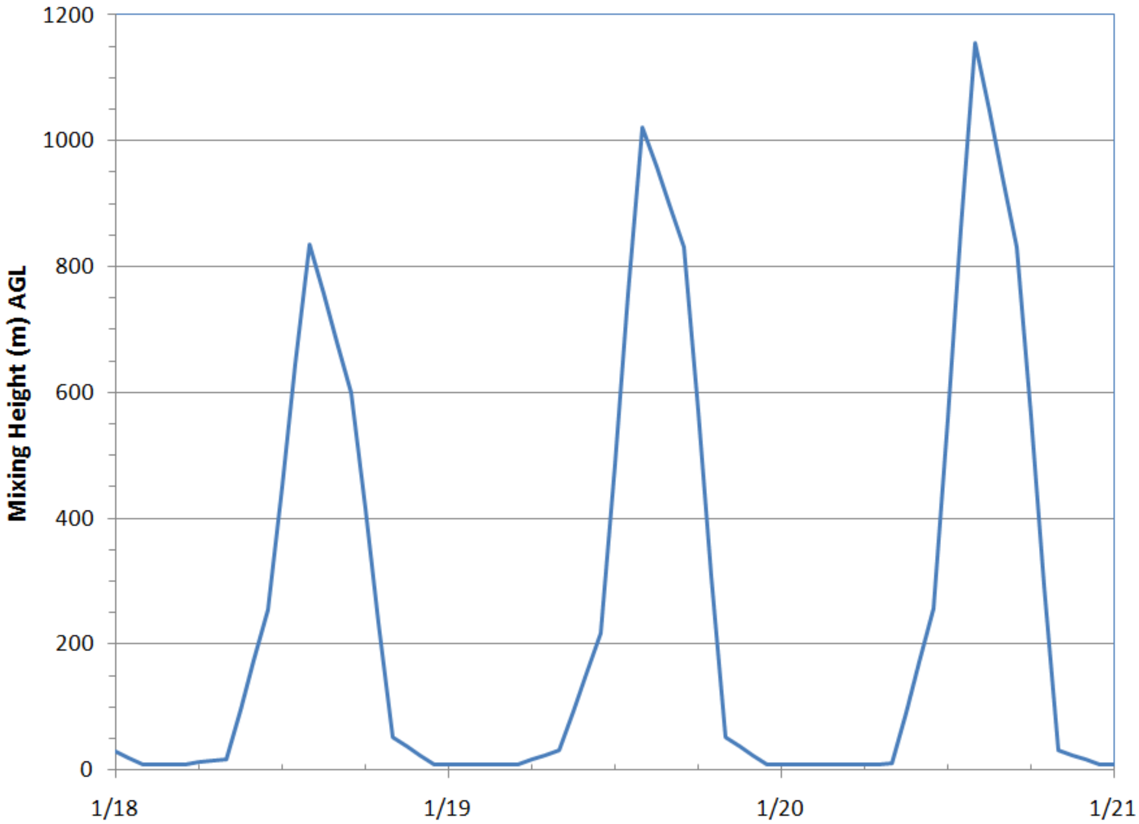

Figure 4-66. Mixing heights before and during the episode based on the 12-km NAM model

Backtrajectories from the 12-km NAM model produced winds from the north to northeast sector throughout this episode.

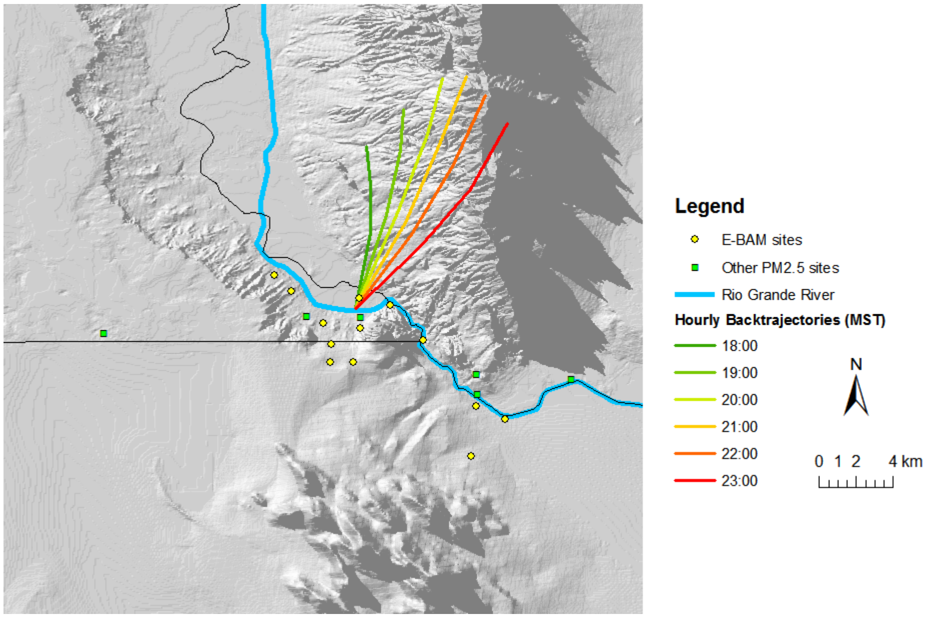

Figure 4-67. Backtrajectories during this episode based on the 12-km NAM model

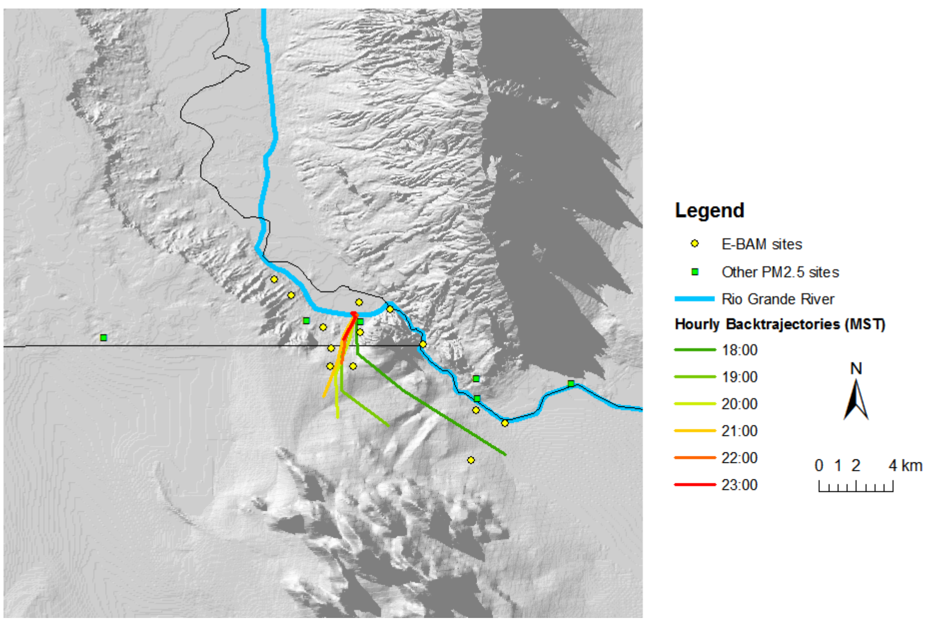

Figure 4-68. Backtrajectories during this episode based on the winds from 6ZG

However, winds from the model were considerably different from the winds observed at the SPCY and E-BAM monitoring sites. Winds near the river valley were terrain following while the winds outside of the Paso del Norte have an northerly component. This figure shows wind flow vectors at 7 pm and shows patterns of downslope winds.

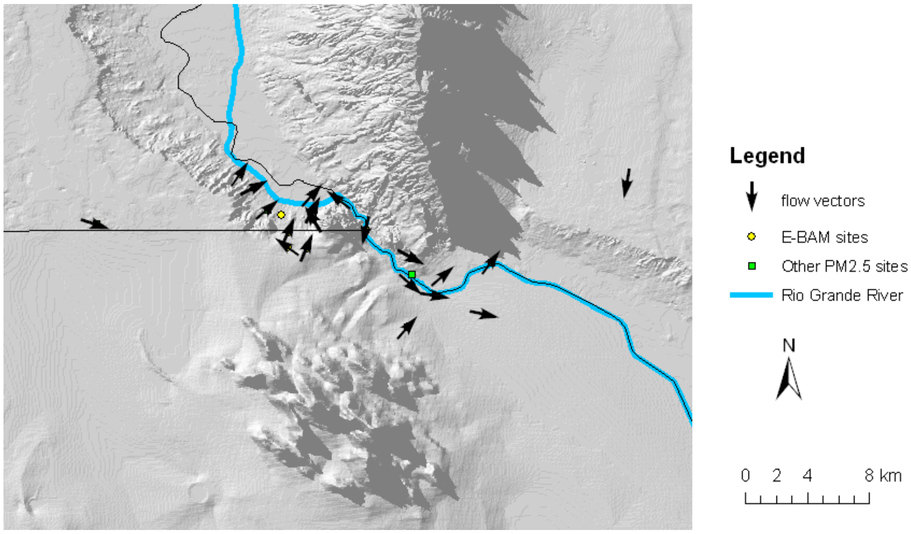

Figure 4-69. Flow vectors from winds measured at each site at 19:00 MST on January 19, 2009

Because of the low winds and the terrain effects, the NAM model did not capture this episode well.

Spatial plots of hourly $PM_{2.5}$ during the episode are shown in the following figures.

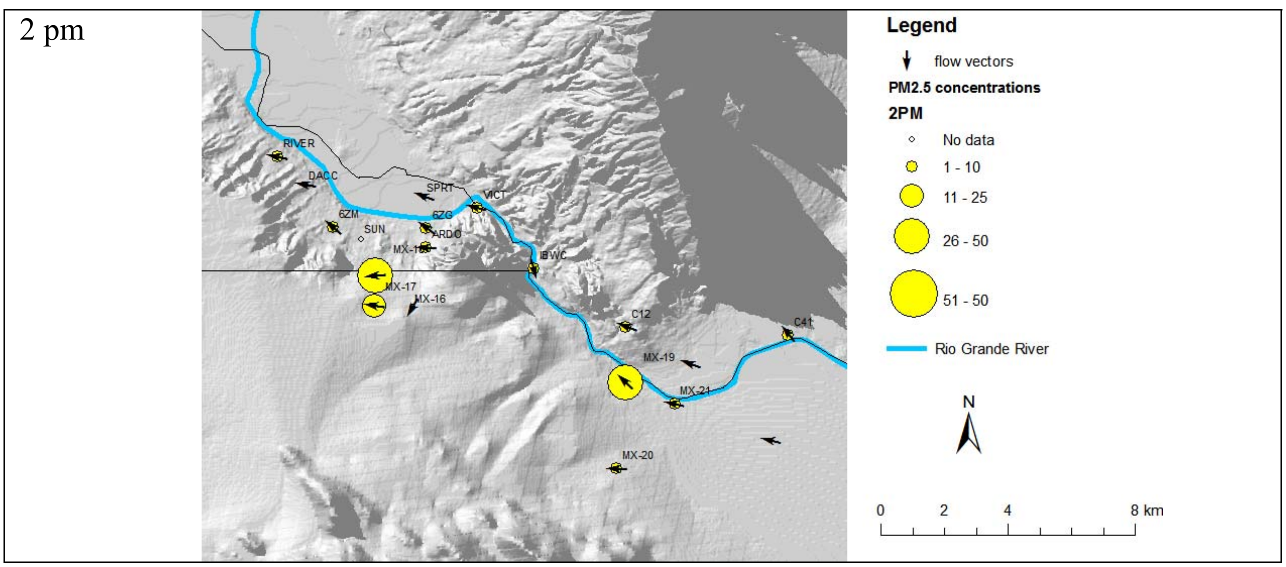

Figure 4-70. Spatial map of hourly $PM_{2.5}$ during this episode at 2 pm

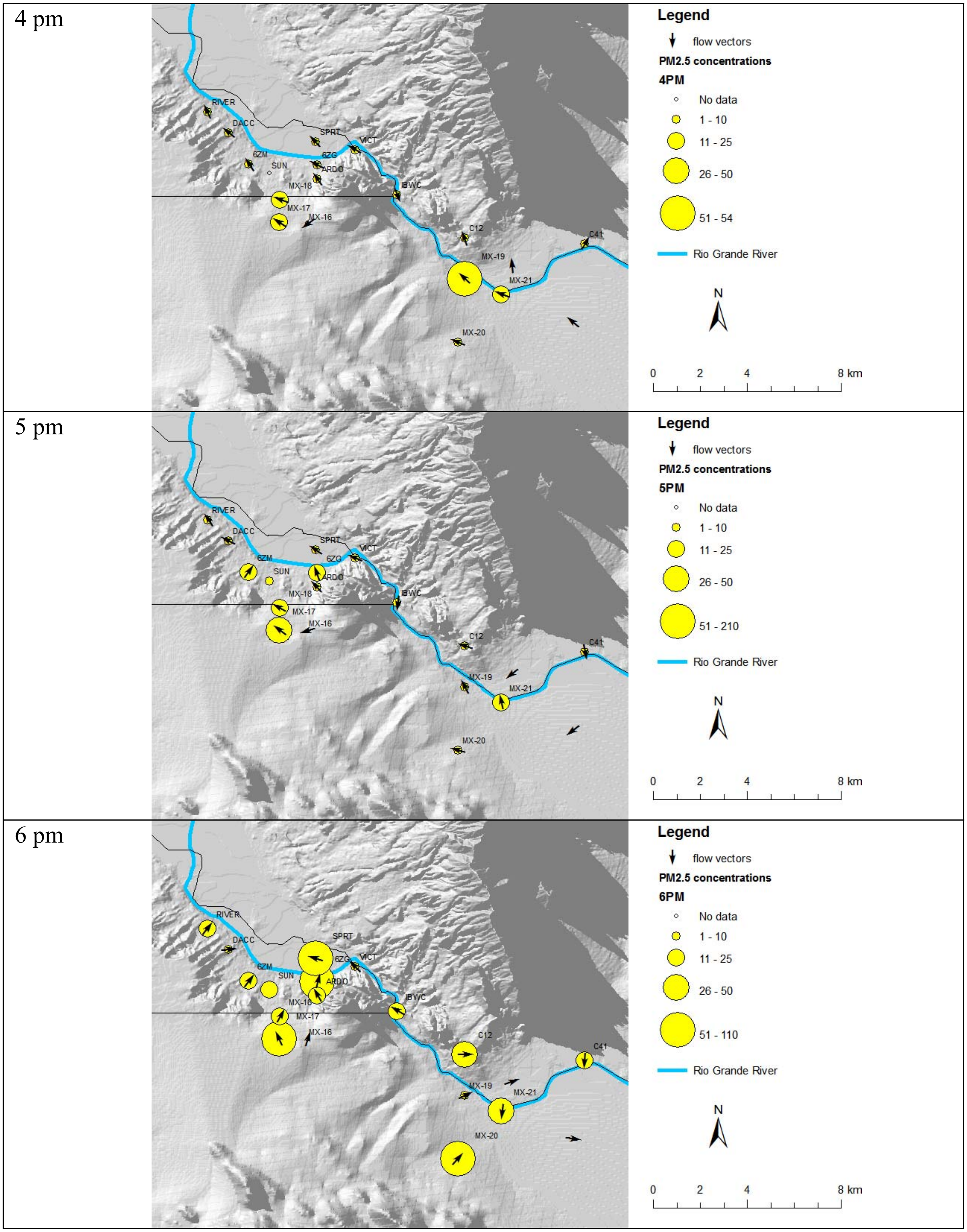

Figure 4-71. Spatial plots of hourly $PM_{2.5}$ during this episode from 4 pm to 6 pm

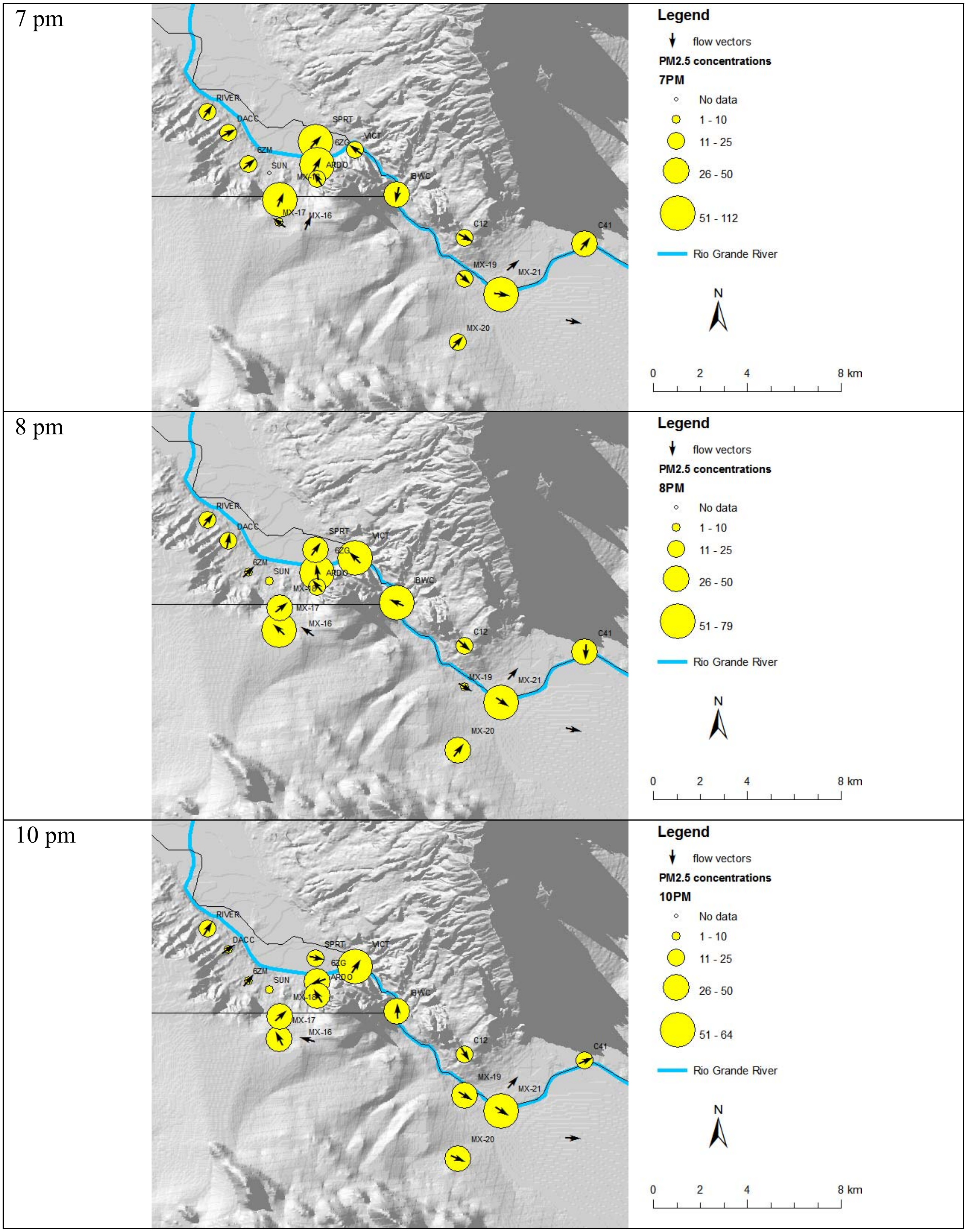

Figure 4-72. Spatial plots of hourly $PM_{2.5}$ during this episode from 7 pm to 10 pm

11 pm

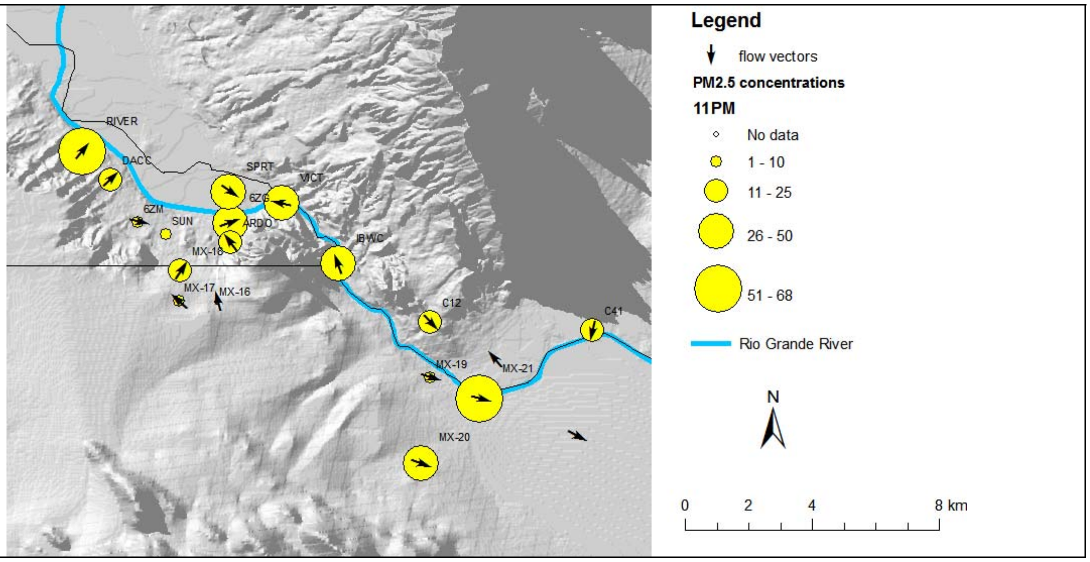

Figure 4-73. Spatial map of hourly $PM_{2.5}$ during this episode at 11 pm

4.3.5 Episode 5: February 5, 2009

This episode occurred during the evening of February 5, 2009. A peak hourly PM2.5 of 82 μg/m^3 at the Sunland Park City Yard site occurred at 7 pm and remained above the 50 μg/m3 level for four hours. The peak concentration at the Desert View Elementary site occurred at 11 pm, four hours after the peak at 6ZG.

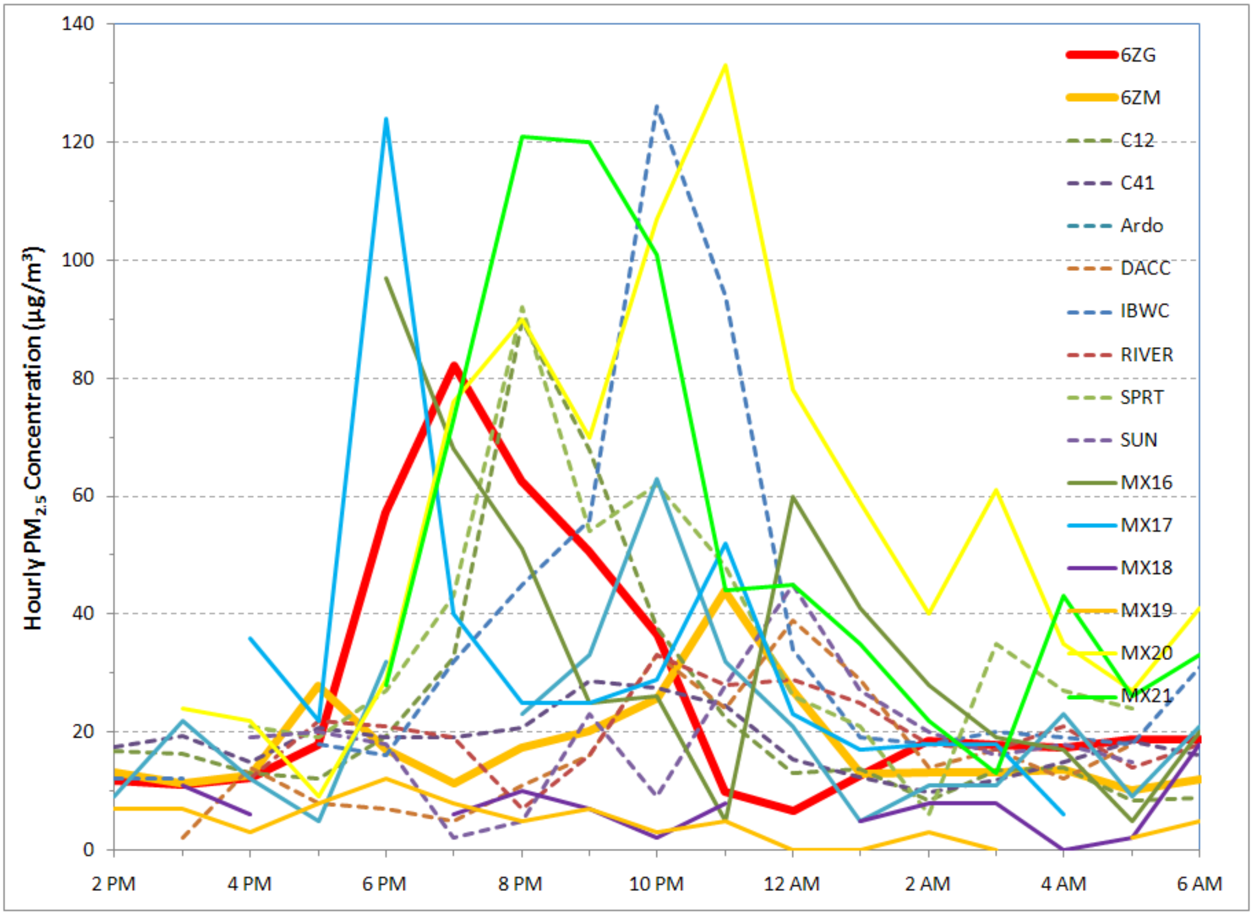

Figure 4-74. Time series plot of hourly $PM_{2.5}$ during the February episode. The two NMED sites are shown as the thick lines. New Mexico E-BAM sites are indicated by dashed lines and Mexican E-BAM sites are thin continuous lines.

Table 4-7. Hourly $PM_{2.5}$ during the February episode. Highlighted area shows episode defined for 6ZG concentrations greater than 50 µg/m^3.

Time	6ZG	6ZM	C12	C41	Ardo	DACC	IBWC	RIVER	SPRT	SUN	VICT	MX16	MX17	MX18	MX19	MX20	MX21
2/5/2009 12:00	5	8	8	12			2		2	21	17	2		9	13	10	1
2/5/2009 13:00	10	11	12	11		9	11		5	3	12			3	25		
2/5/2009 14:00	12	13	17	18			12		17	5	9				7		
2/5/2009 15:00	11	11	16	19		2	12				22			11	7	24	
2/5/2009 16:00	12	13	13	15		14		12	21	19	12		36	6	3	22	
2/5/2009 17:00	18	28	12	21		8	18	22	19	20	5		22		8	9	
2/5/2009 18:00	57	17	19	19		7	16	21	27	18	32	97	124		12	29	28
2/5/2009 19:00	82	11	33	19		5	32	19	43	2		68	40	6	8	76	73
2/5/2009 20:00	63	17	90	21		11	45	7	92	5	23	51	25	10	5	90	121
2/5/2009 21:00	51	20	68	29		16	56	16	54	23	33	25	25	7	7	70	120
2/5/2009 22:00	36	26	38	28		33	126	33	62	9	63	26	29	2	3	107	101
2/5/2009 23:00	10	44	22	24		24	94	28	48	28	32	5	52	8	5	133	44
2/6/2009 0:00	7	27	13	15		39	34	29	26	45	21	60	23		0	78	45
2/6/2009 1:00	13	13	14	12		29	19	25	21	27	5	41	17	5	0	59	35
2/6/2009 2:00	19	13	8	10		14	18	18	6	20	11	28	18	8	3	40	22
2/6/2009 3:00	18	13	14	12		17	20	17	35	16	11	19	18	8	0	61	13
2/6/2009 4:00	17	14	14	15		12	19	21	27	18	23	17	6	0		35	43
2/6/2009 5:00	19	10	8	18		18	18	14	24	15	9	5		2	2	27	26
2/6/2009 6:00	19	12	9	16			31	18			21	20	17	18	5	41	33

Mixing heights peaked at 676 m during the day on February 5 but quickly collapsed to 10 meteres by 8 pm that night as shown in Figure 4-61.

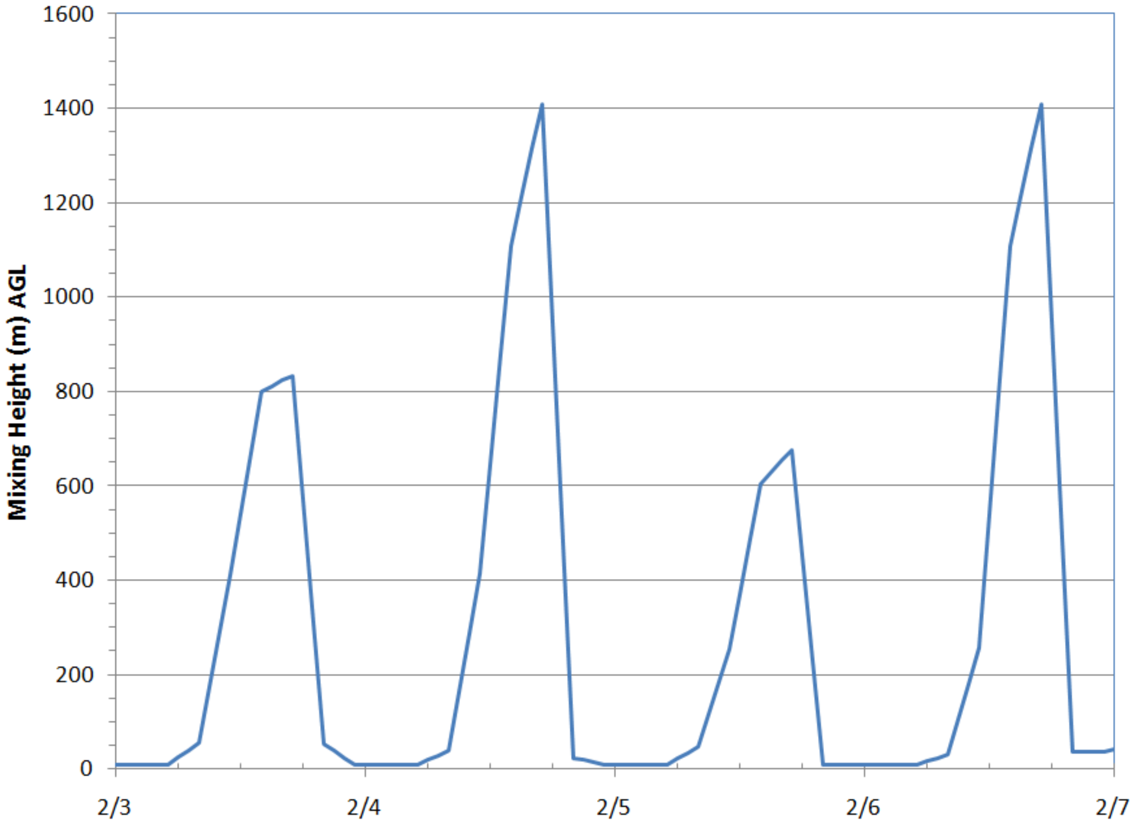

Figure 4-75. Mixing heights before and during the February episode based on 12-km NAM model

Backtrajectories from the 12-km NAM model produced winds from the south, throughout this episode while those backtrajectories generated from the 6ZG station are slower and show a slow turning from up-valley to down-valley through the episode.

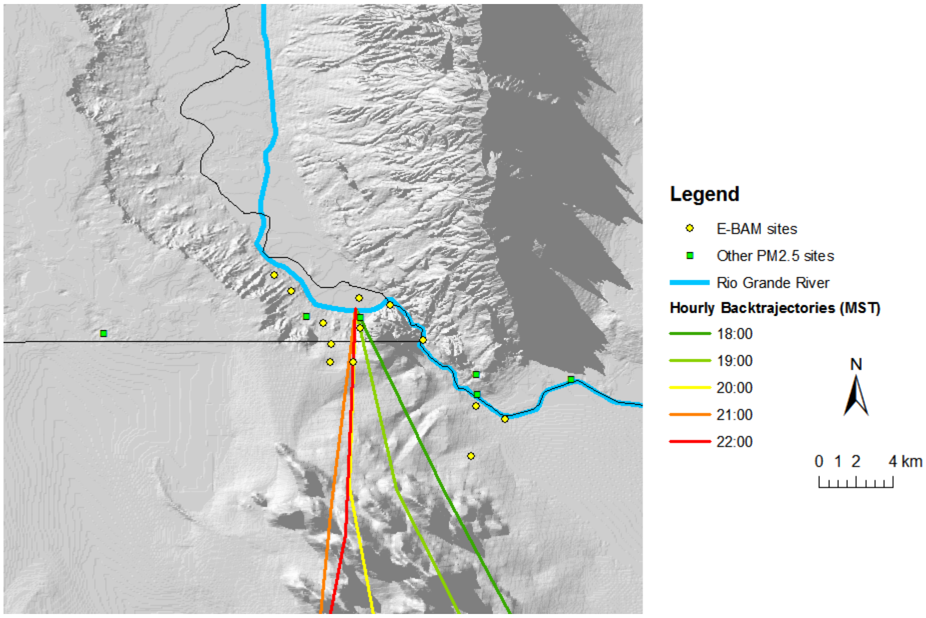

Figure 4-76. Backtrajectories during the February 5 episode based on the 12-km NAM model

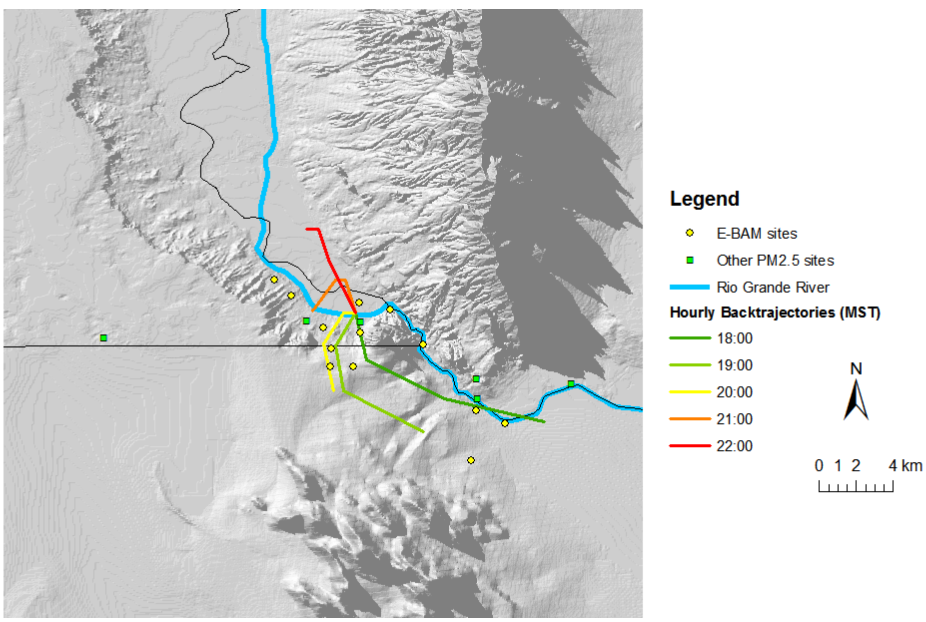

Figure 4-77. Backtrajectories during the February 5 episode based on winds from 6ZG

Spatial plots of hourly $PM_{2.5}$ during the episode are shown in the following figures.

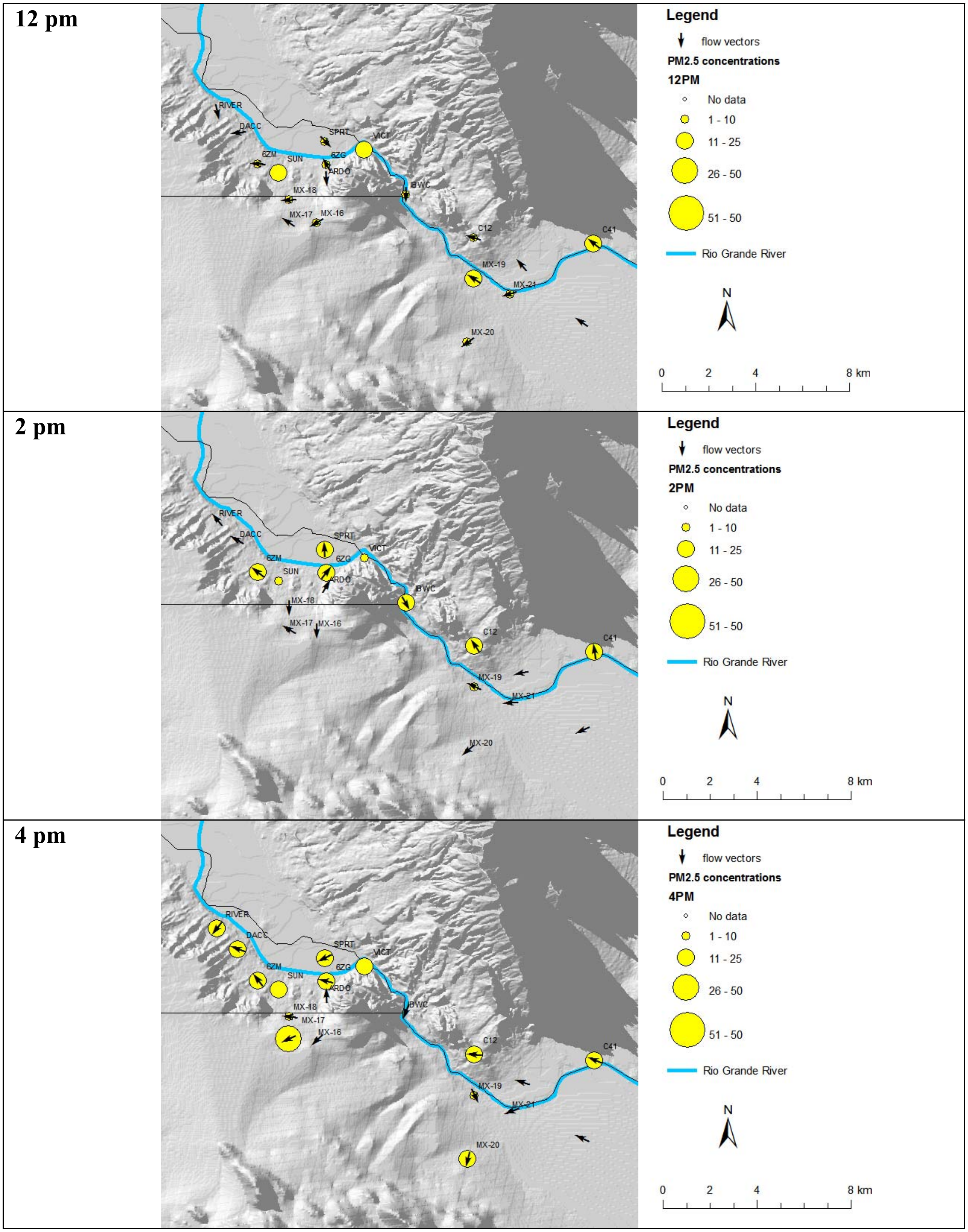

Figure 4-78. Spatial plots of hourly $PM_{2.5}$ during this episode from 12 pm to 4 pm

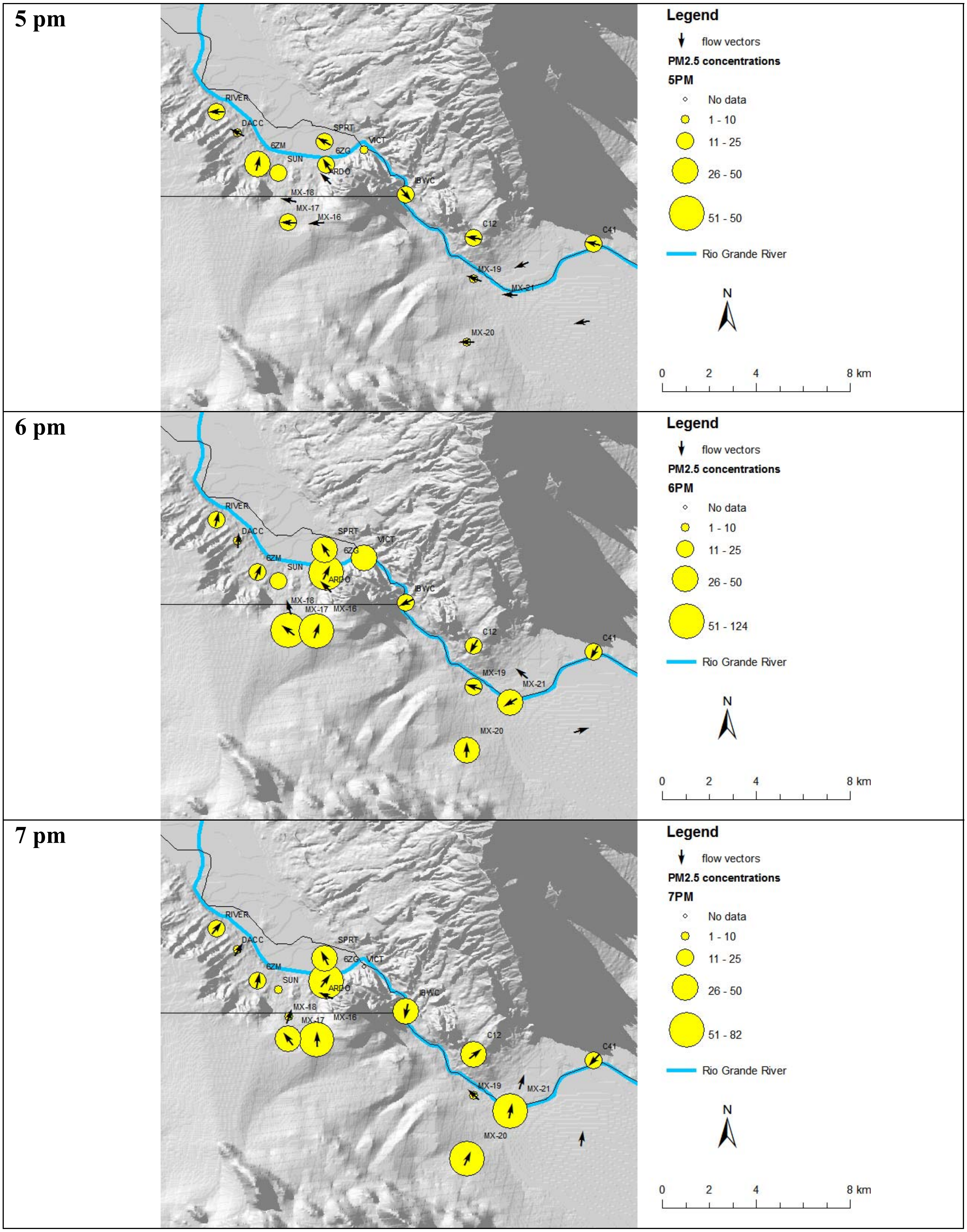

Figure 4-79. Spatial plots of hourly $PM_{2.5}$ during this episode from 5 pm to 7 pm

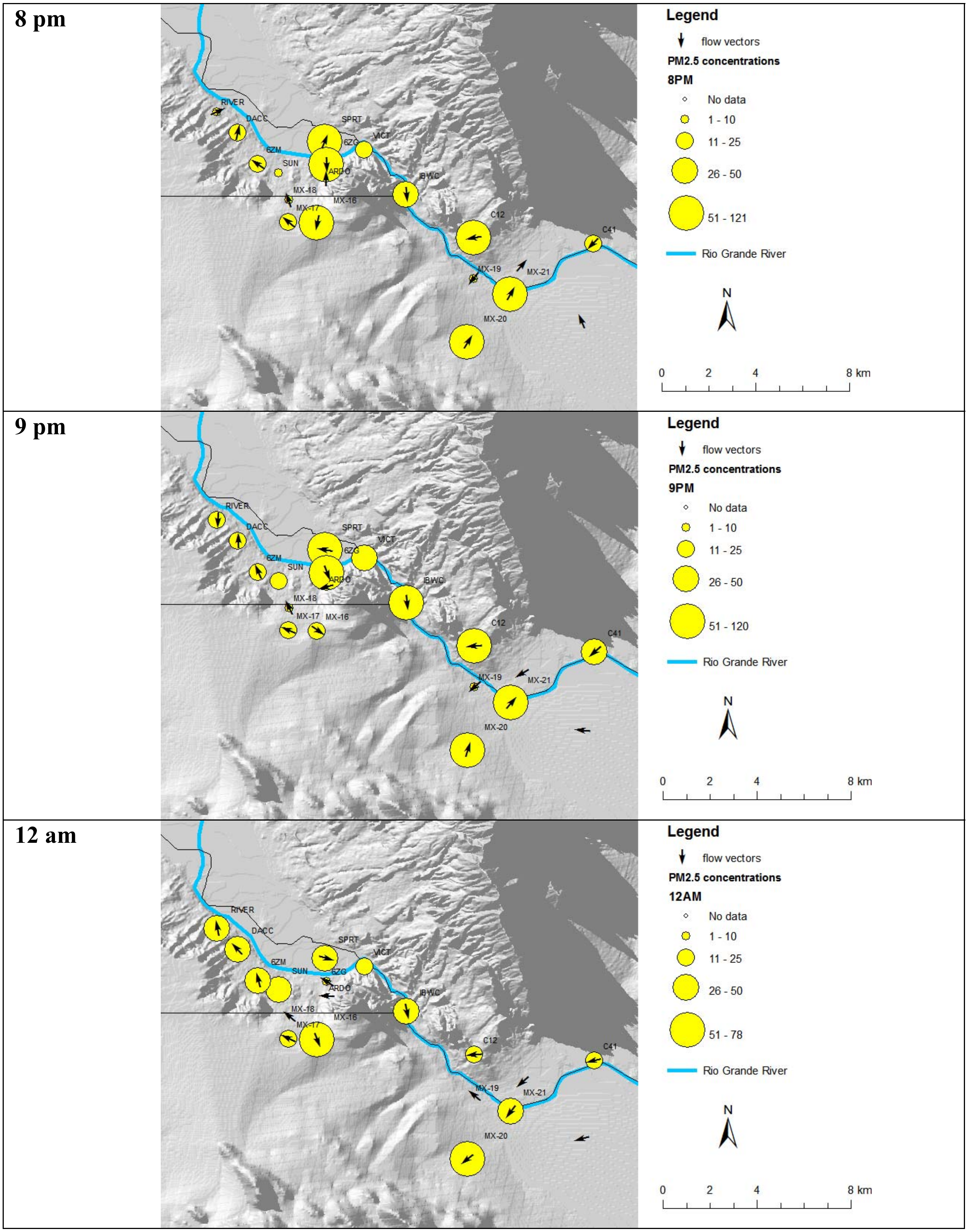

Figure 4-80. Spatial plots of hourly $PM_{2.5}$ during this episode from 8 pm to 12 am

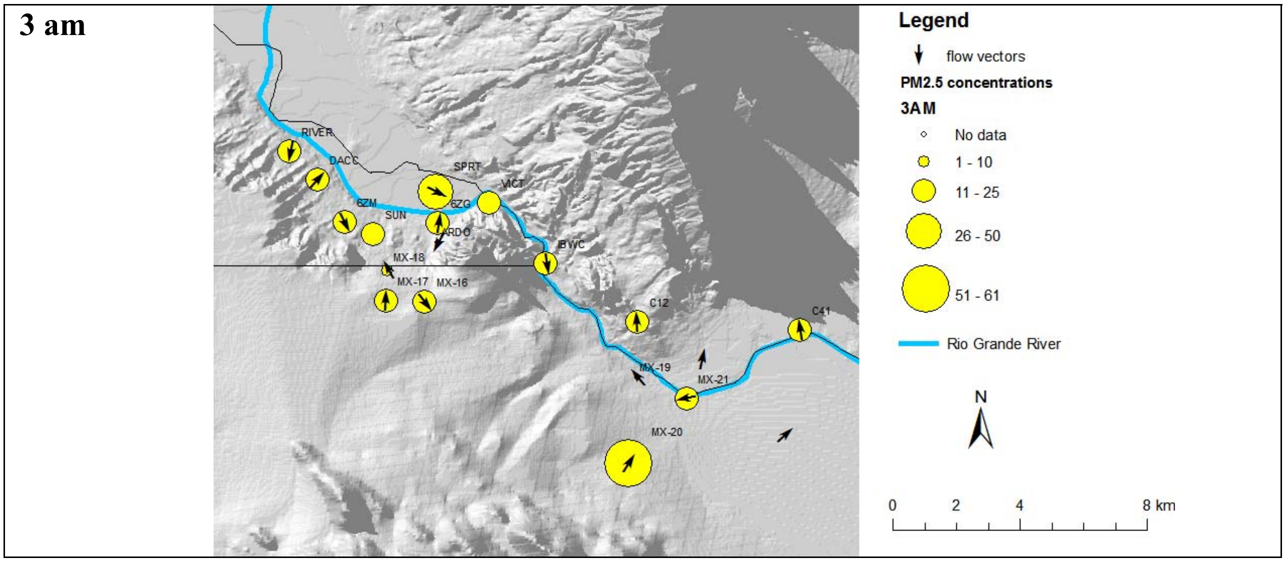

Figure 4-81. Spatial map of hourly $PM_{2.5}$ at the end of this episode at 3am

4.3.6 Episode 6: March 2, 2009

This episode occurred during the late afternoon and evening of March 2, 2009. A peak hourly $PM_{2.5}$ of 55 µg/m^3 at the Sunland Park City Yard site occurred at 10 pm and remained above the 50 µg/m^3 level for two hours in this episode.

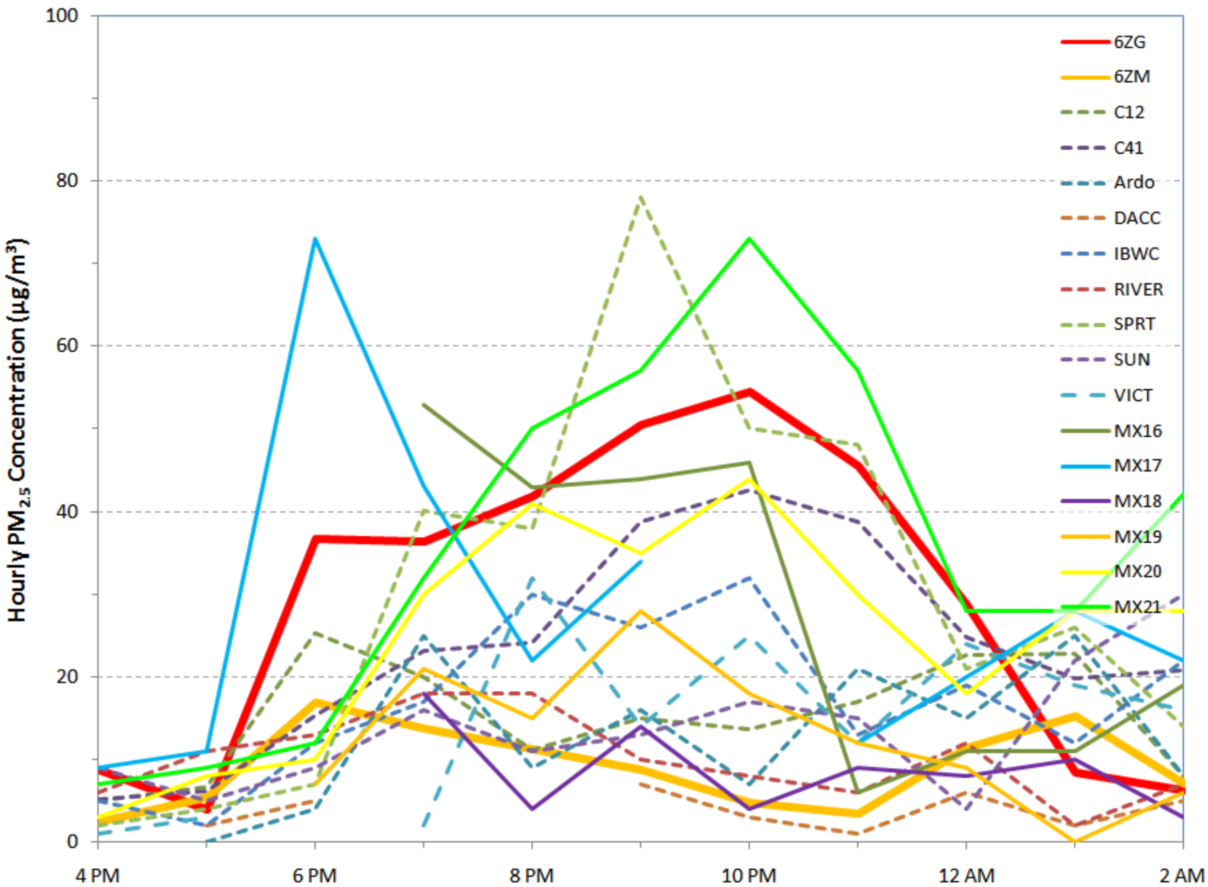

Figure 4-82. Time series of hourly $PM_{2.5}$ during the March episode. The two NMED sites are shown as the thick lines. New Mexico E-BAM sites are indicated by dashed lines and Mexican sites are shown as thin continuous lines.

Table 4-8. Hourly $PM_{2.5}$ during the March 2[nd] episode

Time	6ZG	6ZM	C12	C41	Ardo	DACC	IBWC	RIVER	SPRT	SUN	VICT	MX16	MX17	MX18	MX19	MX20	MX21
3/2/2009 17:00	4	5	7	6	0	2	2	11	4	5	3		11			8	9
3/2/2009 18:00	37	17	25	15	4	5	12	13	7	9			73		7	10	12
3/2/2009 19:00	36	14	20	23	25		17	18	40	16	2	53	43	18	21	30	32
3/2/2009 20:00	42	11	11	24	9		30	18	38	11	32	43	22	4	15	41	50
3/2/2009 21:00	51	9	15	39	16	7	26	10	78	13	14	44	34	14	28	35	57
3/2/2009 22:00	55	5	14	43	7	3	32	8	50	17	25	46		4	18	44	73
3/2/2009 23:00	46	3	17	39	21	1	13	6	48	15	12	6	12	9	12	30	57
3/3/2009 0:00	29	11	23	25	15	6	19	12	21	4	24	11	20	8	9	18	28
3/3/2009 1:00	9	15	23	20	25	2	12	2	26	22	19	11	28	10	0	28	28
3/3/2009 2:00	6	7	8	21	8	5	22	7	14	30	16	19	22	3	6	28	42
3/3/2009 3:00	10	7	7	17	11	9	4	10	10	30	1	21	10	12		12	7

During the day on March 2 the mixing height peaked at 832 m at 5 pm but quickly dropped to 37 m by 8 pm. The very low mixing heights were conducive to pollutant build up and high PM concentrations.

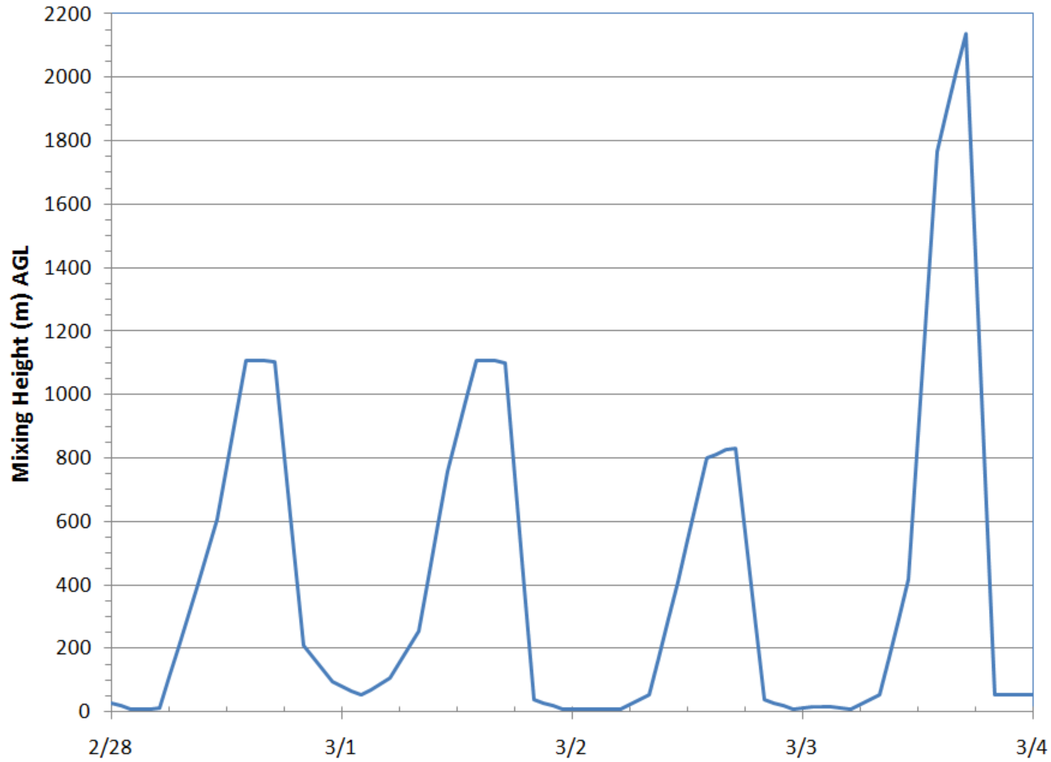

Figure 4-83. Mixing heights leading to and during the episode based on the 12-km NAM model

Backtrajectories from the 12-km NAM model produced winds from the southwest throughout this episode.

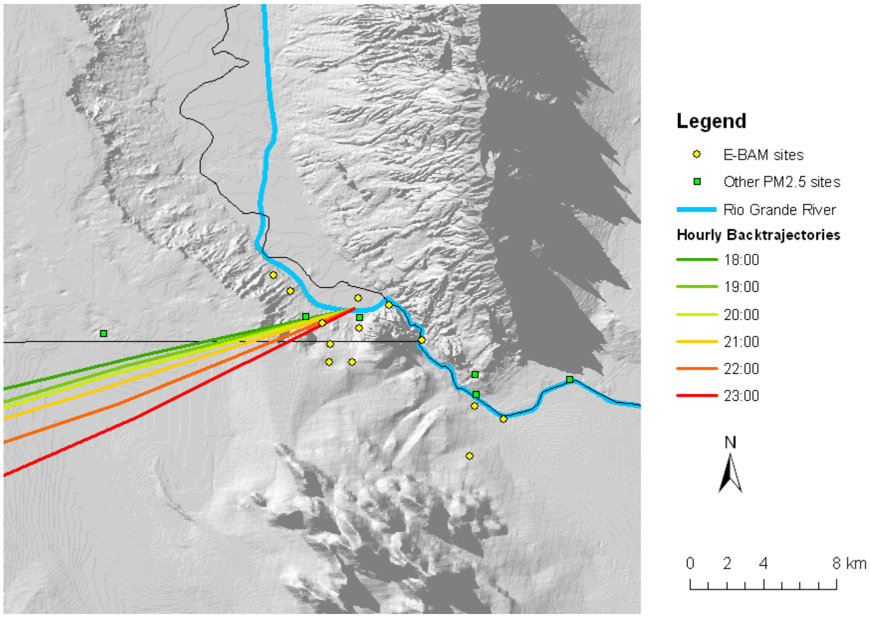

Figure 4-84. Backtrajectories based on the 12-km NAM model

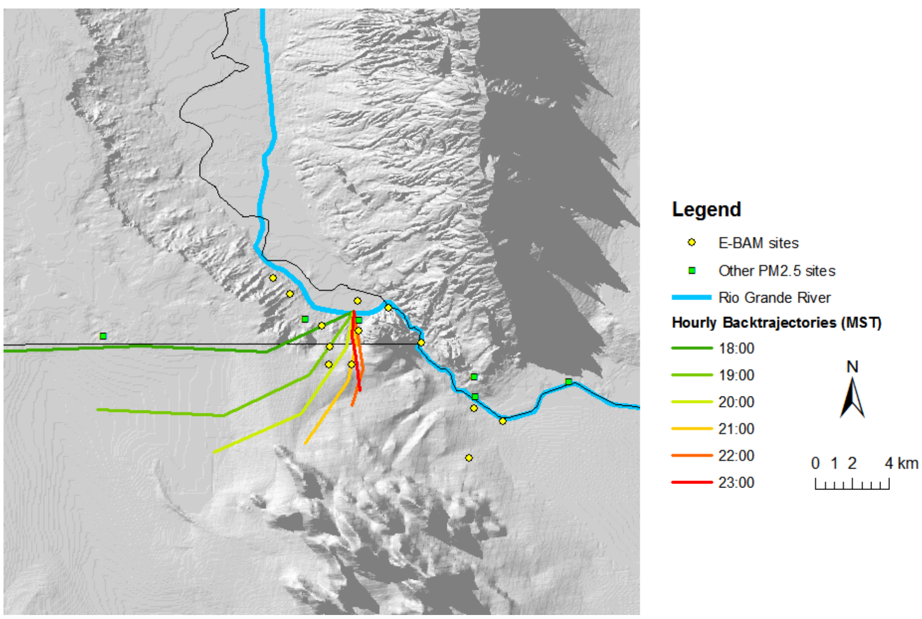

Figure 4-85. Backtrajectories based on data from the 6ZG site

Spatial plots of hourly $PM_{2.5}$ during the episode are shown in the following figures.

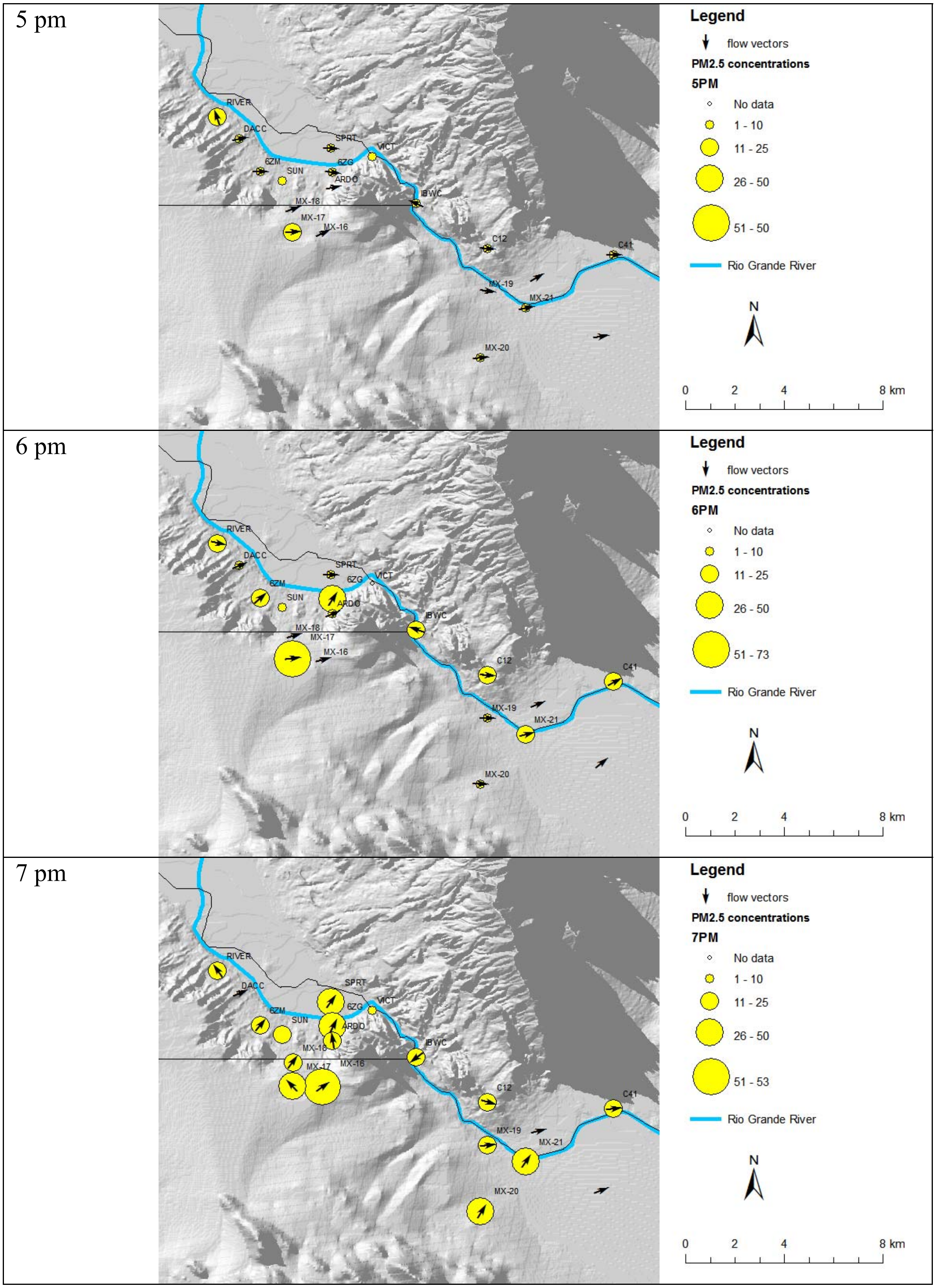

Figure 4-86. Spatial plots of hourly $PM_{2.5}$ during this episode from 5 pm to 7 pm

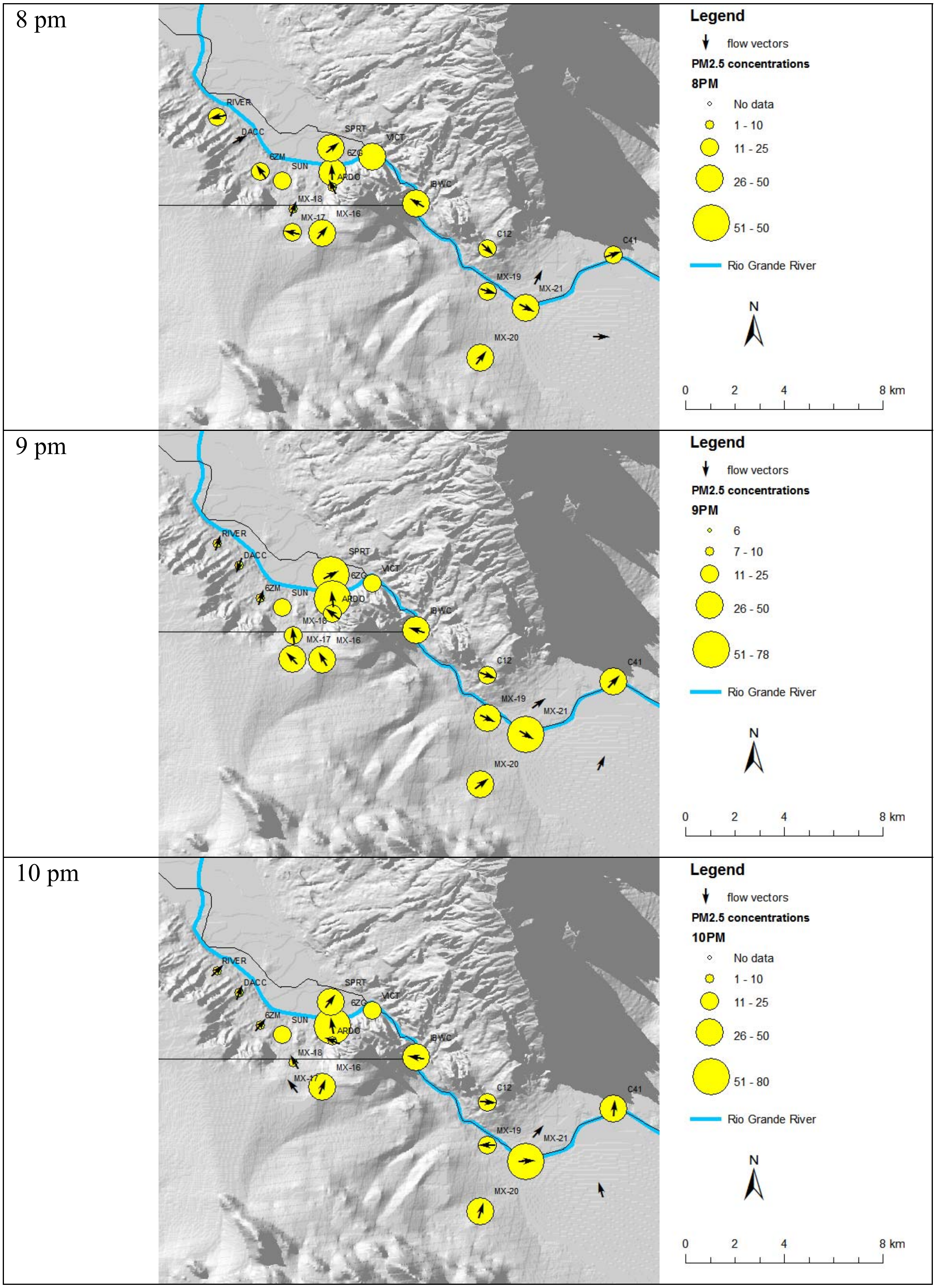

Figure 4-87. Spatial plots of hourly $PM_{2.5}$ during this episode from 8 pm to 10 pm

11 pm

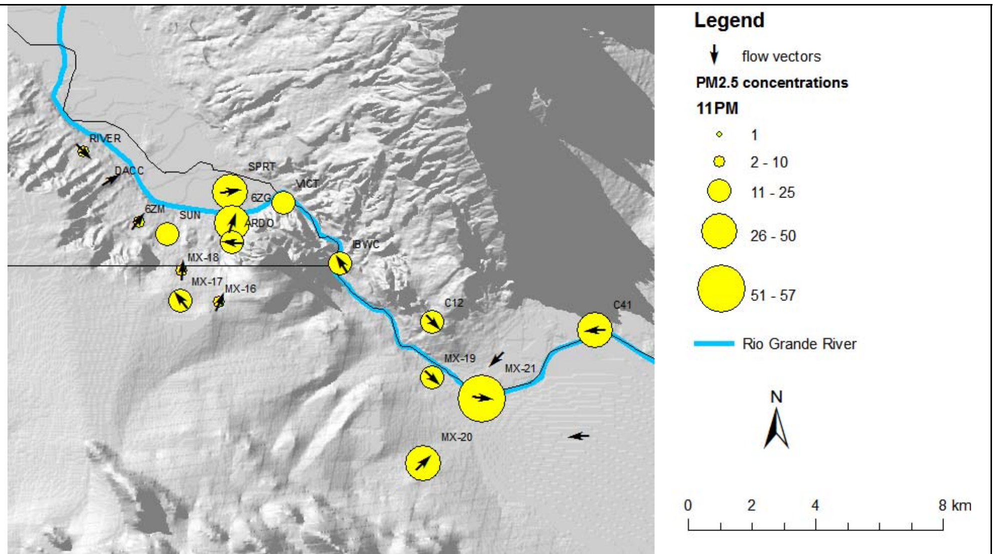

3 am

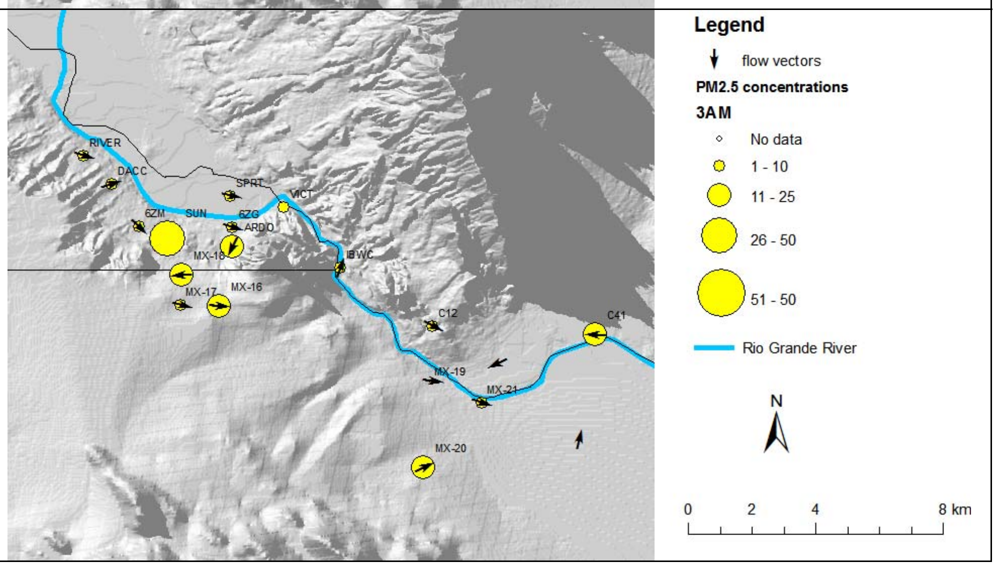

Figure 4-88. Spatial plots of hourly $PM_{2.5}$ during this episode at 11 pm and 3 am

4.4 Potential Source Areas

All of the past work that identified potential source areas was based on a field study from December 2002 to February 2003 with measurement of 3-hour long (6 to 9 pm) speciated $PM_{2.5}$ at the Sunland Park City Yard. Li et al. (2001) referred to brick kilns and unpaved roads as likely sources of $PM_{2.5}$. In a follow up article, Li et al. (2006) used a wind sector analysis and chemical analysis to isolate a potential source area within 5 kilometers south of the Sunland Park City Yard site. In that paper the authors also mentioned possible sources contributing to $PM_{2.5}$ as home heating and uncontrolled burning of waste but not as important as traffic emissions. More recently Garcia et al. (2006) used multivariate statistical techniques on the data and concluded that the evening events were largely due to burning activities south of Sunland Park. Chemical analysis of the filters in these studies found that one of the major constituents of $PM_{2.5}$ was organic carbon, with a likely source of that from residential heating.

The model that we develop here to determine potential source areas is based on backtrajectories, locations of unpaved roads and population density. We compiled known locations of unpaved roads, population density and results from this study in a GIS to investigate a source region. Population density is a surrogate for emissions of residential heating appliances, burn barrels, and trash dumps in Ciudad Juárez. Population density information was obtained from the PdNMapa website for the year 1995. Based on a search for population density in Ciudad Juárez, this data set appeared to be the most recent publicly available GIS data. The map in Figure 4-89 shows population density of the study area based on year 2000 census blocks in the US and year 1995 census tracts in Mexico.

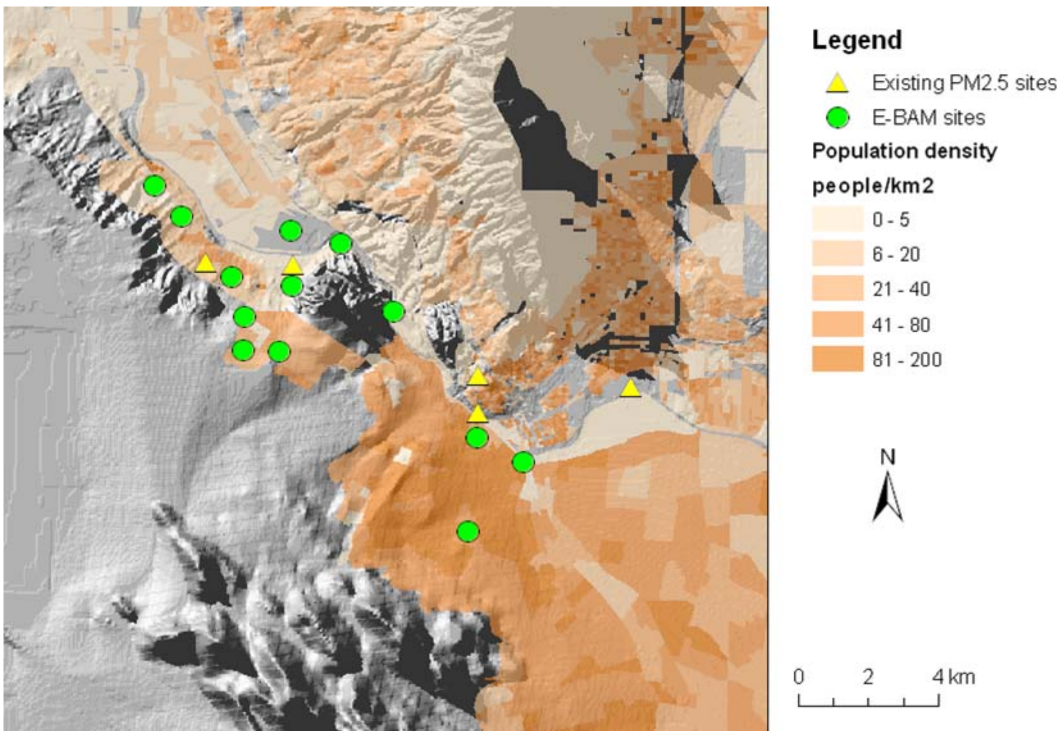

Figure 4-89. Population density surrounding the saturation network

The southern saturation sites are located in very high population density areas compared to the sites in the New Mexico. Since the population density data was from over a decade ago, the population in Ciudad Juárez has inevitably increased and expanded as well as in Colonia Anapra. Unpaved road locations were hand digitized based on high resolution digital aerial photography from 2001 (DuBois, 2003). Despite the lack of a more recent source of unpaved road GIS many of the roads remain unpaved based on an examination of 2008 aerial photos from the National Aerial Photography Program (USGS, 2008). The density of the unpaved road line segments was calculated using the Kernel-type spatial probability density and is shown in Figure 4-90. Unpaved road densities follow very close to the population density since these roads in western Ciudad Juárez in Anapra are spread out in a grid like fashion. There is a high density of unpaved roads directly south of the Sunland Park City Yard site south of the international border.

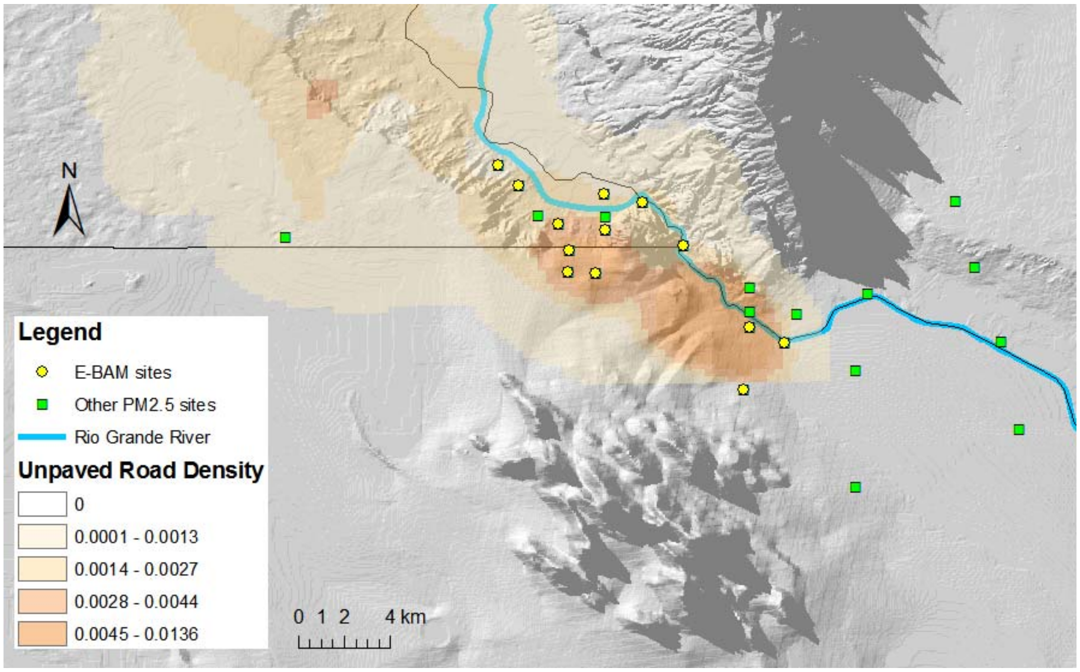

Figure 4-90. Unpaved road density

Backtrajectories from the six episodes were used to extract areas of potential for contributing to the high PM based on proximity of the trajectories to highest population density. Figure 4-91 shows the frequency of 3-hour long backtrajectories over the study area. Each grid cell number represents the number of trajectory end points intersecting each cell divided by the maximum possible that could intersect. As expected, the highest frequencies occur close to the backtrajectory starting location adjacent to the 6ZG site. The map shows a higher number of backtrajectories coming from the western quadrants compared to the other directions. There were a few cases of winds from the north but they were few. Figure 4-92 shows the backtrajectory frequency multiplied by the population density on a grid cell by grid cell basis. Here the map product would show highest numbers where there would be the greatest number of trajectories passing over the most populated areas. This figure shows the product of these two, highest in an area south of Sunland Park within 3 to 4 km of the 6ZG site. We interpret this map subjectively with the highest values having greater weight for being labeled as a potential source area. While the results of this analysis are based on a small number of episodes and trajectories, nevertheless this confirms previous work done with wind sector analysis and speciated $PM_{2.5}$ data. An analysis that includes more episodes would yield more information than provided here and should be done in the future.

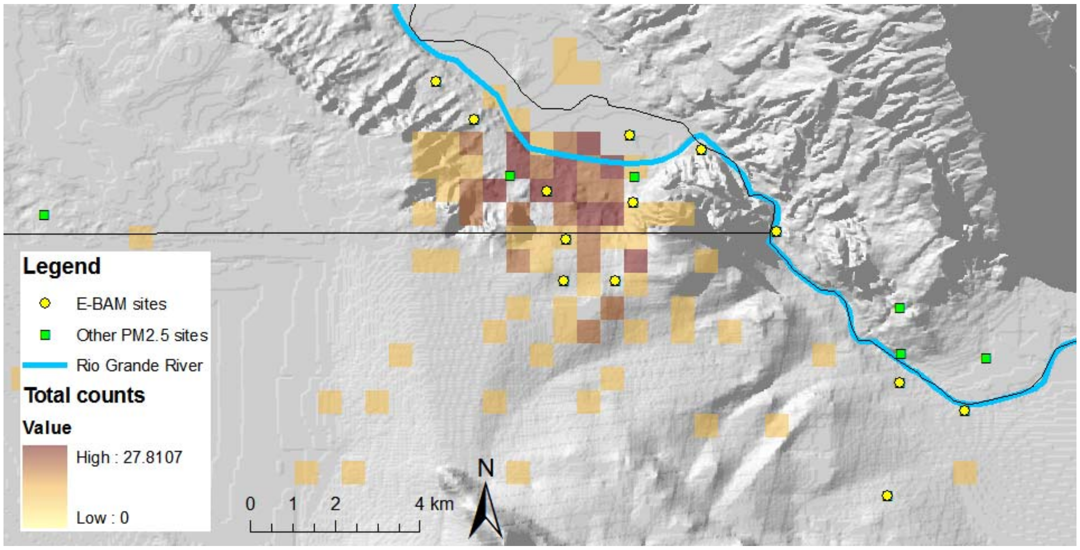

Figure 4-91. Backtrajectory density during the six episodes

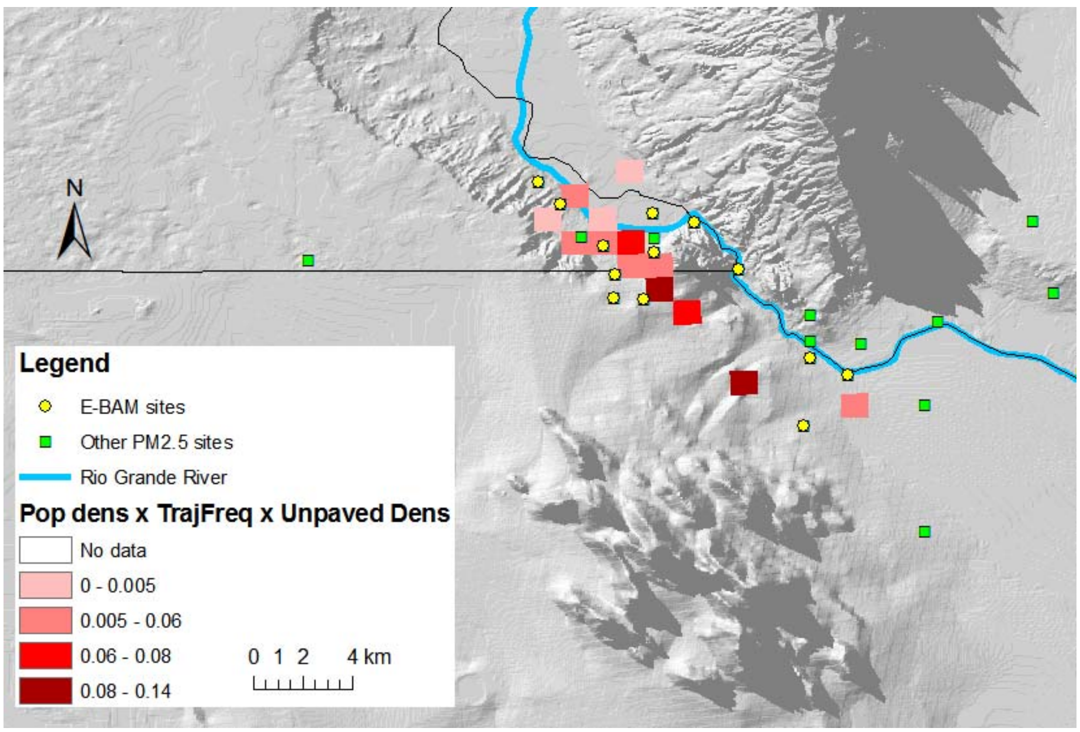

Figure 4-92. Potential source areas defined by the product of population density, trajectories and unpaved road density

5 Conclusions and Recommendations

This study investigated the spatial and temporal behavior of $PM_{2.5}$ during numerous winter episodes in the saturation monitoring network. We quantified over 63 episodes where the hourly $PM_{2.5}$ concentration exceeded 30 $\mu g/m^3$ over one or more hours. Episodes were defined based on the measurements at the NMED Sunland Park City Yard site, with code name 6ZG. The majority of the episodes occurred during the hours between 18:00 and 20:00 MST. Episodes occurred on average every 3 days and varied in duration between one and nine hours and often went past midnight. There were 37 episodes where hourly concentrations exceeded 50 μg/m^3 at 6ZG. The highest hourly $PM_{2.5}$ concentration observed at the NMED 6ZG site was 184 μg/m^3 and was measured on New Year's Day at 1 am. Because of the holiday this would likely have been the result of a combination of home heating wood burning, and pyrotechnics, with some unpaved road traffic emissions. Exceedances of the 24-hour $PM_{2.5}$ standard of 35 μg/m^3 did not occur at the permanent NMED or Texas sites during this study. However, exceedances of the standard were observed multiple times at the saturation sites in New Mexico and Ciudad Juárez. The highest 24-hour averaged $PM_{2.5}$ measured at the Sunland Park City Yard site was 30.8 μg/m^3, 88 percent of the standard. However, four exceedances of the 24-hour standard were observed at the saturation sites in New Mexico. Exceedances occurred at the Ardovinos (Dec. 16, 2008), Dona Ana Community College (Dec. 25, 2008), Riverside Elementary (Feb. 25, 2009) and at the Sunland Park Race Track (April 28, 2009). Substantially higher $PM_{2.5}$ concentrations were measured at the saturation sites in Ciudad Juárez with 24-hour average concentrations as high as 230 μg/m^3 at site MX-16. For those sites with both PM_{10} and $PM_{2.5}$ we observed that the New Mexico side had a smaller $PM_{2.5}$ to PM_{10} ratio of 0.11 than the El Paso sites with a ratio of around 0.22. This is an indication that there are differences in the size distribution of the aerosol particles. This is consistent with general location differences between the sites and previous studies that looked at the size distribution. One hypothesis is that the El Paso sites are more influenced by urban sources such as passenger vehicles and diesels, while the New Mexico sites are dominated by unpaved roads and wind blown dust with the mobile source signature not as significant. A day-of-week pattern in the $PM_{2.5}$ concentrations was observed across several sites. Sundays showed the lowest concentrations followed by a mid-week peak. At multiple sites, Saturday also showed peak concentrations, indicating traffic emissions and non-work related activities.

We successfully demonstrated the utility of using backtrajectories in identifying a potential source area. With the limited number of trajectories used in this study the potential source area confirmed past published research of an area south of Sunland Park and within 5 kilometers of the 6ZG site. We also found out that a commonly used forecast model was not adequate to address transport during these low wind events. This was shown by comparing the North American Model (NAM) model backtrajectories with the trajectories generated using the winds from the 6ZG station. The problem with using a large scale forecast model is its lack of detail in areas that are strongly influenced by terrain. The 12-kilometer grid scale does not resolve the hills and valleys necessary to predict these wind flows. The backtrajectories generated with the NAM input match well with the winds observed at the El Paso International Airport. The airport winds do not reflect winds observed near the Rio Grande River valley. The most appropriate method for using backtrajectories in this region is to use a prognostic mesoscale meteorological model such as MM5, WRF, RAMS or similar model operating at very fine resolution less than 1 kilometer grid scale. Based on this study the wind fields in this locale are not spatially homogeneous and are strongly influenced by downslope and upslope winds along the sides of the hills as well as a river drainage flow following the Rio Grande river. The HYSPLIT model could be driven by these MM5 or WRF wind fields to hopefully yield better predictions of source areas.

While saturation monitoring networks collecting only mass concentrations are useful in providing detail regarding the spatial extent of particulate matter across an area and how it varies in time, they are limited by telling only the magnitude of the problem. Based on past work in chemical speciation of the $PM_{2.5}$, a suggested further study would be to focus on the organic carbon fractions during these episodes at several sites. Tracers for burning various materials would be useful as well as differentiating the carbon from diesel emissions. Following the study from 2002 to 2003, an organic analysis of short-term filter samples of the evening spike would be useful in identifying some compounds used in burning trash, wood, and fuels.

Another possible follow up study that would further describe the source area and the complex wind flow patterns would be to use a tracer release in one or more neighborhoods in Ciudad Juárez and measure the tracer concentrations in the Sunland Park area with high time resolution instruments. In this type of study an inert tracer such as Sulfur Hexafluoride (SF_6) or some other gas is released at one location with a known rate. A sampling network is designed to measure the small concentrations over time. Estimates of the plume's horizontal dispersion can be obtained from this data. This type of measurement study has been done successfully for many years to investigate the behavior of power plant emissions, motor vehicle plumes, and hazardous releases within urban areas. While performing the study a LIDAR type of instrument that measures vertical profiles of aerosol backscatter would also be useful to track the plume's vertical extent.

6 Bibliography

Barr,S.; Buttler,W.F.; Clark,D.A.; Cottingame,W.B.; and Eichinger,W.E. (1994). Lidar-observed wind patterns in the Mexico-New Mexico-Texas border region: 9-11 September, 1994. Prepared by Lidar/Environmental Applications, Los Alamos National Laboratory, Los Alamos, NM.

Draxler, R R, and G D Hess. "An overiveiw of the HYSPLIT_4 modelling system for trajectoreis dispersion and deposition." *Australian Meteorological Magazine*, 1995: 295-308.

Draxler, R. R. and G. D. Hess, (1997). Description of the Hysplit_4 modeling system. Report No. NOAA Tech Memo ERL ARL-224, December 1997. Prepared by Air Resources Laboratory, NOAA, Silver Spring, MD.

DuBois, D.W. Applications of air quality monitoring network design strategies, Unpublished Ph.D. dissertation, University of Nevada, Reno. 2003.

ERG, (2003). Development of an area source emissions inventory for Ciudad Juárez, Chihuahua, Mexico, Eastern Research Group, report number 0141.00.055.001

Finlayson-Pitts, B J, and Jr, J N Pitts. *Chemistry of the upper and lower Atmosphere.* London, UK: Academic Press, 1999.

Fujita, E M, D E Campbell, W Stockwell, P T Roberts, W Main, and L R Chinkin. *Weekend/weekday ozone observations in the South Coast Air Basin, Volume I-Executive Summary.* Final, Atlanta, GA: Desert Research Institute and Sonoma Technology, 2002.

Garcia, J. H., W.-W. Li, N. Cardenas, R. Arimoto, J. Walton and D. Trujillo. "Determination of PM2.5 sources using time-resolved integrated source and receptor models." *Chemosphere*, 1996: 2018-2027.

Graham, J.P., Gurian, P.L., Corella-Barud, V., Avilla R. Periurbanization and in-home environmental health risks: the side effects of planned and unplanned growth. *Int J Hyg Environ Health*. 2004;207(5):447–54.

Graham, J.P., V. Corella-Barud, R. Avitia-Diaz and P. Gurian. The in-home environment and household health: A cross-sectional study of informal urban settlements in Northern Mexico, *Int. J. Env. Res. and Public Health*. 2005; 2(3): 394-402

Kavouras, I G, V Etyemezian, D DuBois, J Xu, and M Pitchford. "Source reconciliation of dust sources in western United States." *Journal of Geophysical Research-Atmospheres*, 2009: D02308.

Kemp, M., (1992). El Paso/Juárez saturation PM-10 study, December 8, 1989 – December 18, 1989, US EPA Region 6, report number 906-R-92-001.

Li, W.-W., R. Orquiz, J.H. Garcia, T.T. Espino, N.E. Pingitore, J. Gardea-Torresdey, J.C. Chow and J.G. Watson, (2001). Analysis of temporal and spatial dichotomous PM air samples in the El Paso-Cd. Juárez air quality basin, J. Air & Waste Mgmt. Assoc. 51: 1551-1560.

Li, W.-W., N. Cardenas, J. Walton, D. Trujillo, H. Morales, and R. Arimoto, (2005). PM source identification at Sunland Park, New Mexico, using a simple heuristic meteorological and chemical analysis, J. Air & Waste Mgmt. Assoc. 55: 352-364.

Marr, L. .C, D. R. Balck, and R. A. Harley. "Formation of a photochemical pollution in central California 1. Development of a revised mobile vehicle emissions inventory." *Journal of Geophysical Research*, 2002: S1-S9, doi:10.1029/2001JD000689.

Motallebi, N, H Tran, B E Croes, and L C Larsen. "Day-of-week patterns of particulate matter and its chemical components at selected sites in California." *Journal of Air and Wastes Management Association*, 2003: 876-888.

Orris,G.J. (2000). New Mexico aggregate production sites, 1997-1999. USGS Open-File Report 00-011-A. Prepared by USGS.

Pfeil,J. (2001). New Mexico's natural resources 2001. Prepared by Energy, Minerals and Natural Resources Department, Santa Fe, NM.

PNEG, (2003). Development of GIS-based Maps for the Ciudad Juárez Area Source Emissions Inventory Project. Prepared for the Texas Commission on

Environmental Quality. Prepared by the Texas Commission on Environmental Quality. Prepared by the Paso del Norte Environmental Group, El Paso, Texas. August 24.

Seinfeld, J H, and S N Pandis. *Atmospheric Chemistry and Physics: From Air Pollution to Climate Change*. New York: Wiley-Interscience, 1998.

Smith, T.B., and D.E. Lehrman, (1996). SARMAP II Design, Analysis of San Joaquin Valley Meteorological Environment During High PM Loading, Final Report, Technical & Business Systems, Santa Rosa, CA

US Bureau of Transportation Statistics (BTS), U.S. Border Crossings/ Entries by State/Port and Month/Year Sorted by Year. 2009, http://www.transtats.bts.gov/BorderCrossing.aspx

USGS, The National Aerial Photography Program (NAPP), 2008, http://edcsns17.cr.usgs.gov/EarthExplorer/

Appendix A: Site Descriptions

Sunland Park City Yard, NMED Air Quality Bureau permanent site (6GZ)

Above is an aerial photo of 6ZG from the 2009 National Agricultural Imagery Program (NAIP) with 1-meter resolution.

Sunland Park City Yard Site, location of PM2.5 TEOM Monitor

Desert View Elementary School, NMED Air Quality Bureau, Permanent site (6ZM)

Above is an aerial photo of 6ZM from the 2009 National Agricultural Imagery Program (NAIP) with 1-meter resolution.

Santa Teresa Border Crossing, NMED Air Quality Bureau permanent site, (6ZN)

Above is an aerial photo of 6ZN from the 2009 National Agricultural Imagery Program (NAIP) with 1-meter resolution.

E-BAM Site #12, Ardovinos (ARDO)

Above is an aerial photo of ARDO from the 2009 National Agricultural Imagery Program (NAIP) with 1-meter resolution.

E-BAM #12, Ardovino's

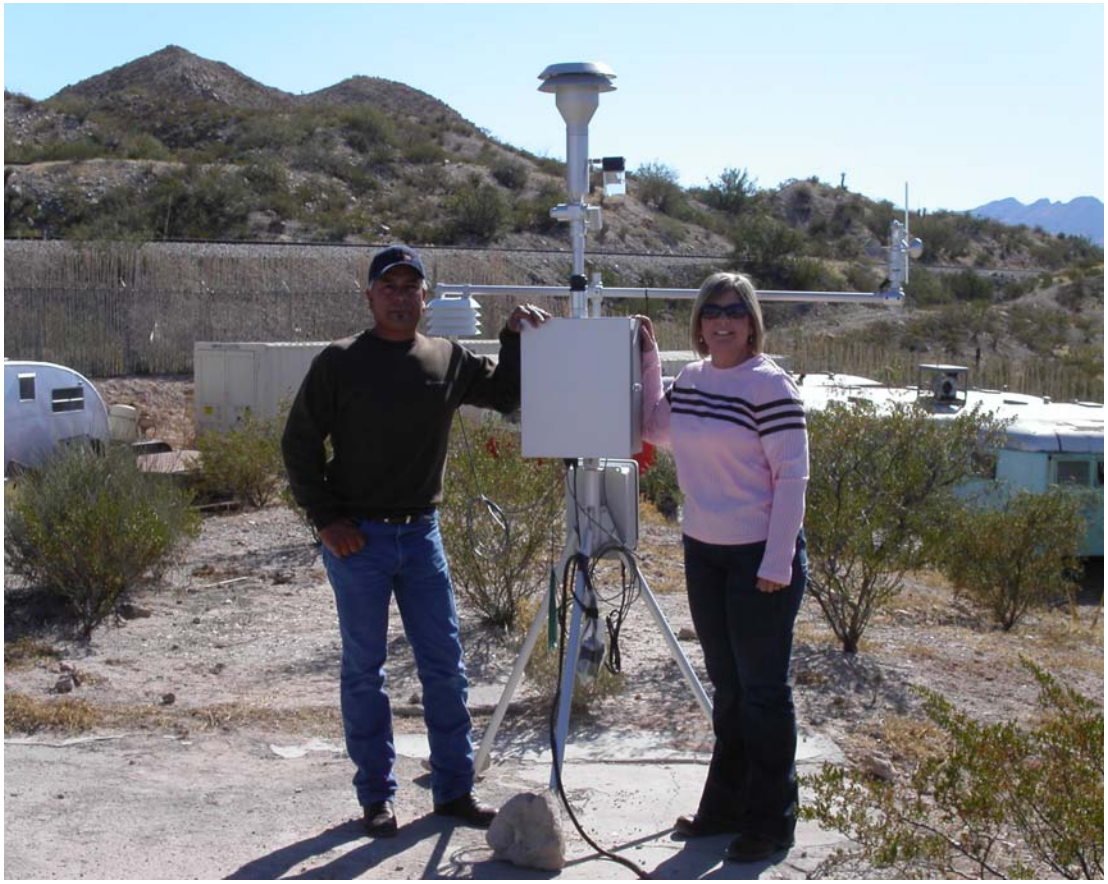
Ardovino site with US Operators Abel Ramirez and Michaela Lane-Sanchez

E-BAM Site #14, Dona Ana County Community College (DACC)

Above is an aerial photo of DACC from the 2009 National Agricultural Imagery Program (NAIP) with 1-meter resolution.

E-BAM #14, Dona Ana County Community College

E-BAM Site #10, International Border and Water Commission (IBWC)

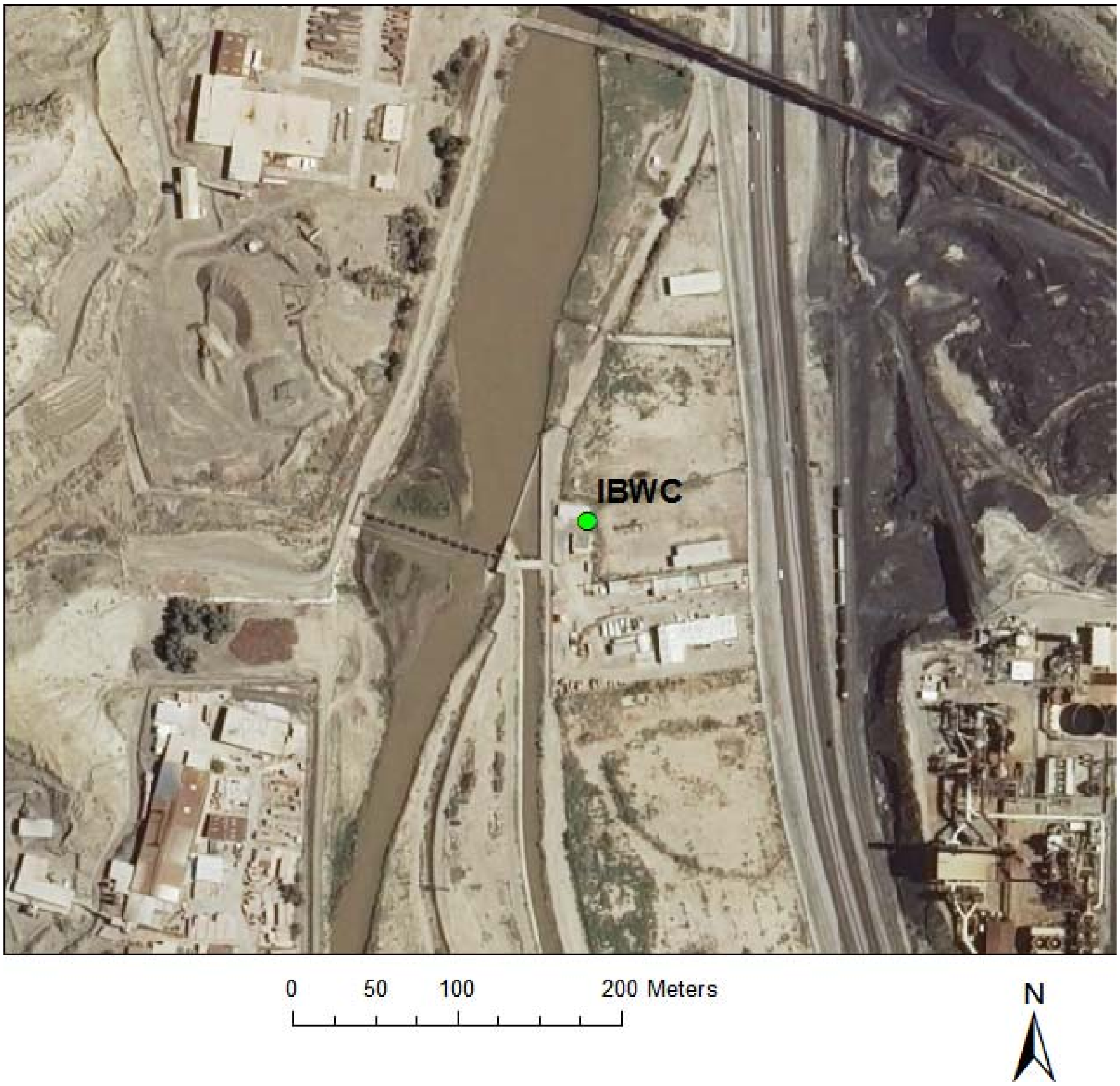

Above is an aerial photo of IBWC from the 2009 National Agricultural Imagery Program (NAIP) with 1-meter resolution.

E-BAM #10, International Border and Water Commission
Note: The ASARCO stack is no longer active; not emitting particulates

E-BAM Site #13, Riverside Elementary School (RIVER)

Above is an aerial photo of RIVER from the 2009 National Agricultural Imagery Program (NAIP) with 1-meter resolution.

E-BAM #13, Riverside Elementary School

E-BAM site #11, Sunland Park Race Track (SPRT)

Above is an aerial photo of SPRT from the 2009 National Agricultural Imagery Program (NAIP) with 1-meter resolution.

E-BAM #11, Sunland Park Race Track

E-BAM Site #15, Sunland Park Elementary School (SUN)

Above is an aerial photo of SUN from the 2009 National Agricultural Imagery Program (NAIP) with 1-meter resolution.

E-BAM #15, Sunland Park Elementary School

E-BAM Site #15A, Victoria En Jesucristo Templo (VICT)

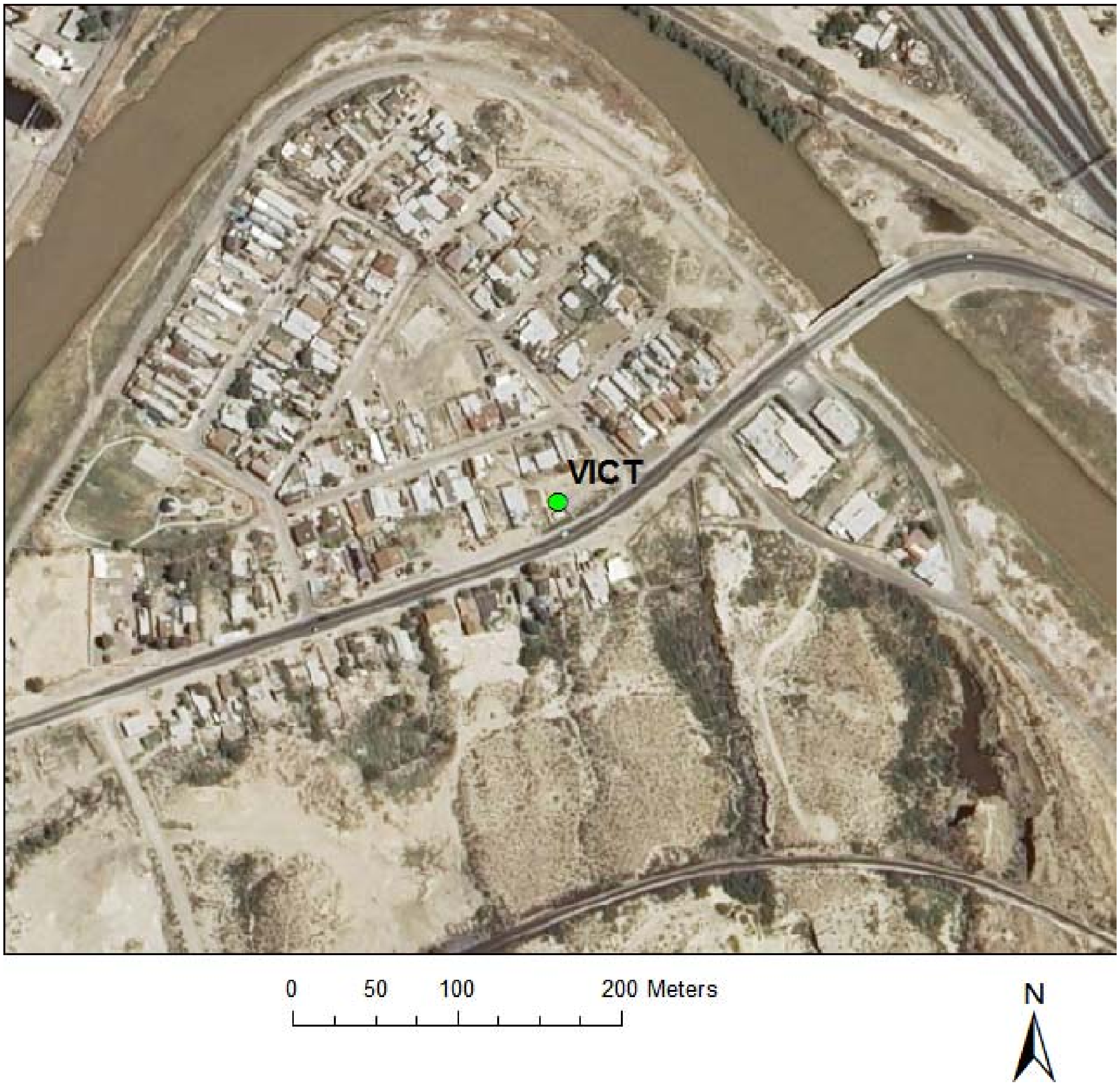

Above is an aerial photo of VICT from the 2009 National Agricultural Imagery Program (NAIP) with 1-meter resolution.

E-BAM #15A, Victoria En Jesucristo Templo

E-BAM Site #16, Bomberos Anapra (MX-16)

Above is an aerial photo of MX-16 from the 2009 National Agricultural Imagery Program (NAIP) with 1-meter resolution.

DOMICILIO: Calle 6 esquina con Raya Col. Anapra
COORDENADAS: Lat. 31° 46’ 25.26” N, Long. 106° 33’ 40.83”
FECHA DE INICIO: 06 DE NOVIEMBRE DE 2008

E-BAM #16, Bomberos Anapra


Foto 2. Sitio 16, Monitor instalado en azotea de Estación de Bomberos


Foto 3. Sitio 16, Vista Norte

Foto 4. Sitio 16, Vista Sur

Foto 5. Sitio 16, Vista Poniente

Foto 6. Sitio 16, Vista Oriente

E-BAM Site #17, Ferretaria la Mas Barata (MX-17)

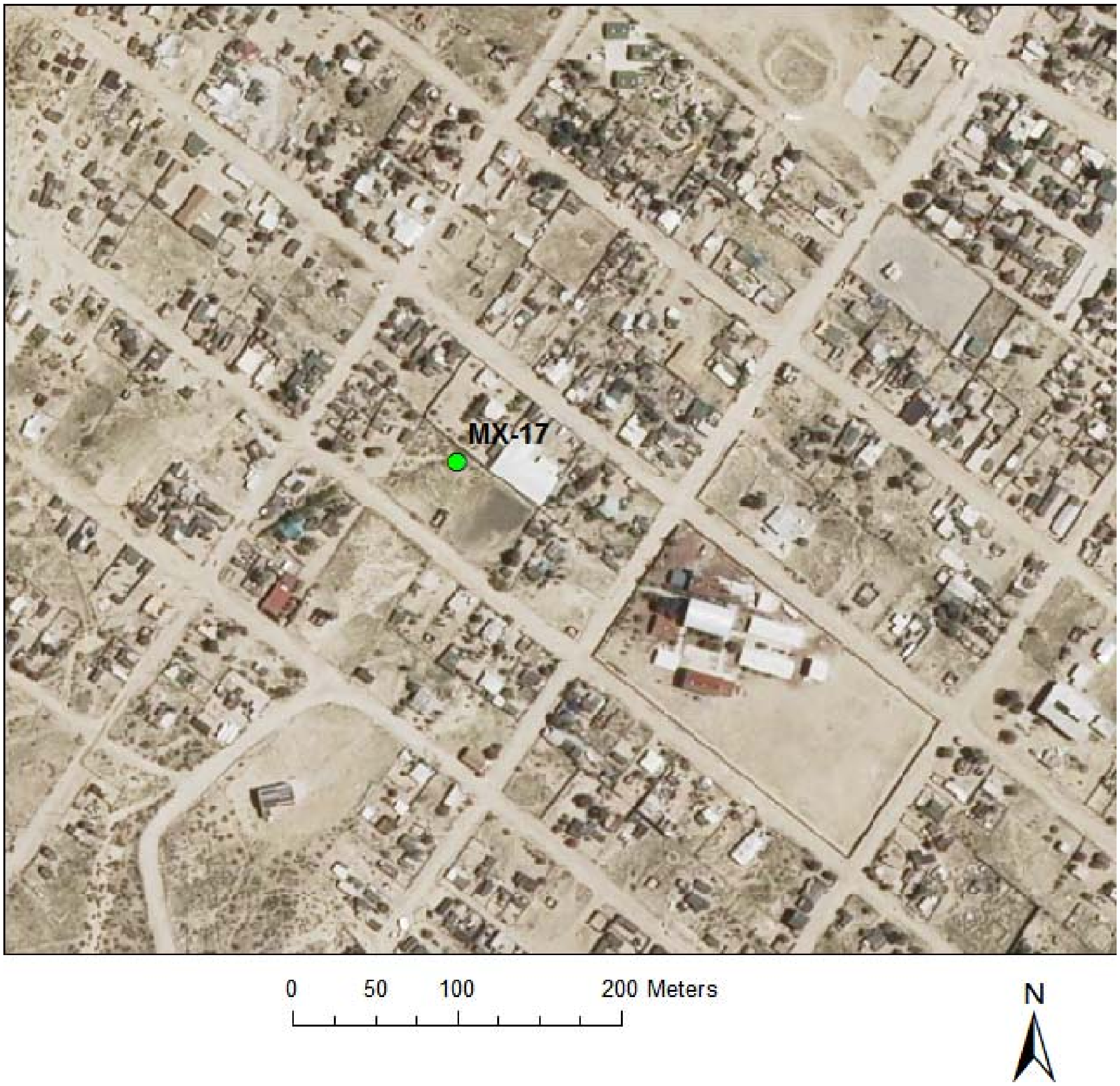

Above is an aerial photo of MX-17 from the 2009 National Agricultural Imagery Program (NAIP) with 1-meter resolution.

DOMICILIO: Rancho Anapra No. 10604, Col. Puerto Anapra
CORDENADAS: Lat. 31° 46’ 26.07”, Long. 106° 33’ 20.16”
FECHA DE INICIO: 07 DE NOVIEMBRE DE 2008

E-BAM #17, Ferretaria la Mas Barata


Foto 2. Sitio 17, Monitor instalado en azotea de Ferretería.

Foto 3. Sitio 17, Vista Norte


Foto 4. Sitio 17, Vista Sur


Foto 5. Sitio 17, Vista Poniente

Foto 6. Sitio 17, Vista Oriente

E-BAM Site #18, Iglesia Anglicana de San Jose de Anapra (MX-18)

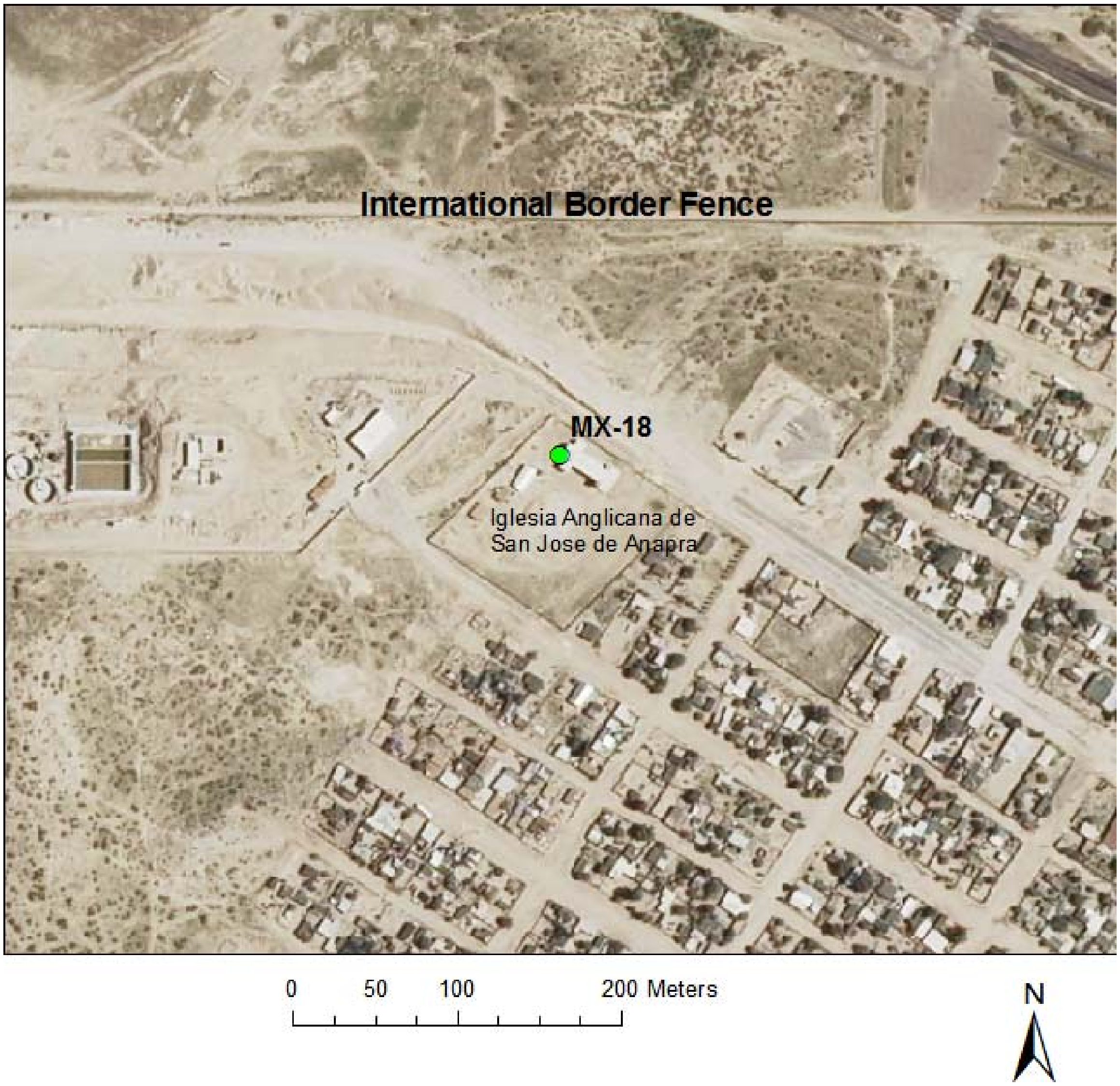

Above is an aerial photo of MX-18 from the 2009 National Agricultural Imagery Program (NAIP) with 1-meter resolution.

DOMICILIO: Camino a Rancho Anapra No. 11248, Col. Anapra
COORDENANDAS: Lat. 31° 46’ 57.40”, Long. 106° 34’ 18.47”
FECHA DE INICIO: 12 DE NOVIEMBRE DE 2008

E-BAM #18, Iglesia Anglicana de San Jose de Anapra


Foto 2. Sitio 18, Monitor instalado en azotea de Iglesia.

Foto 3. Sitio 18, Vista Norte

Foto 4. Sitio 18, Vista Sur

Foto 5. Sitio 18, Vista Poniente

Foto 6. Sitio 18, Vista Oriente

E-BAM Site #19, Maquiladora ACS (MX-19)

Above is an aerial photo of MX-19 from the 2006 National Aerial Photography Program (NAPP) with 1-meter resolution.

DOMICILIO: Calle Cloro s/n entre Blvd. Fronterizo y Geranios, Col. Altavista
COORDENADAS GEOGRAFICAS: Lat 31° 45’ 08, Long. 106° 30’ 04
FECHA DE INICIO: 12 DE NOVIEMBRE DE 2008

E-BAM #19, Maquiladora ACS

Foto 2. Sitio 19, Monitor instalado en Estación ACS.

Foto 3. Sitio 19, Vista Norte

Foto 4. Sitio 19, Vista Sur

Foto 5. Sitio 19, Vista Poniente

Foto 6. Sitio 19, Vista Oriente

E-BAM Site #20, Secundaria Federal No. 3 (MX-20)

Above is an aerial photo of MX-20 from the 2006 National Aerial Photography Program (NAPP) with 1-meter resolution.

DOMICILIO: Viaducto Díaz Ordaz y Lucio Blanco, Col. E. Zapata
COORDENADAS GEOGRAFICAS: Lat. 31° 43’ 41” N, Long. 106° 30’13” O
FECHA DE INICIO: 13 DE NOVIEMBRE DE 2008

E-BAM #20, Secundaria Federal No. 3


Foto 2. Sitio 20, Monitor instalado en Sec. Federal No. 3.


Foto 3. Sitio 20, Vista Norte


Foto 4. Sitio 20, Vista Sur

Foto 5. Sitio 20, Vista Poniente


Foto 6. Sitio 20, Vista Oriente

E-BAM Site #21, Bomberos Estacion Central (MX-21)

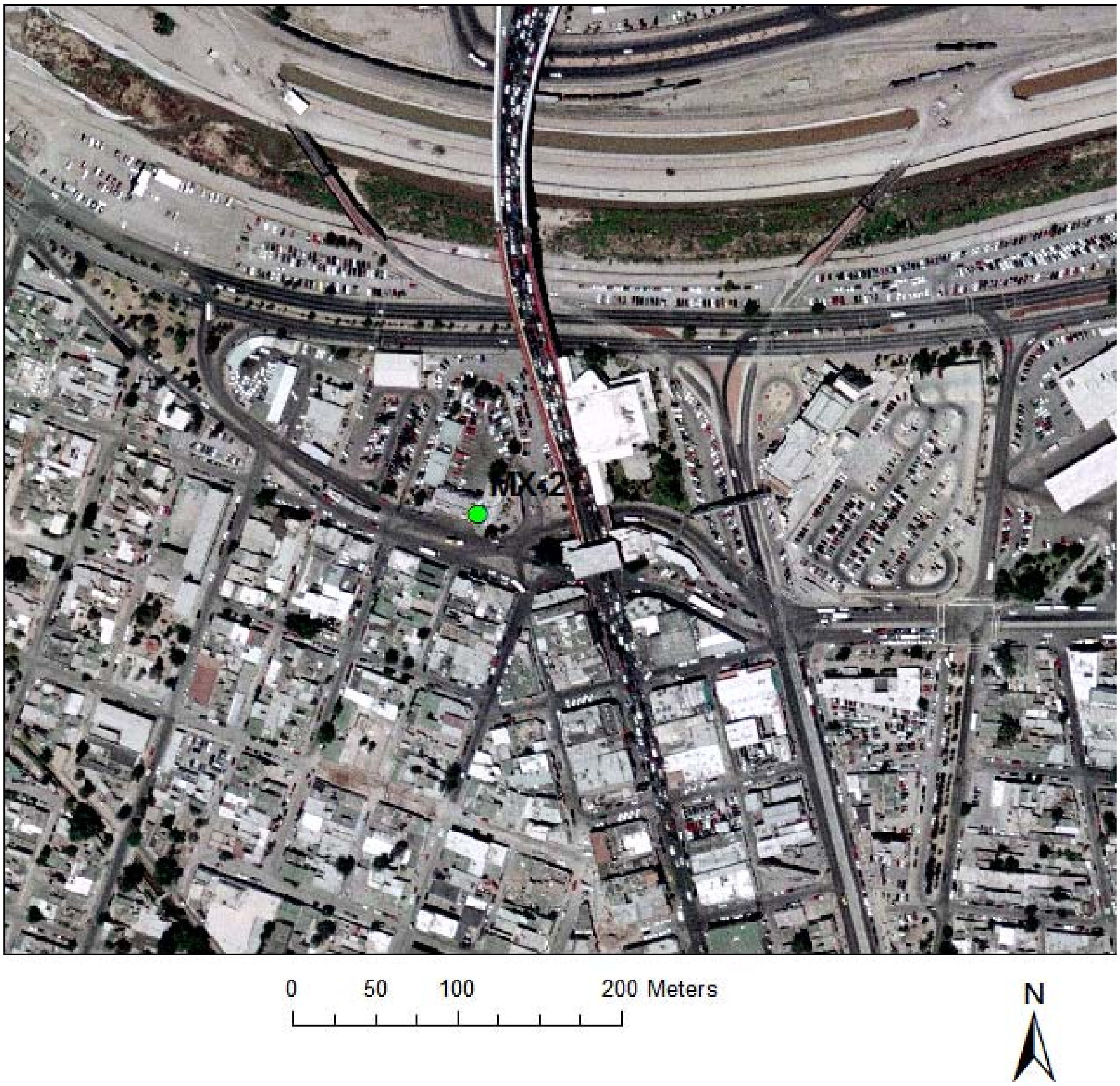

Above is an aerial photo of MX-21 from the 2006 National Aerial Photography Program (NAPP) with 1-meter resolution.

DOMICILIO: Gardenias y Amapolas, Col. Centro
COORDENADAS GEOGRAFICAS: Lat. 31° 44' 46" N, Long. 106° 29'14" O
FECHA DE INICIO: 01 DE DICIEMBRE DE 2008

E-BAM #21, Bomberos Estacion Central

Foto 2. Sitio 21, Monitor instalado en Azotea de Central de Bomberos.

Foto 3. Sitio 21, Vista Norte


Foto 4. Sitio 21, Vista Sur

Foto 5. Sitio 21, Vista Poniente


Foto 6. Sitio 21, Vista Oriente

US Operator Abel Ramirez (middle) with MX Operators Pedro Mora (l.) and Ricardo Aragon (r.)

Appendix B: List of episodes during the study

Episodes at 6ZG based on at least one hour with $PM_{2.5}$ concentration of 50 $\mu g/m^3$ or higher and for winds less than 2 mph. Using this criteria there were 37 episodes in the study.

Episode No.	Date	Max PM2.5	Mean PM2.5	Number Hours	Mean DeltaT (C)
1	10/30/2008	67.7	60.2	2	2.5
2	10/31/2008	71.0	63.1	4	2.4
3	11/2/2008	53.7	53.7	1	2.3
4	11/7/2008	64.7	64.7	1	2.9
5	11/8/2008	83.7	81.3	4	2.7
6	11/16/2008	55.7	55.6	2	2.6
7	11/17/2008	79.7	71.3	2	3.1
8	11/18/2008	61.7	61.7	1	3.5
9	11/19/2008	78.3	69.6	2	2.7
10	11/21/2008	69.0	69.0	1	1.3
11	11/22/2008	101.9	62.3	6	2.1
12	11/25/2008	50.5	50.5	1	0.0
13	11/26/2008	50.2	50.2	1	1.7
14	12/5/2008	72.2	70.1	2	2.0
15	12/6/2008	83.0	83.0	1	2.1
16	12/11/2008	63.7	56.9	2	1.7
17	12/24/2008	53.8	53.8	1	1.4
18	12/29/2008	84.5	70.1	4	2.4
19	12/30/2008	76.6	69.2	3	2.5
20	12/31/2008	184.1	112.1	8	1.7
21	1/10/2009	51.9	51.9	1	1.9
22	1/14/2009	71.9	61.3	2	2.7
23	1/16/2009	74.3	62.7	2	2.3
24	1/18/2009	85.4	78.8	2	2.8
25	1/19/2009	110.3	89.8	4	2.4
26	1/21/2009	73.3	65.2	3	2.2
27	1/25/2009	56.1	56.1	1	2.2
28	1/30/2009	75.6	69.2	2	2.3
29	2/5/2009	82.1	63.2	4	2.8
30	2/16/2009	51.2	51.2	1	1.3
31	2/22/2009	56.2	56.2	1	2.3
32	2/23/2009	63.6	57.6	2	2.6
33	3/2/2009	54.6	52.6	2	2.6

Episode No.	Date	Max PM2.5	Mean PM2.5	Number Hours	Mean DeltaT (C)
34	3/3/2009	66.6	59.1	3	4.1
35	3/16/2009	50.9	50.9	1	2.6
36	3/21/2009	60.6	60.6	1	3.2
37	4/21/2009	50.5	50.5	1	3.3

Episodes at 6ZG based on at least one hour with $PM_{2.5}$ concentration of 40 $\mu g/m^3$ or higher and for winds less than 2 mph. Using this criteria there were 49 episodes in the study.

Episode No.	Date	Max PM2.5	Mean PM2.5	Number Hours	Mean Delta T (C)
1	10/30/2008	67.7	60.2	2	2.5
2	10/31/2008	71.0	63.1	4	2.4
3	11/2/2008	53.7	47.5	3	2.6
4	11/7/2008	64.7	64.7	1	2.9
5	11/8/2008	83.7	81.3	4	2.7
6	11/9/2008	45.2	42.7	2	2.0
7	11/16/2008	55.7	55.6	2	2.6
8	11/17/2008	79.7	56.8	4	2.9
9	11/18/2008	41.4	41.4	1	1.4
10	11/18/2008	61.7	52.5	2	3.9
11	11/19/2008	78.3	53.5	5	2.5
12	11/21/2008	69.0	69.0	1	1.3
13	11/22/2008	101.9	58.2	8	2.0
14	11/25/2008	50.5	50.5	1	0.0
15	11/26/2008	50.2	46.6	5	1.6
16	12/3/2008	47.0	47.0	1	3.2
17	12/5/2008	72.2	70.1	2	2.0
18	12/6/2008	83.0	83.0	1	2.1
19	12/11/2008	63.7	51.3	4	1.5
20	12/24/2008	53.8	53.8	1	1.4
21	12/29/2008	84.5	59.6	7	2.3
22	12/30/2008	76.6	69.2	3	2.5
23	12/31/2008	184.1	112.1	9	1.7
24	1/10/2009	51.9	47.8	2	1.7
25	1/14/2009	71.9	52.9	4	2.7
26	1/16/2009	74.3	50.2	6	2.2
27	1/18/2009	85.4	78.8	2	2.8
28	1/19/2009	110.3	81.4	5	2.4

Episode No.	Date	Max PM2.5	Mean PM2.5	Number Hours	Mean Delta T (C)
29	1/21/2009	73.3	57.2	5	2.0
30	1/25/2009	56.1	56.1	1	2.2
31	1/29/2009	45.6	44.3	9	1.7
32	1/30/2009	75.6	60.4	3	2.0
33	2/3/2009	40.9	40.8	2	3.3
34	2/5/2009	82.1	63.2	4	2.8
35	2/11/2009	42.0	42.0	3	1.3
36	2/13/2009	46.5	46.2	2	2.2
37	2/16/2009	51.2	46.9	2	1.9
38	2/19/2009	47.2	47.2	1	2.7
39	2/22/2009	56.2	51.7	2	2.2
40	2/23/2009	63.6	52.2	3	2.5
41	3/2/2009	54.6	48.2	4	2.7
42	3/3/2009	66.6	59.1	3	4.1
43	3/16/2009	50.9	50.9	1	2.6
44	3/21/2009	60.6	60.6	1	3.2
45	4/18/2009	43.5	43.5	1	2.0
46	4/21/2009	50.5	50.5	1	3.3
47	4/28/2009	41.1	41.1	1	-0.1
49	4/30/2009	42.6	42.6	1	2.7

Episodes at 6ZG based on at least one hour with $PM_{2.5}$ concentration of 30 $\mu g/m^3$ or higher and for winds less than 2 mph. Using this criteria there were 63 episodes in the study.

Episode No.	Date	Max PM2.5	Mean PM2.5	Number Hours	Mean Delta T (C)
1	10/30/2008	67.7	48.1	4	2.4
2	10/31/2008	71.0	57.2	5	2.3
3	11/1/2008	31.4	31.4	1	1.5
4	11/2/2008	53.7	47.5	3	2.6
5	11/3/2008	34.5	34.5	1	2.8
6	11/7/2008	64.7	47.4	2	2.6
7	11/8/2008	83.7	81.3	4	2.7
8	11/9/2008	45.2	40.1	3	1.8
9	11/12/2008	34.6	32.3	2	2.5
10	11/16/2008	55.7	47.8	3	2.6
11	11/17/2008	79.7	49.2	6	2.7
12	11/18/2008	61.7	46.5	4	2.4

Episode No.	Date	Max PM2.5	Mean PM2.5	Number Hours	Mean Delta T (C)
13	11/19/2008	78.3	49.7	6	2.2
14	11/21/2008	69.0	47.3	3	1.5
15	11/22/2008	101.9	55.4	9	1.9
16	11/25/2008	50.5	50.5	1	0.0
17	11/25/2008	32.6	32.6	1	1.3
18	11/26/2008	50.2	46.6	5	1.6
19	12/1/2008	36.0	36.0	1	2.5
20	12/3/2008	47.0	47.0	1	3.2
21	12/5/2008	72.2	70.1	2	2.0
22	12/6/2008	83.0	49.5	4	1.8
23	12/11/2008	63.7	51.3	4	1.5
24	12/24/2008	53.8	53.8	1	1.4
25	12/27/2008	34.7	34.7	1	1.9
26	12/29/2008	84.5	55.9	8	2.3
27	12/30/2008	76.6	69.2	3	2.5
28	12/31/2008	184.1	103.2	9	1.7
29	1/3/2009	34.3	34.3	1	1.8
30	1/10/2009	51.9	42.5	3	1.7
31	1/14/2009	71.9	49.9	5	2.6
32	1/16/2009	74.3	48.2	6	2.2
33	1/18/2009	85.4	78.8	2	2.8
34	1/19/2009	110.3	74.2	6	2.4
35	1/21/2009	39.0	39.0	1	1.0
36	1/21/2009	73.3	53.7	6	2.0
37	1/25/2009	56.1	44.9	2	2.2
38	1/26/2009	31.1	31.1	1	2.6
39	1/28/2009	30.8	30.8	1	1.7
40	1/29/2009	45.6	40.7	3	1.7
41	1/30/2009	42.9	42.9	1	1.6
42	1/30/2009	75.6	53.5	4	1.9
43	2/2/2009	34.4	34.4	1	1.1
44	2/3/2009	40.9	40.8	2	3.3
45	2/5/2009	82.1	63.2	4	2.8
46	2/11/2009	42.0	42.0	2	1.3
47	2/13/2009	46.5	46.2	2	2.2
48	2/16/2009	51.2	46.9	2	1.9
49	2/19/2009	47.2	47.2	1	2.7
50	2/22/2009	56.2	51.7	2	2.2
51	2/23/2009	63.6	52.2	3	2.5
52	3/2/2009	54.6	43.6	6	2.3

Episode No.	Date	Max PM2.5	Mean PM2.5	Number Hours	Mean Delta T (C)
53	3/3/2009	66.6	59.1	3	4.1
54	3/6/2009	30.9	30.9	1	1.1
55	3/16/2009	50.9	44.3	2	2.6
56	3/17/2009	31.6	31.6	1	2.3
57	3/21/2009	60.6	60.6	1	3.2
58	3/31/2009	35.6	35.6	1	2.1
59	4/18/2009	43.5	37.7	3	2.1
60	4/20/2009	36.5	36.5	1	3.4
61	4/21/2009	50.5	40.5	2	2.9
62	4/28/2009	41.1	39.7	2	0.8
63	4/30/2009	42.6	42.6	1	2.7

Appendix C: Theory of E-BAM Operation

"E-BAM" stands for "Environment Proof Instrument-Beta Attenuation Measurement."

When the high-energy electrons emanating from the radioactive decay of ^{14}C (carbon-14) interact with nearby matter, they lose their energy and, in some cases, are absorbed by the matter. These high-energy electrons emitted through radioactive decay are known as *beta rays* and the process is known as *beta-ray attenuation*. When matter is placed between the radioactive ^{14}C source and a device designed to detect beta rays, the beta rays are absorbed and/or their energy diminished, resulting in a reduction in the number of beta particles detected. The magnitude of the reduction in detected beta particles is a function of the mass of the absorbing matter between the ^{14}C beta source and the detector. [1]

Page two of the MetOne E-BAM brochure (below) shows the mechanism of the unit.

In this study, glass fiber tape on reels was the medium used to collect the particulate matter, which was introduced by a vacuum pump at a flow rate of 16.7 liters per minute. The tape was advanced every 24 hours. During any given 24-hour period, particulate matter would collect on the tape and 60-minute averages of particulate concentrations were recorded by the software.

As the particulate matter accumulated on the tape, the software of the E-BAM calculated a particulate concentration in milligrams per cubic meter of air volume sampled. The units used for particulate concentration data in this report were converted to micrograms per cubic meter.

PM2.5 was collected for the project, rather than PM10. This was accomplished by the addition of a "Sharp Cut Cyclone" to every E-BAM. The "SCC" is shown on page 66 of the operating manual.

In addition to the particulate measurement capability, the E-BAMs used in this project had the capability to collect wind speed and wind direction data. This data was also captured as 60-minute averages.

For more details, see the E-BAM operating manual which can be found on the Air Quality Bureau's web site under "My Air" in the Library, in both English and Spanish versions.

E-BAM is a complete measurement system it comes with the following standard components:

- 6 Channel Datalogger
- Internal DC Vacuum Pump
- Real-Time Concentration
- PM10 Dichot Head
- Aluminum Tripod
- Ambient Temperature Sensor
- Volumetric Flow Control
- Weatherproof Enclosure
- Filter Temperature
- Filter RH
- Filter Pressure
- Calibration Membranes

Options and Accessories

- Flow Calibrator
- WINS Impactor
- PM2.5 Sharp-Cut Cyclone
- TSP Inlet, External AC Vacuum Pump
- Power Solar Panel Array, AC Power Supply
- Sensor inputs Wind Sensor,
- Ambient RH,
- Communications Transfer Module, Modem, Radio Modem
- Calibration: Zero Calibration Kit, Flow Calibration Kit

UX-961

Specifications

Range	0 -100 mg per cubic meter
Accuracy	2.5 µg in 24 hour period
Measurement Cycle	Standard @ 60 Minutes, actual sampling time 59 Minutes
Beta Source	C14, less than 75 microcurie, Half life of 5730 years
Detector:	Scintillation probe
Analog Output	0-1V, 0-5V, 0-10V selectable, 12 bit accuracy
Filter Tape	Continuous glass fiber filter
Inlet	PM10 impactor type
Flow Rate:	16.7 liters per minute, adjustable
Flow accuracy	+/- 3% of reading, volumetric flow controlled
Sample Pump	Dual diaphragm type, internally mounted
Alarm Signals	Filter, flow, power and operation failure
Input Power	12 Volts DC @ 36 Watts, 25°C , 48 Watts Max
Alarm Contact Closure	2 Amp @ 240 VAC
Operating Temperature	-30 Deg C to 40 Deg C
Enclosure	
BX-807	PM 2.5 Sharp Cut Cyclone
390062	Battery, 12VDC 100AHR,
390052	Battery Charger, 12 VDC @ 4 A / .3A hold AC adaptor, 100-240 VAC in, 12VDC @ 6A,
EX-0B4	Wind speed and direction sensor
EX-593	Humidity sensor
MMP	MicroMet Plus Software
EX 121	AC Power Supply
UX-961	Transfer Module

Consumables	Part Number
Filter tape, roll	460130

Met One Instruments, Inc.
Corporate Sales & Service: 1600 Washington Blvd., Grants Pass, Oregon 97526 • Tel (541) 471-7111 • Fax (541) 471-7116
Regional Sales & Service: 3206 Main Street, Suite 106, Rowlett, Texas 75088 • Tel (972) 412-4747 • Fax (972) 412-4716
http://www.metone.com • metone@metone.com

E-BAM

The Met One E-BAM is a portable real-time beta gauge traceable to US-EPA requirements for automated PM 2.5 and PM 10 measurement.

The Met One E-BAM has been built to satisfy users, regulators and those from the health community by providing truly accurate, precise, real time measurement of fine particulate matter automatically. In addition, it is rugged, portable battery operated, deployable in 15 minutes.

The E-BAM offers the following advanced features:

1. Accuracy and precision consistent with US-EPA requirements for Class III designation for $PM_{2.5}$.
2. Real-time, accurate results without correction factors, regardless of season or geographic location.
3. True ambient sampling provides accurate measurement of semi-volatile nitrates and organic compounds.
4. Lightweight, rugged construction is easily mounted on a tripod in minutes.
5. All-weather construction allows for true ambient sampling.
6. Operates on AC or DC power. Battery and Solar options available upon request.

Met One Instruments, Inc.

Met One Instruments, Inc.

Continuous Monitoring

E-BAM automates particulate measurement by continuously sampling and reporting particulate concentration, data is updated every second, and data records updated every minute. E-BAM eliminates the old process of filter collection and manual filter weighing, and eliminates the need for more expensive, high maintenance instruments. Today, with the adaptation of Beta Attenuation to ambient monitoring this process became simple streamlined and inexpensive.

About Accuracy

Real-time accurate, reliable, and repeatable measurement of ambient fine particulate matter has been the elusive goal of environmental regulators and health professionals for many years. Met One Instruments has developed advanced particulate monitoring instrumentation which will meet or exceed all US-EPA requirements for Class-III PM2.5 designation, is reliable, and is easy to operate. It will also report results in real time and is automatic thereby eliminating the need for high levels of human intervention.

Because sampling occurs under true ambient conditions semi-volatile organic compounds and nitrates are easily detected thereby avoiding under measurement.

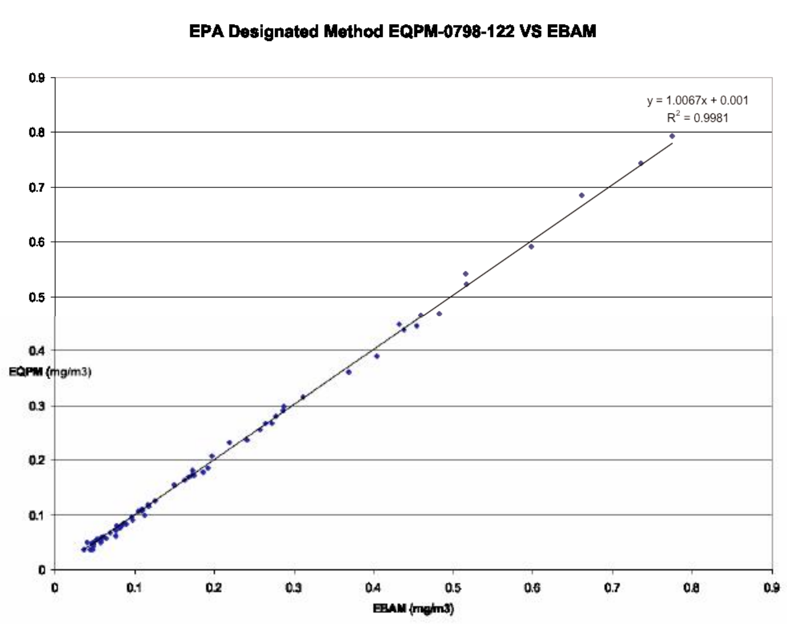

Continuous Sampling

Mobility

E-BAM is a lightweight portable instrument that operates directly in hostile environments without exterior enclosure. E-BAM is a very robust portable sampler system that is easily installed in less than 15 minutes. No other sampler matches the portability and flexibilty of the E-BAM.

Set up

Quick setup of the E-BAM is assured with a series of prompts instructing the installer on the sequence to follow. Then the E-BAM performs a series of self test diagnostics and alerts the installer of any corrective action, upon completion the E-BAM automatically places itself in normal operate mode.

Particulate size selection

Size selective concentration measurements are made using a variety of sampling inlets, the E-BAM may be supplied with TSP (Total Suspended Particulate), PM-10, PM 2.5 or PM 1 inlets. Flow dependent cut points in the size selective inlets are maintained using integral flow meter, pressure sensor and ambient temperature sensor.

The PM-10 inlet removes particles larger than 10 microns, the inlet is not affected by wind speed and wind direction. For PM 2.5 or PM 1 secondary size selection is made using a second downstream inlet.

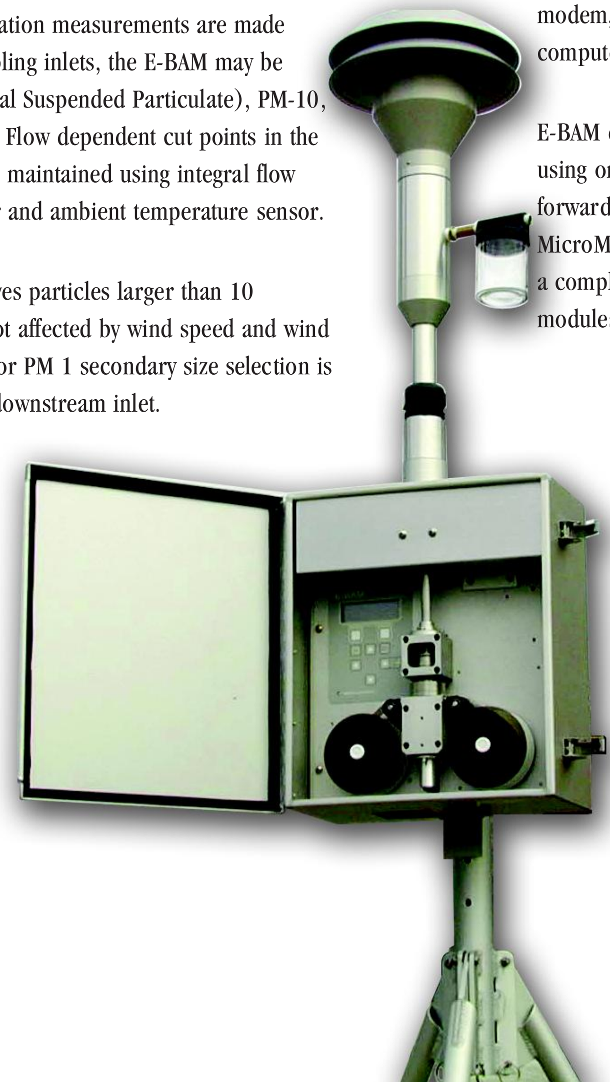

Construction etc.

The standard configuration of the E-BAM is a self-contained environmentally sealed aluminum enclosure placed on a rugged tripod. This system can be permanently placed on rooftops, near roads, at industrial sites or rapidly deployed to monitor emergency situations.

'E- 'represents Environment Proof instrument, E-BAM has been specifically designed to work in hostile environments without additional protection.

Direct Field Reporting

Collecting real time or historical particulate data from a field site has never been easier. Advanced communication options include cellular phone, Line of Sight Radio, and for very remote sites satellite communications are now available. E-BAM also supports the full line of standard MET ONE options, such as data transfer module, phone modem, and direct communications to a portable computer.

E-BAM data is recorded internally and may be retrieved using one of the communication options or data may be forwarded to third party data acquisition system. MicroMet Plus Software supports the E-BAM and provides a complete communication, data base and reporting modules with charting.

Digital, Analog and Alarm Outputs

The E-BAM provides both continuous digital and analog outputs, alarm output may be set for any concentration level. Analog output is selectable to either voltage or current, digital output is supplied as RS-232 or USB.

Reporting modes

The internal data logger can store up over 200 days of concentration data at one hour sample times, and collect data from six other measurements at the same time! Both digital and analog outputs are included to enable users to connect to other data recording systems and to network with other monitors.

Easy to Operate

E-BAM has been programmed to operate, at all times, except during calibration verification. Current data, historical data, and status information are available at all times without interrupting normal E-BAM operation.

Data Validation

The operator may select various criteria for data validation, including deviation from rolling average, high value excursions, power failure and others. If an error occurs it is entered into the error log with date, time and type of error.